universität wien

DISSERTATION / DOCTORAL THESIS

Titel der Dissertation /Title of the Doctoral Thesis

"Studies on the toxicological impact of selected secondary metabolites from *Alternaria* and *Fusarium* fungi"

verfasst von / submitted by

Katharina Jarolim MSc

angestrebter akademischer Grad / in partial fulfilment of the requirements for the degree of

Doktorin der Naturwissenschaften (Dr. rer. nat.)

Wien, 2018 / Vienna 2018

Studienkennzahl lt. Studienblatt / degree programme code as it appears on the student record sheet:	A 796 605 419
Dissertationsgebiet lt. Studienblatt / field of study as it appears on the student record sheet:	Chemie
Betreut von / Supervisor:	Prof. Dr. rer. nat. Doris Marko

Table of contents

1 Introduction

According to conservative estimations, up to 3 million fungi exist worldwide, of which approximately 100 000 have been characterized (Russell et al. 2016). Molds are a number of fungal species that are predominately found on food (Viegas and Baum 2017). Under favorable conditions, molds produce secondary metabolites which are non-essential compounds of low molecular weight that play an indirect role in the growth of the fungus by enhancing the chance of survival in the natural biotope (Martín et al. 2014). Secondary metabolites from fungi have been the subject of scientific investigations for decades and some were identified as beneficial for humans, as for instance antibiotics from *Penicillium spp.* (Fleming 1929). On the other hand, pathogenic fungi produce secondary metabolites that might cause adverse health effects, so called mycotoxins. Among the different genera of toxigenic food-infesting fungi, *pergillus* and *Fusarium* are two examples of molds that have been investigated more thoroughly in the last decades (Patriarca and Fernández Pinto 2017). In contrast, the toxicological significance of fungi of the genus *Alternaria* has moved into scientific focus recently and the respective secondary metabolites are thus referred to as "emerging mycotoxins" (Miceli and Lee 2011).

In order to protect humans and animals from the detrimental effects to health associated with the consumption of food contaminated with mycotoxins, regulatory limits have been established for some of these compounds. *Alternaria* fungi produce a broad range of secondary metabolites and to date the toxicological data are not sufficient to establish regulatory limits for any secondary metabolite produced by *Alternaria spp.* Hence, further investigations on the toxicological relevance of these contaminants represent an important contribution to food safety, as noted by the European Food Safety Agency previously (EFSA 2011; EFSA 2016). The presented PhD thesis aimed to contribute to the elucidation of the toxicological profile of selected secondary metabolites from food-infesting fungi of the genus *Alternaria*, in comparison to selected *Fusarium* mycotoxins.

2 Objective

Alternaria spp. produce a broad spectrum of secondary metabolites from different chemical classes. One major group are the perylenequinone-derivatives, to which altertoxin I (ATX I) and II (ATX II) belong (Fig 1). The two molecules are structurally closely related, only differing at position C-7,8, where ATX II bears an epoxide and ATX I a hydroxyl moiety. This minor chemical difference affects the toxicological potency of the two altertoxins. The reactive epoxy group of ATX II has been associated with the more potent mutagenic and genotoxic characteristics of the compound, compared to ATX I (Schrader et al. 2006; Schwarz et al. 2012; Stack and Prival 1986). Recently it was reported that this structural difference also affects the reactivity of the two altertoxins towards thiol compounds (Fleck et al. 2014). It was observed that ATX II formed conjugates with the tripeptide glutathione (GSH), whereas ATX I did not undergo any reactions with the monothiols tested in this study. These results raised the question, whether ATX II affects a major detoxification route, the Nuclear factor (erythroid-derived 2)-like 2–antioxidant responsive element (Nrf2/ARE)-pathway. This important signaling pathway serves as a cellular defense against many xenobiotics and oxidative stress via the induction of phase II enzymes (Ma 2013). Molecules that act as inducers were described to react with thiol groups (Dinkova-Kostova et al. 2001). Thus, according to the results of Fleck et al. (2014), ATX II might represent a suitable candidate for a Nrf2-inducer. On the contrary, ATX I is expected not to affect this pathway, since it was not identified as thiol reactive by Fleck et al. (2014).

This question was investigated in the first publication of the PhD thesis, which aimed to assess the impact of ATX I and ATX II on the Nrf2/ARE-pathway in human colon adenocarcinoma cells. In order to evaluate this hypothesis, the effect of the two altertoxins on

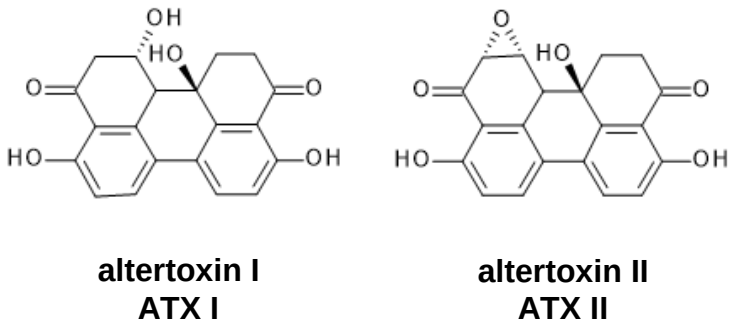

Figure 1 Chemical structures of the perylene quinones ATX I and II from *Alternaria alternata* fungi.

Nrf2 was investigated using immunochemical histochemistry and confocal microscopy, which allowed monitoring the translocation of the transcription factor Nrf2 from the cellular cytoplasm to the nucleus. Furthermore, additional endpoints along the Nrf2/ARE signaling cascade, following the ATX II-mediated translocation of Nrf2, were investigated. In this respect, the impact on the transcription of the Nrf2-dependent phase II gene γ-glutamate cysteine ligase (γ-GCL) was assessed with quantitative real-time polymerase chain reaction (rtPCR). γ-GCL is the rate-determining enzyme in the biosynthesis of GSH (Wild et al. 1999). The intracellular level of GSH was measured as additional indicator of a potential impact of ATX II on the Nrf2/ARE-pathway. Oxidative stress has been described as a major inducer of the Nrf2/ARE-pathway (Rushmore et al. 1991), therefore the level of oxidized GSSG and the intracellular formation of reactive oxygen species (ROS) by ATX II were evaluated as well in order to assess a potential impact on the cellular redox equilibrium.

The induction of phase II metabolism by a mycotoxin that was investigated in Publication 1 made a contribution to understanding the impact of secondary fungal mycotoxins on cellular metabolism and potential detoxification pathways. In this respect, phase II detoxification constitutes an important cellular mechanism to cope with a potent toxic contaminant like ATX II, a mycotoxin that was reported as genotoxic, mutagenic and cytotoxic *in vitro* (Fleck et al. 2014; Schwarz et al. 2012; Stack and Prival 1986). The impairment of topoisomerase II (topo II) by ATX II was described as a potential underlying mechanism (Tiessen et al. 2013). The enzyme is involved in regulating the topological state of DNA during processes like replication, transcription and DNA repair, thus a malfunction may result in detrimental effects to the cellular survival (Holm et al. 1989). Interestingly, interference with the activity of topo II is not restricted to ATX II, but has been reported for the *Alternaria* dibenzo-α-pyrones alternariol (AOH) and its monomethyl ether (AME) as well (Fehr et al. 2009; Tiessen et al. 2016; Tiessen et al. 2013).

Based on these observations, the aim of the second publication of the PhD project was to clarify if the impairment of topo II represents a toxicological mechanism of action that could be observed for further secondary metabolites produced by *Alternaria* fungi as well. For this purpose, eleven *Alternaria* metabolites were studied for their effect on the activity of human topo II α in the cell-free decatenation assay. Thereby the discrimination between active and inactive/ inhibited topo II is assessed via the electrophoretic mobility of the substrate kinetoplast DNA (Sahai and Kaplan 1986). To take into account the broad range of chemically diverse secondary metabolites produced by *Alternaria spp.*, test substances with a

spectrum of differing structures were chosen for the experiments. These included the perylenequinone derivatives ATX I, ATX II, alterperylenol (ALP) and stemphyltoxin III (STTX III), which share the same basic structure except for the double bond and an epoxide group in case of ATX II and STTX III (Fig 2A). ATX II was included for comparison, since the altertoxin has already been reported to inhibit topo II, as well as the dibenzo-α-pyrones AOH and AME (Fig 2B) (Fehr et al. 2009; Tiessen et al. 2016; Tiessen et al. 2013). Further tested *Alternaria* metabolites included the macrodiolide pyrenophorol (PYR), the anthraquinone macrosporin (MAC), the cyclic tetrapeptide tentoxin (TEN), the diphenol altenusin (ALS) and the tetramic acid derivative altersetin (ALN) (Fig 2C).

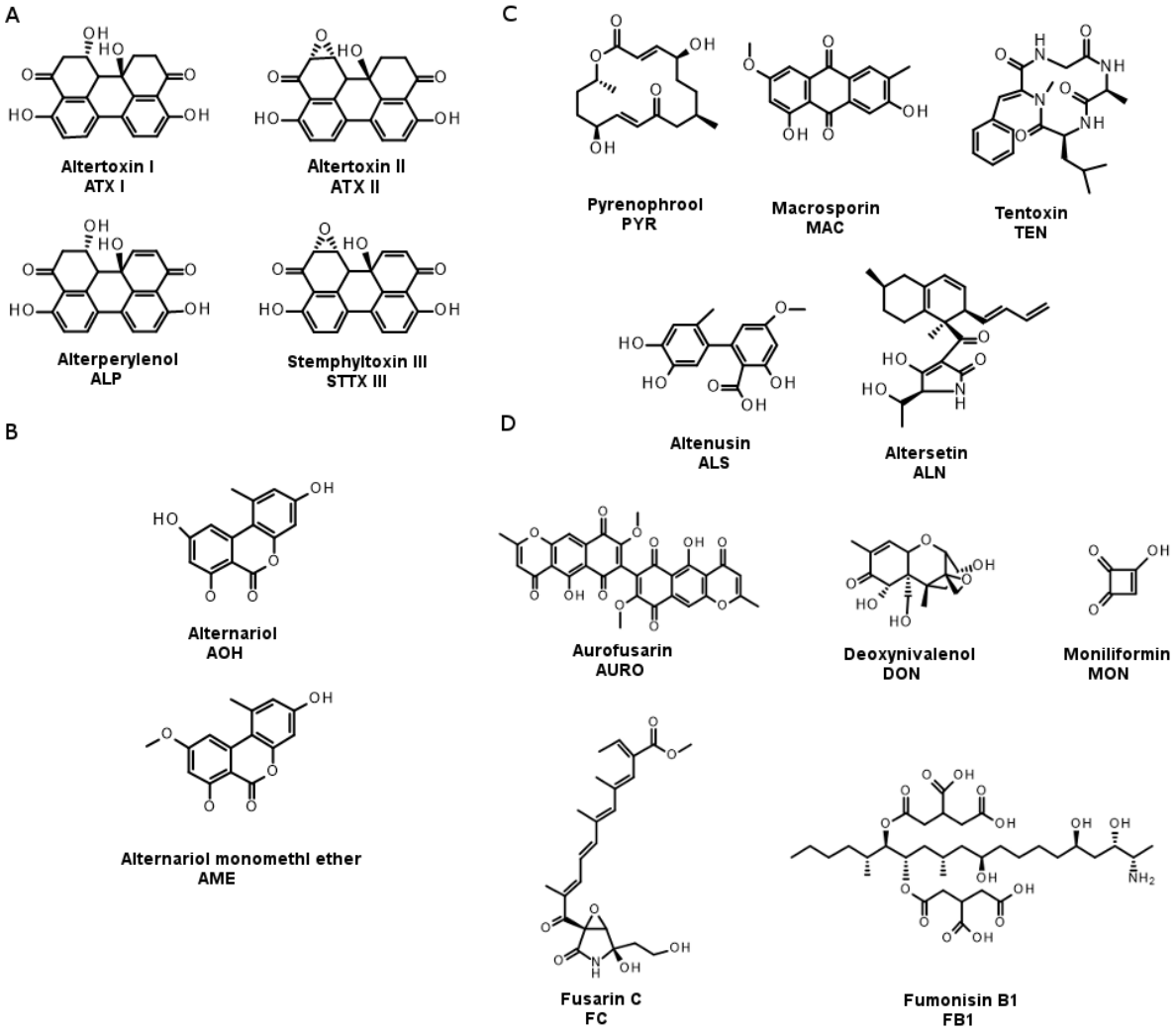

Figure 2 Chemical structures of the investigated secondary metabolites from *Alternaria* and *Fusarium* fungi: A) perylene quinones B) dibenzo-α-pyrones, C) diverse *Alternaria* secondary metabolites, and D) secondary metabolites from *Fusarium* species.

The observation that several secondary metabolites from *Alternaria spp.* affected the activity of topo II gave rise to the question, whether inhibition of the human enzyme by mycotoxins was limited to this fungal genus. For comparison, four mycotoxins produced by *Fusarium spp.* were included in the testing. The test substances from *Fusarium spp.* were selected to cover a broad spectrum of chemical diversity and included the naphthoquninone Aurofusarin (AURO), fumonisin B1 (FB1), the trichothecene deoxynivalenol (DON), the semiquadric acid moniliformin (MON) and the pyrrolidin derivative fusarin C (FC) (Fig 2D).

Apart from the question of genus-specifity, the impairment of human topo II by secondary metabolites from a pathogenic mold gave further rise to question why a fungus produces metabolites that affect a human enzyme. Thus the hypothesis was tested whether the observed impairment might be based on the structural homology between human and bacterial topo II (Dong and Berger 2007). Since bacteria and fungi are naturally competing for resources, the reduction of bacterial growth by the inhibition of a vital bacterial enzyme could serve as a defense mechanism of the mold that suppresses bacterial growth. Thus, a dual impairment of human topo II and gyrase may indicate that bacteria are the primary target of the secondary metabolites, but human topo II is affected due to the similar enzymatic structure. In order to examine this theory, the fourteen selected secondary metabolites from *Alternaria* and *Fusarium spp.* that were tested for their effect on human topo II, were assessed for their impact on bacterial topo II, gyrase from *E. coli*. This was done with a gel-based gyrase supercoiling assay, which enabled the assessment of gyrase activity by quantification of the different electrophoretic mobilities of relaxed and supercoiled DNA in an agarose gel (Gellert et al. 1976).

In the second publication, in total sixteen secondary metabolites from *Alternaria* and *Fusarium spp.* were investigated for their impact on human topo II in the cell-free decatenaton assay. Of these substances, one compound showed to be the most potent inhibitor of human topo II and the only active secondary metabolite from *Fusarium spp.*, the dimeric naphthoquinone AURO (Fig 2D). The toxicological relevance of this metabolite has been investigated scarcely, although the compound has frequently been found in high concentrations in contaminated food (Ezekiel et al. 2012; Matumba et al. 2015). Available literature on the toxicity of AURO *in vitro* was limited to the observation that the naphthoquinone was cytotoxic to colon cells, but the underlying mechanism was not known yet (Vejdovszky et al. 2016). Studies about quinone-derivatives have shown that this compound class affects topo II by stabilizing the topo II-DNA (cleavage) complex, a process

referred to as poisoning due to the associated onset of DNA-damage (Bandele and Osheroff 2008; Barthelmes et al. 2001; Esteves-Souza et al. 2007; Lindsey Jr et al. 2004). Based on these results and the observation that AURO potently inhibited the activity of topo II in the decatenation assay, the question arose, whether the *Fusarium* metabolite indeed acts as topo II poison and inducer of DNA-damage as well. This question was addressed in the third publication of the PhD project, where the stabilization of the cleavage complex by AURO in HT29 cells is evaluated with the in vivo complex of enzyme (ICE) assay. In order to examine whether a potential impairment of topo II by AURO was associated with genotoxicity, the DNA-damaging potential of the naphthoquinone was investigated in the comet assay. Poisoning of topo II by xenobiotics is associated with DNA double strand breaks (Liu et al. 1980). The formation of DNA double strand breaks after incubation with AURO was assessed with immunocyctochemical staining of γH2AX and p53 and subsequent detection through confocal microscopy in the colon carcinoma and non-transformed cell lines HT29 and HCEC-1CT.

Quinoid compounds have been reported to cause DNA damage not only via topo II-mediated DNA cleavage, but also through DNA intercalation (Pullman 1986). To investigate if this mechanism was also applicable to AURO, the intercalating potential of the metabolite was tested by evaluating the replacement of the intercalating dye ethidium bromide from calf thymus DNA by AURO, according to the method of Lepecq and Paoletti (1967). In order to assess if the impairment of topo II, that was observed in the cell-free decatenation assay, could be linked to cytotoxic effects in the colon cell line HT29 or in the non-transformed cell line HCEC-1CT, the impact of AURO on mitochondrial activity and the proliferation of these two cell lines was examined with the watersoluble tetrazolium salt-1 assay (WT-1) and the sulforhodamin B (SRB) assay. Impact on cell cycle distribution was examined by flow cytometry in the cell lines HT29 and HCEC-1CT.

One of the few studies about the toxicological relevance of AURO reported that in quail eggs and embryos the metabolite showed pro-oxidative effects (Dvorska et al. 2001; Dvorska et al. 2002). In general, the formation of ROS and induction of oxidative stress has been described as major toxic mechanism of naphthoquinoide compounds (O'Brien 1991). Therefore, the pro-oxidative potential of the compound was assessed in the study as well. In a first step thereof, formamidopyrimidine-DNA-glycosylase (fpg) was added to the comet assay, which allowed the detection of several types of DNA damage, as for instance oxidative damage, by conversion to additional strand breaks (Chetsanga et al. 1981). To further assess the pro-

oxidatve potential of AURO, the formation of ROS in HT29 cells by the metabolite was investigated with the DCF assay. The formation of ROS by naphthoquinones was previously associated with an elevated oxidation of cellular GSH, resulting in the depletion of GSH and a shift towards GSSG (Di Monte et al. 1984). In order to evaluate if this effect was observable for AURO as well, the impact of the secondary metabolite on the ratio of GSH and GSSG was assessed in the PhD study.

The generation of ROS by quinones is caused by a repeating cycle of electron transfer and associated redox reactions between the quinone and oxygen, so called redox cycling (Lown 1983). This effect was shown to be alleviated by NAD(P)H quinone dehydrogenase 1 (NQO1) (O'Brien 1991). Based on these data, we investigated whether the naphthoquinoide AURO induced the expression of NQO1 by quantification of the respective gene expression in HT29 cells, with q-PCR. The impact if AURO on the Arylhydrocarbon receptor (AhR) was investigated by assessment of cytochrome P450 1A1 (CYP1A1) in q-PCR and the ethoxyresorufin (EROD) assay (Lubet et al. 1985). Furthermore, a potential induction of the Nrf2/ARE-pathway was tested by measurement of the mRNA levels of γ-GCL, using q-PCR.

3 Overview of publications and manuscripts

Publication 1 (Jarolim *et al.*, 2016a)

status:	Published
title:	**Activation of the Nrf2‑ARE pathway by the *Alternaria alternata* mycotoxins altertoxin I and II**
authors:	Katharina Jarolim [a], Giorgia Del Favero [a], Gudrun Pahlke [a], Victoria Dostal [a], Kristin Zimmermann [b], Elke Heiss [b], Doris Ellmer [c], Timo D. Stark [c], Doris Marko [a]
affiliations of authors:	**a:** University of Vienna, Department of Food Chemistry and Toxicology, Waehringer Str. 38, A-1090 Vienna, Austria **b:** Department of Pharmacognosy, Faculty of Life Sciences, University of Vienna, Althanstraße 14, 1090 Vienna, Austria **c**: Chair of Food Chemistry and Molecular Sensory Science, TU München, Lise‑Meitner‑Strase 34, 85354 Freising, Germany
published in:	Archives of Toxicology, Volume 91, Issue 1, pages 203 – 216
year:	2016
accepted for publication:	13th May 2016
DOI	http://dx.doi.org/10.1007/s00204-016-1726-7
author´s contribution:	Katharina Jarolim performed the reporter gene assay, the WST-1 assay and the dichlorofluorescein assay. Giorgia Del Favero performed the microscopy experiments. Gudrun Pahlke performed the q-PCR measurement. Victoria Dostal performed the glutathione assay. Katharina Jarolim made the statistical evaluation of all experimental data and wrote the manuscript.

Publication 2 (Jarolim *et al.*, 2016 b)

status:	Published
title:	**Dual effectiveness of *Alternaria* but not *Fusarium* mycotoxins against human topoisomerase II and bacterial gyrase**
authors:	Katharina Jarolim [a], Giorgia Del Favero [a], Doris Ellmer [b], Timo D. Stark [b], Thomas Hofmann [b], Michael Sulyok[c], Hans-Ulrich Humpf [d], Doris Marko [a]
affiliations of authors:	**a:** University of Vienna, Department of Food Chemistry and Toxicology, Waehringer Str. 38, A-1090 Vienna, Austria **b:** Chair of Food Chemistry and Molecular Sensory Science, TU München, Lise-Meitner-Strase 34, 85354 Freising, Germany **c**: Department IFA-Tulln, University of Natural Resources and Life Sciences Vienna (BOKU), 3430 Tulln, Austria **d**: Institute of Food Chemistry, Westfälische Wilhelms-Universität Münster, 48149 Münster, Germany
published in:	Archives of Toxicology, epub ahead of publication
year:	2016
accepted for publication:	15th September 2016
DOI	http://dx.doi.org/ 10.1007/s00204-016-1855-z
author´s contribution:	Katharina Jarolim performed all the experiments in this study and did the statistical evaluation of the data. The concept and design of the study was designed by all co-authors together. The manuscript was written by Katharina Jarolim

Publication 3 (Jarolim *et al.*, submitted for publication)

status:	Published
title:	**The secondary *Fusarium* metabolite aurofusarin induces cytotoxicity, genotoxicity and oxidative stress in human colon cells**
authors:	Katharina Jarolim[a], Konstantin Wolters[a], Lydia Wölflingseder[a], Gudrun Pahlke[a], Julia Beisl[a], Hannes Puntscher[a], Dominik Braun[a], Michael Sulyok[b], Benedikt Warth[a], Doris Marko[a]
affiliations of authors:	**a:** University of Vienna, Department of Food Chemistry and Toxicology, Waehringer Str. 38, A-1090 Vienna, Austria **b:** University of Natural Resources and Life Sciences Vienna (BOKU), Department IFA-Tulln, 3430 Tulln, Austria
Published in:	Toxicology letters
Accepted for publication	14th December 2017
DOI	10.1016/j.toxlet.2017.12.008
author´s contribution:	Katharina Jarolim performed the topoisomerase assays, the intercalation and the EROD assay. Konstantin Wolters was introduced to the cytotoxicity, genotoxicity, DCF and glutathione assays by Katharina Jarolim and performed them. Statistical evaluation of the data was done by Katharina Jarolim and Konstantin Wolters. Hannes Puntscher, Dominik Barun and Benedikt Warth performed the analytical experiments as well as the evaluation of the data. The manuscript was written by Katharina Jarolim.

4 Theoretical background

4.1 Nrf2/ARE-pathway

In publication 1 of the PhD thesis, the impact of the altertoxins I and II on the Nrf2/ARE-pathway was assessed. This signaling pathway constitutes a crucial part of the cellular defense against oxidative and electrophilic stress. Induction of this pathway leads to the transcription of a broad spectrum of phase II enzymes.

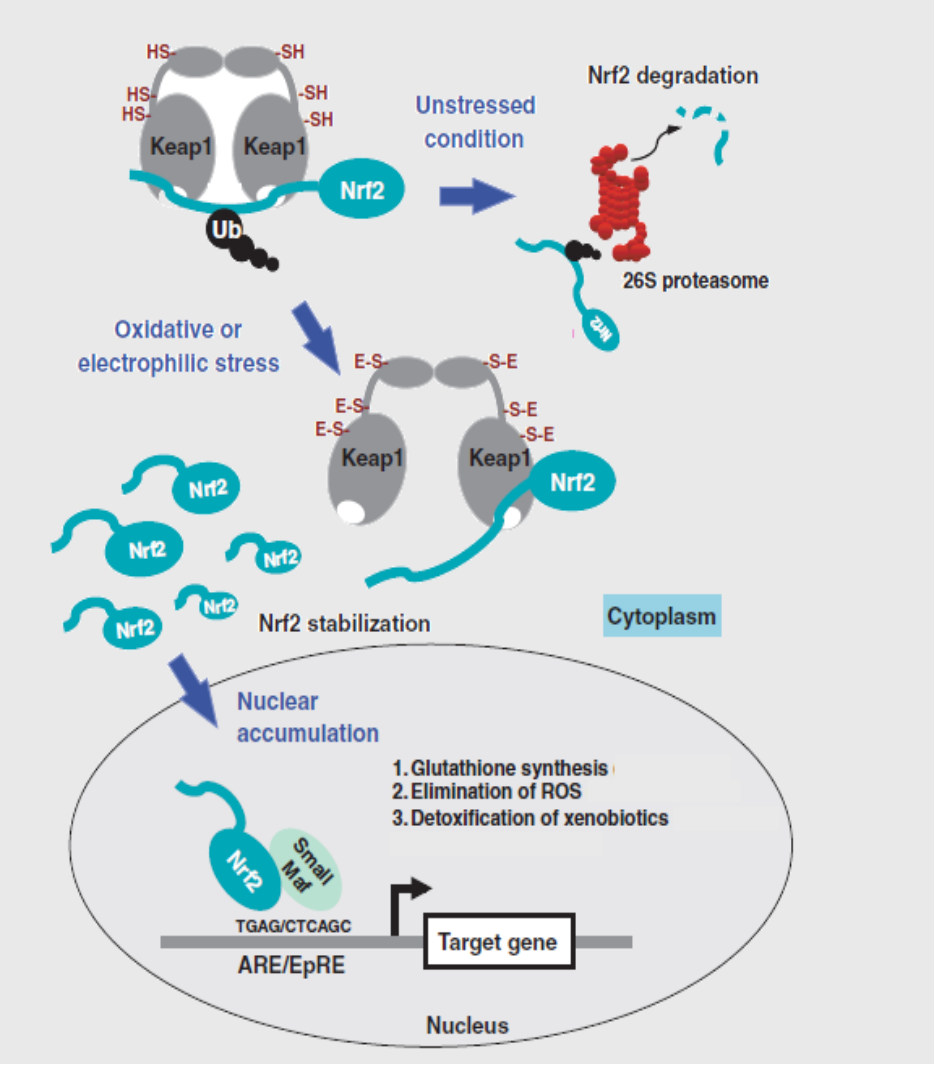

Figure 3 The Nrf2/ARE signaling pathway. Under unstressed conditions Nrf2 is bound to its adaptor protein Keap1 and gets polyubiquinated and subsequently degraded by the 26S proteasome. In case of oxidative or electrophilic stress the cysteine residues of Keap1 are modified, inducing a transformational change and dissociation of Nrf2, which is translocated from the cytoplasm to the nucleus. In the nucleus Nrf2 induces the induction of a spectrum of target genes upon binding to the ARE. Modified after Taguchi et al. (2011).

4.1.1 Introduction

Under homeostatic conditions the cap”n”collar transcription factor Nrf2 is bound to two monomers of the suppressor protein Kelch-like ECH-associated protein 1 (Keap1) in the cytoplasm (Fig 3) (Itoh et al. 1995; Itoh et al. 1999; Moi et al. 1994). Keap1 is anchored to the actin cytoskeleton and acts as a substrate adaptor of the ubiquitin ligase cullin 3. The cul3-Keap1 E3 ligase complex inhibits transcriptional activity of Nrf2 via ubiquination and proteosomal degradation (Cullinan et al. 2004; Kobayashi et al. 2004). Therefore, the amount of Nrf2 in the cytoplasm is regulated by the equilibrium between de novo synthesis and degradation by the ubiquitin-dependent 26S proteasome (Nguyen et al. 2003). Due to this rapid turnover, the half-life of cytoplasmic Nrf2 was estimated to be less than 20 minutes under redox-balanced conditions (Kobayashi et al. 2004). In case of oxidative or chemical stress, Nrf2 dissociates from the negative regulator Keap1 and is translocated to the nucleus. As potential mechanism behind the dissociation of the Nrf2-Keap1 complex, the modification of the thiol groups of the cystein-rich Keap1 by Nrf2-inducers has been discussed (Dinkova-Kostova et al. 2002; Zhang and Hannink 2003). In this respect, four cysteins of Keap1 were identified to be especially reactive towards Nrf2/ARE-pathway inducers (Dinkova-Kostova et al. 2002). Following translocation to the nucleus, Nrf2 heterodimerizes with a small Maf protein and induces the transcription of Nrf2-dependent genes after binding to the respective ARE in the regulatory region (Itoh et al. 1997; Rushmore et al. 1991). The Nrf2-dependently transcribed gene products are cytoprotective enzymes, such as NQO1, heme oxygenase 1 (HO-1), γ-GCL and glutathione S transferase. These enzymes catalyze reactions involved in the detoxification of ROS and protection against oxidative stress.

An example of a naturally occurring inducer of the Nrf2/ARE-pathway is the isothiocyanate sulforaphane from broccoli (McMahon et al. 2001; Zhang et al. 1992).

4.1.2 NAD(P)H quinone oxidoreductase 1 (NQO1)

The cytotoxic effects of 1,4-naphthoquinones have been attributed to the formation of ROS, an effect which is meliorated by NQO1 (O'Brien 1991). The flavoenzyme catalyzes the two-electron reduction of quinones to stable hydroquinones and therefore contributes to the detoxification of this reactive substance class (Ernster et al. 1960; Joseph et al. 2000; Radjendirane et al. 1998).

4.1.3 γ-Glutamylcysteine ligase (γ-GCL)

γ-GCL is the rate-limiting enzyme in the synthesis of the tripeptide γ-L-glutamyl-L-cysteinylglycine or GSH, a cellular antioxidant (Meister and Anderson 1983). GSH supports the cellular defense against oxidative and xenobiotic stress by acting as nucleophile and

reductant (Booth et al. 1961). In the latter case, GSH is oxidized to GSSG. The two forms constitute a redox pair and the corresponding GSSG/GSH ratio serves as indicator for the redox state of a cell (Schafer and Buettner 2001; Toborek and Hennig 1994).

4.2 DNA-topoisomerases

DNA-topoisomerases are vital enzymes that alter the topology of the genetic material by introducing transient DNA strand breaks and relieving torsional stress during cellular processes like replication and chromosome segregation (Champoux and Dulbecco 1972; DiNardo et al. 1984; Jazwinski and Edelman 1984).

4.2.1 Introduction

Topoisomerases are classified as type I or type II, according to their mechanism of action. While topoisomerase I cleaves a single DNA strand, the ATP-dependent topo II introduces transient double strand breaks (Champoux 2001). The subfamily of topoisomerase II A comprises the human topo II and bacterial homologue gyrase, which were examined in the PhD project and will be discussed in the next chapters (Baldi et al. 1980; Bergerat et al. 1997).

4.2.2 Human topo II

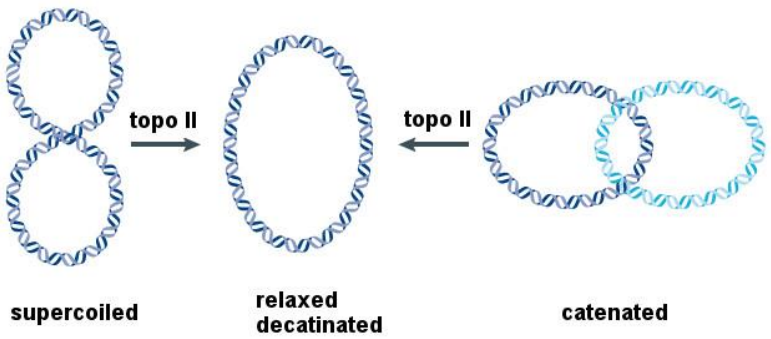

Figure 4 Catalyzed reactions by topo II. Relaxation of supercoiled DNA (left) and decatenation of catenated plasmids (right).

Human topo II can be divided into two isoforms, topo IIα and β, encoded by the genes *TOP2A* and *TOP2B*, respectively (Lang et al. 1998). Both catalyze the relaxation of negatively supercoiled DNA and decatenation, which describes the separation of interlinked duplex DNA circles (catenates) into separate decatenates, a process needed at the end of the replication to enable chromosome segregation (Fig 4) (Baldi et al. 1980). However, while topo IIα is also involved in chromosome condensation, the β isoform is essential for transcription in differentiated, non-dividing cells (Ju et al. 2006; Rattner 1996; Yang et al. 2000). The molecular mechanism behind the DNA cleavage of topo II involves the formation of a covalent 5'-phosphotyrosyl bond between the phosphate sugar backbone of the DNA strand and the active tyrosine of the enzyme (Fig 5). Since topo II is a homodimer, the nucleophilic attack is performed simultaneously by both active center tyrosines, which ultimately results in a double strand break (Champoux 1981; Depew et al. 1978). The DNA-bound topo II complex is referred to as cleavage complex. In the next step, a second DNA duplex is passed through the break, which is religated afterwards by binding of the terminal hydroxyl group to the phosphate (Fig 6).

Since topo II plays a critical role in maintaining the topological equilibrium of DNA,

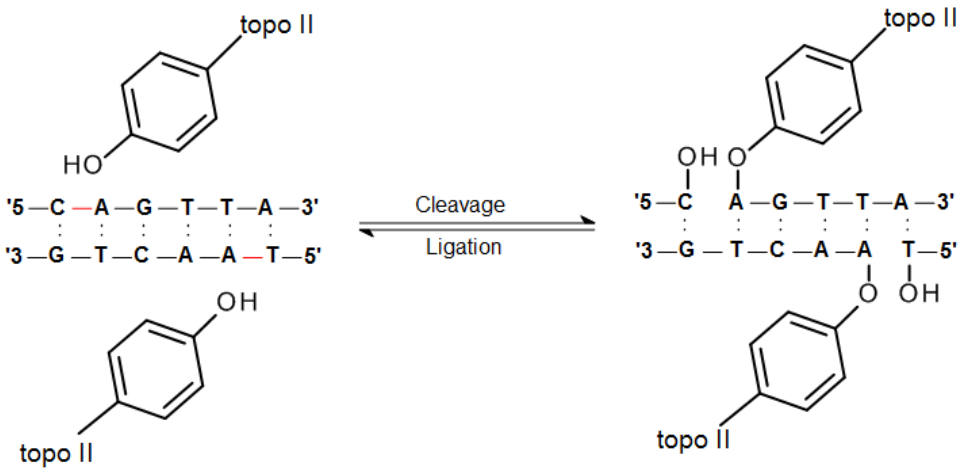

Figure 5 Molecular mechanism of topo II-induced cleavage of double stranded DNA. The homodimeric topo II attacks with the hydroxyl moieties of the tyrosine groups in the active centers. In the course of a nucleophilic attack, the hydroxyl binds to a phosphate group in the phosphate sugar backbone of the DNA double strand, forming a phosphoytyrosine bond, which leads to a transient double strand break. The reverse reaction of sealing the double strand break is called ligation. Modified after Deweese and Osheroff (2009).

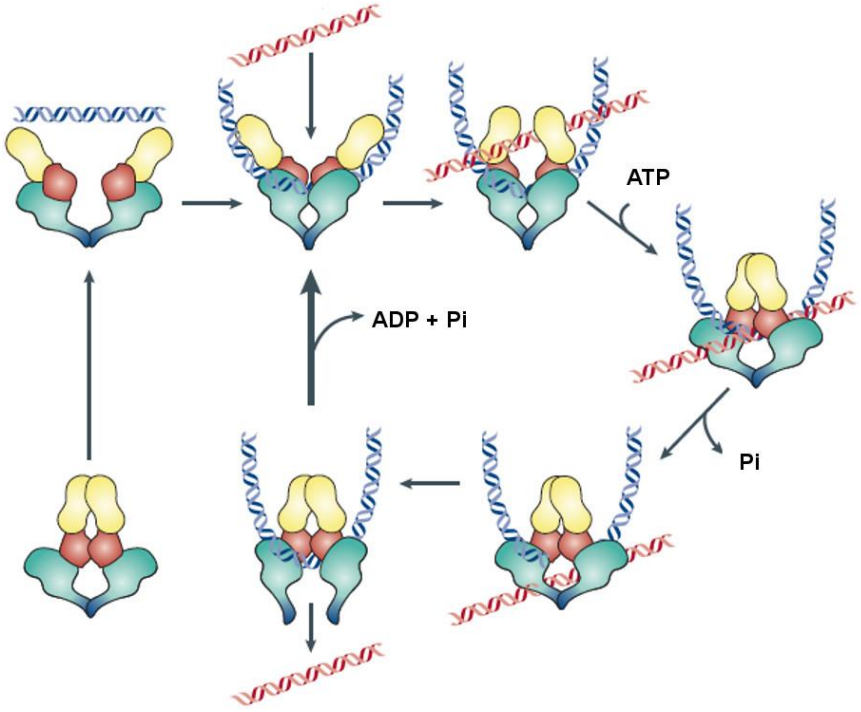

Figure 6 Catalytic cycle of topo II. The enzyme introduces a transient double strand break into a DNA strand, which requires ATP. Afterwards a second DNA double helix is transported through the break, followed by ligation and release of the first DNA strand. Modified after Nitiss (2009).

interference with the enzymatic function by xenobiotics has detrimental effects on the cell and may result in the activation of cell death pathways if repair is not sufficient (Kaufmann 1998). Since cell growth reduction is a desired characteristic of antineoplastic drugs, topo II-targeting molecules are applied as anticancer medications. Chemotherapeutics that function by stabilizing the topo II-DNA complex, so called poisoning, belong to such diverse chemical classes like, for instance, etoposide, a semisynthetic derivative of podophyllotoxin, the anthracenedione mitoxantrone or doxorubicin, which belongs to the group of anthracyclines (Fig 7A) (Greenspan et al. 1950; Hong et al. 2010; Tewey et al. 1984). Apart from these semisynthetic molecules several natural substances, which also differ greatly in their chemical structures, have been identified as topo II poisons, for instance lycobetaine, a phenantridine alkaloid from mmaryllidacae, epigallocatechin gallate, a catechin contained in green tea or the isoflavon genistein, a phytoestrogen found in soybeans (Fig 7B) (Bandele and Osheroff 2008; Barthelmes et al. 2001; Markovits et al. 1989). The mycotoxins AOH and AME from *Alternaria spp.* have also been identified as topo poisons (Fehr et al. 2009).

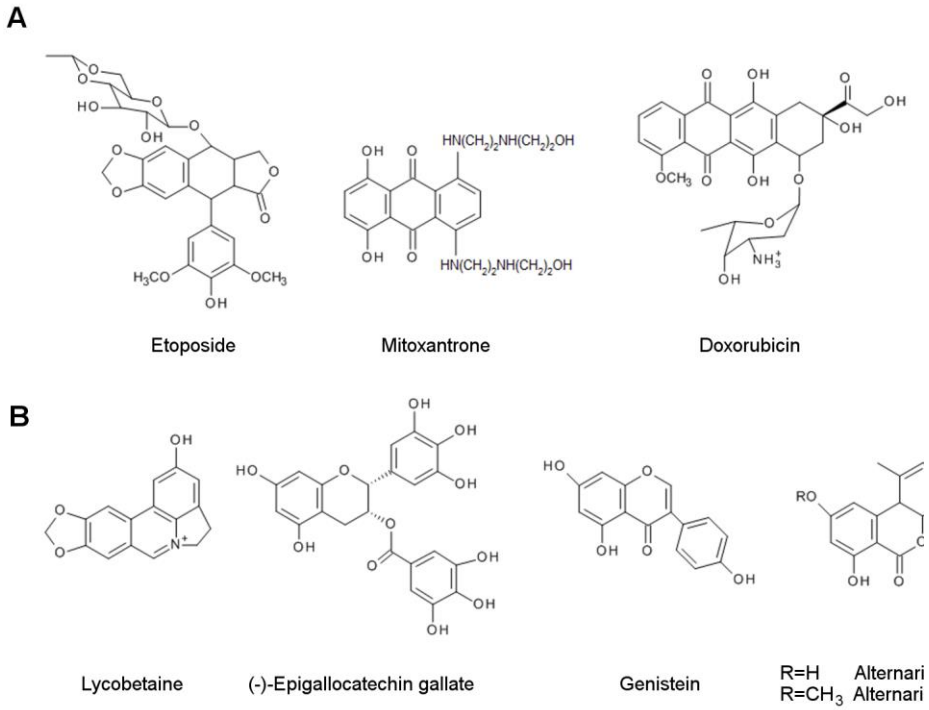

Figure 7 Examples of semi-synthetic and natural topo II poisons. A) The semi-synthetic topo II poisons used in cancer therapy, etoposide, mitoxantrone and doxorubicin and B) natural topo II poisons lycobetaine, epigallocatechine gallate and genistein

4.2.3 Bacterial topoisomerase II

Bacterial DNA predominately occurs either in a relaxed state or in the supercoiled form, which refers to an underwound duplex writhed about itself (Fig 5). Bacteria contain gyrase, a topoisomerase that is responsible for the interconversion of these topoisomers. On the contrast to homodimeric topo II, the bacterial enzyme is heterotetrameric, but also catalyzes the introduction of DNA double strand breaks, and transport of the second duplex through this break (Mizuuchi et al. 1980). Although human and bacterial topo II share a high degree of homology, only gyrase is able to introduce supercoils into relaxed closed duplex DNA (Kato et al. 1990). Comparably to human topo II, which can be affected by certain anticancer therapeutics, gyrase constitutes a target of antimicrobial drugs. Known antibiotics that function by impairing gyrase are grouped into two major classes, aminocoumarins and quinolones. A member of the aminocoumarin derivatives is novobiocin (Kucers 1997). Novobiocin was found to interfere with the ATP-binding of gyrase and is thus a catalytic inhibitor (Gellert et al. 1976; Sugino et al. 1978). On the contrary, nalidixic acid, the first of a broad range of quinolone antibiotics to be synthesized, was reported to act as a gyrase poison, stabilizing the cleavage complex (Shen and Pernet 1985).

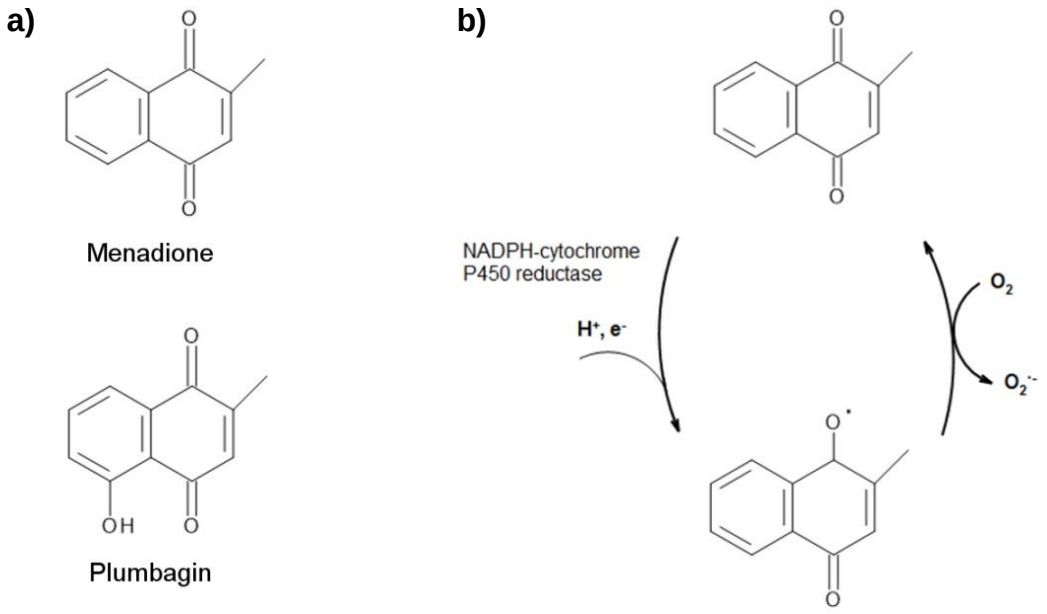

Figure 8 The 1,4-naphthoquinones menadione and plumbagin act as redox cycles. a) Structures of the two molecules and the b) redox cycle process. Illustrated with menadione, which undergoes a one-electron reduction to the semiquinone radical and is subsequently reoxidized back to the full diquinone by transfering the single electron to oxygen.

4.3 Naphthoquinones

Napthoquinones are naphthalene-derivatives that belong to the family of quinones. Quinone-dervatives are used as anticancer agents due to their cytotoxicity to human cancer cells, which is mainly caused by the intracellular formation of ROS (Goodman and Hochstein 1977). An example of a naphthoquinone -containing antineoplastic drug is doxorubicin, which, apart from poisoning topo II, was found to induce oxidative stress. A further naphthoquinone -derivate that was formerly used clinically is the vitamin K mimetic 2-methyl-1,4-naphthoquinone or Menadione (Fig 8a) (Suttie 2009). An example of a naturally occurring 1,4-naphtquinone is 5-hydroxy-2-methyl-1,4-naphthoquinone or plumbagin, a yellow dye of the *Plumbago* plant. Menadione and plumbagin were both described to act as redox cyclers, a mechanism that is frequently observed for quinonoid compounds (Miller et al. 1986; Srinivas et al. 2004).

4.3.1 Redox cycling

Redox cycling is a process which generates ROS, while a quinone is reduced and re-oxidized, thus undergoing a redox cycle. This cycle is initiated by a one-electron reduction, giving the respective semiquinone radical (Fig 8b). The semiquinone radical then transfers the single

electron to molecular oxygen (O'Brien 1991). In this process, toxic ROS, like the superoxide anion radical $O_2^{\bullet-}$, are generated, while the semiquinone is re-oxidized to the quinoid form and may restart the cycle (Apel and Hirt 2004). The initial one-electron reduction may take place non-enzymatically or be catalyzed, for instance, by NADPH cytochrome P450 reductase, with NADPH as radical donor (Bachur et al. 1979). Non-enzymatic one-electron reduction can take place via conjugation to a thiol group or oxidation of a thiol compound, such as GSH, which is an important reaction for naphthoquinones due to their high electronegativity (O'Brien 1991; Wilson et al. 1987). In this regard, menadione was described to increase the amount of oxidized disulfide GSSG at the expense of GSH in rat hepatocytes (Di Monte et al. 1984).

5 Results & Discussion

Fungi of the genus *Alternaria* produce a range of diverse secondary metabolites, some of which can be grouped according to the respective chemical structures (Barkai-Golan 2008). Of these, the perylene quinones have been associated with potent toxic effects *in vitro*, with being ATX II being the most toxic perylene quinone. ATX II has been identified as mutagenic and as the main genotoxic impact component in *Alternaria alternata* infested rice (Schwarz et al. 2012; Stack and Prival 1986). Unfortunately, the available data about the cellular detoxification mechanism of perylene quinones in general are limited. In this respect, ATX II was identified as activator of the Nrf2/ARE-pathway in publication 1 of the PhD project. The altertoxin was shown to potently induce the translocation of Nrf2 in cell culture. Interestingly, ATX I did not show any impact in the same concentration range, which indicated that the epoxide of ATX II played an important role in the activation of Nrf2, since ATX I is structurally equivalent to ATX II, except for the missing epoxy group (Fig 1). It was observed that incubation with ATX II led to a decrease of GSH in HT29 cells after 1h of incubation. However, this initial reduction was followed by am increase of the intracellular amount of the thiol after longer incubation periods of 3h and 24h, presumably as a response to the activation of Nrf2, which led to an increase of transcribed γ-GCL and ultimately an elevated synthesis of GSH.

Generally, induction of the Nrf2/ARE-pathway by a toxin is associated with beneficial effects to the cell due to the upregulated expression of cytoprotective enzymes like γ-GCL (Kensler et al. 2007). This effect was observed, for instance, for the mycotoxin aflatoxin B1 from *Aspergillus spp.*, which was reported to elicit weaker pro-carcinogenic effects in rat liver after the induction of the Nrf2/ARE-pathway (Yates et al. 2006). However, in case of ATX II an increased biosynthesis of GSH through Nrf2-activation and thus an elevated conjugation to GSH might not reduce the genotoxicity of the altertoxin. Fleck et al. (2014) reported that prior depletion of cellular GSH in mammalian cells did not lower the genotoxicity of ATX II and speculated that this was due to different kinetics of ATX II-mediated DNA-damage and GSH-conjugation (Fleck et al. 2014). Therefore, induction of the Nrf2/ARE-pathway by ATX II might not make a significant contribution to the detoxification of the mycotoxin.

Apart from the detoxifying properties associated with activation of the Nrf2/ARE system, the role of the pathway in cancer progression has moved into scientific focus lately. A dysfunctional regulation of the pathway, resulting in a abnormally active Nrf2, has been discussed as a promoting factor for tumor growth. In the recent years oncogenic mutations

and epigenetic changes in the genes *NRF2* and/or *KEAP1* have been detected in cancers from esophagus, lung, head, neck, skin and gallbladder (Kim et al. 2010; Shibata et al. 2008a; Shibata et al. 2008b; Singh et al. 2006; Wang et al. 2008). Although the underlying molecular mechanisms are not clarified yet, the observation that over-active Nrf2 is associated with cancer progression sheds a new light on the results of the PhD thesis, which indicated that a mycotoxin induces the Nrf2/ARE-pathway. This is especially intriguing, considering that ATX II naturally occurs in a mixture with other secondary metabolites from different fungi genera in contaminated food (Patriarca et al. 2007). So far, several mycotoxins have been described as mutagenic or carcinogenic and it might be speculated that the co-occurrence of these molecules with the Nrf2-activating mycotoxin ATX II might enhance the overall pro-carcinogenic potency of such a mixture.

The mentioned broad spectrum of chemically different secondary metabolites produced by molds is a challenge for the toxicological impact of the resulting mycotoxin mixture, to which the consumer is exposed, difficult, since each molecule elicits different toxic effects. However, some mycotoxins, though structurally diverse, share toxicological mechanisms of action, as for instance the inhibition of topo II that was reported for the *Alternaria* mycotoxins AOH, AME and ATX II (Fehr et al. 2009; Tiessen et al. 2016; Tiessen et al. 2013). Since impairment of human topo II was described several *Alternaria* toxins, the question was adressed whether this important enzyme represents a target to further structurally diverse *Alternaria* metabolites. Accordingly, the results indicated that nine of ten tested Alternaria metabolites reduced the activity of human topo II in the decatenation assay. The most potent inhibitors were the dibenzo-α-pyrones AOH and AME, followed by the perylene quinones, where the two epoxide-containing ATX II and STTX III had a stronger inhibitory potential than ATX I and ALP. The weaker inhibitors were ALN, ASN, MAC and PYR. The phytotoxin TEN was the only *Alternaria* metabolite that was not active against human topo II.

In search for an explanation, why a fungus produces secondary metabolites that target a human enzyme, we could demonstrate that this was based on the structural similarity between human and bacterial topo II, gyrase. In the experiments, six of the ten test substances from *Alternaria spp.* were identified as dual inhibitors against both human and bacterial topo II, the four perylene quinones and the two dibenzo-α-pyrones. These data substantiate the thesis that impairment of human topo II by the *Alternaria* metabolites is a side effect of the competition between bacteria and fungi. Interestingly, not all topo II-inhibitors were active against both human and bacterial topo II in the experiments. This was probably based on the choice of

bacterium species of gyrase in the supercoiling assay, which originated from *E. coli*. The metabolites that were not active against *E.coli* gyrase, but against human topo II, might target gyrases from other bacterium genera. This might be the subject to further investigations in the future.

For comparison, the impairment of human topo II by selected Fusarium metabolites was investigated. Of the five tested Fusarium toxins, only one was active against human topo II, but not gyrase, the dimeric naphthoquinone AURO (Fig 2D).

The naphthoquinone AURO proved to be the most potent inhibitor of human topo II of all tested *Alternaria* and *Fusarium* substances in the decatenation assay. The third publication of the PhD thesis focused on the investigation of the associated toxicological relevance of the secondary compound, which has not been studied previously. In this regard, the authors could demonstrate that AURO was cytotoxic to both the colon adencocarcinoma cell line HT29 and the non-tumorigenic colon epithelial cells HCEC-1CT. These effects were also demonstrated by means of cell cycle distribution, which showed that incubation with AURO led to an increase of HT29 cells in the S-phase and an arrest in G_2/M, while the cell cycle distribution of the extended primary cell line HCEC-1CT was not significantly affected by incubation with AURO. Both cell lines showed an increase of p53 after incubation with AURO, measured confocal microscopy.

In order to find the underlying mechanism of action, AURO, which was shown to potently inhibit human topo II in the cell-free decatenation assay, was tested for its impact on the stabilization of the cleavage complex in HT29 cells, using the ICE assay. The results showed that AURO did not potently poison human topo II in this test system. In order to investigate whether the stability of AURO might be limited in the used solvent DMSO, stability assessments were conducted with HPLC-MS/MS. The experiments showed that the compound was light- and temperature-sensitive and suggested that AURO was not stable under the cell culture conditions. The limited stability most probably also affected the experiments that were conducted under the cell culture experiments, as for instance the ICE assay.

The impact of AURO on DNA-integrity was assessed with the comet assay in HT29 cells, where the naphthoquinone induced mild DNA-damage. Since topo II poisoning is associated with an increase of DNA double strand breaks, the amount of γH2AX following incubation with AURO was assessed with confocal microscopy. The data suggested that incubation with AURO did not lead to an induction of DNA double strand breaks in either HT29 or HCEC-

1CT cells, thus a stabilization of the cleavage complex by AURO seemed unlikely.

Since AURO was shown to be cytotoxic and genotoxic, but presumably not a topo II poison, another mechanism of action was searched for. A common mechanism of action of naphthoquinones is DNA-intercalation, which could also be demonstrated for AURO, that was identified as weak intercalator in calf thymus DNA. Since AURO induced fpg-sensitive sites in the comet assay, it was also assumed that the molecule was pro-oxidative, which is another common mechanism of quinone-derivatives. Accordingly, AURO led to the intracellular formation of ROS in the DCF assay at a concentration of 5 µM in HT29 cells. Furthermore, the secondary metabolite caused a shift of the GSSG/GSH ratio in the cells, also indicative of pro-oxidative effects. The same held true for the AURO-induced upregulation of the gene transcription of CYP1A1 and an elevated activity of the enzyme in the EROD assay.

Evaluation of the chemical stability showed that AURO was light- and temperature-sensitive, but nevertheless induced pronounced toxicological effects. Despite the apparent disintegration of AURO in the cell culture conditions, incubation with the substance was shown to be toxic, as was assessed by several endpoints, to both the colon cell line HT29 and the primary cells HCEC-1CT. However, the metabolite did not lead to an upregulation of NQO1 in the q-PCR experiments, an enzyme that has been described to metabolize quinoide substances and was thus expected to be affected by the exposure to AURO (Iyanagi and Yamazaki 1969). Instead, AURO led to an upregulation of the transcription of CYP1A1, as well as higher activity of the phase I enzyme in the EROD assay, which has not been reported for naphthoqunoide substances previously. Since CYP1A1 transcription is triggered by the AhR (Fujii-Kuriyama et al. 1992), the results suggest that AURO acts as a ligand of this receptor.

6 Conclusion

Secondary metabolites from food-infesting fungi pose a potential health risk to consumers. The presented PhD thesis aimed to contribute to the toxicological understanding of so called "emerging mycotoxins", selected secondary metabolites from the emerging genus *Alternaria altenara,* as well as from fungi of the *Fusarium spp.*

The present PhD thesis could demonstrate that one of the most potent genotoxic impact compounds of *Alternaria alternata,* the perylene quinone ATX II, acts as an inducer of the Nrf2/ARE-pathway and increases the biosynthesis of GSH via this pathway. Though Nrf2-activation is usually associated with cellular detoxification, it was previously reported that the genotoxic potential of ATX II is not reduced by GSH-conjugation due to the presumably faster kinetics of DNA-damage than adduct formation. On the contrary, activation of Nrf2 has been shown to be associated with tumor progression; hence the induction of the Nrf2/ARE-pathway by the altertoxin might contribute to a potential overall pro-carcinogenicity of a mycotoxin mixture in which ATX II is contained, rather than lead to a reduction of the genotoxicity of the altertoxin. This is intriguing, since several potentially co-occuring mycotoxins have been reported as genotoxic as well. One example thereof is AOH, which belongs to the class of dibenzo-α-pyrones.

The mechanism of action for the DNA-damage caused by AOH has been identified as interference with human topoisomerase II. In this regard, the current PhD project could show that this enzyme constitutes a target to 90% of the tested *Alternaria* metabolites. Furthermore, it was demonstrated that the majority of the tested *Alternaria* metabolites target both the human and the bacterial topo II, gyrase. These results indicate that human topo II was probably affected by the mold due structural similarity of the bacterial and the human enzyme. Interestingly, this effect was largely limited to the *Alternaria* metabolites, since only one of the tested metabolites from *Fusarium spp.* that were also assessed in the PhD work was active against human topo II, the dimeric naphthoqunoide AURO. However, these results are not representative, since the amount of tested *Fusarium* toxins was comparably smaller than the investigated *Alternaria* substances.

The secondary *Fusarium* metabolite AURO was the most potent inhibitor of human topo II in the experiments, but studies about the toxicological relevance of the compound are scarce. This is especially intriguing, since AURO is routinely found in comparably high concentrations in diverse food and feed. Hence, the cytotoxic profile of this abundant secondary *Fusarium* metabolite was assessed in the PhD project. The experiments showed

that AURO was cytotoxic in HCEC-1CT and HT29 cells and mildly genotoxic in the cell line HT29, presumably caused by the pro-oxidative effects of the compound. Although very potent as reducer of the activity of human topo II in the decatenation assay, under cell-free conditions, AURO did not act as topo II poison. However, the naphthoquinone could be identified as mild DNA intercalator and an inducer of the phase II enzyme CYP1A1, which is indicative for AhR activation.

Taken together the results of the PhD thesis, which indicated that AURO caused a variety of toxicologically relevant effects in the tested in a colon cancer cell line HT29 and the non-transformed cell line HCEC-1CT, suggested that the secondary metabolite from *Fusarium spp.* might be considered to contribute a potential health risk to consumers of contaminated food. The toxicity of the substance should be validated in *in vivo* studies, to provide further evidence for consideration of AURO as a full mycotoxin.

7 References

Apel K, Hirt H (2004) REACTIVE OXYGEN SPECIES: Metabolism, Oxidative Stress, and Signal Transduction. Annual Review of Plant Biology 55(1):373-399 doi:doi:10.1146/annurev.arplant.55.031903.141701

Bachur NR, Gordon SL, Gee MV, Kon H (1979) NADPH cytochrome P-450 reductase activation of quinone anticancer agents to free radicals. P Natl Acad Sci USA 76(2):954-957

Baldi MI, Benedetti P, Mattoccia E, Tocchini-Valentini GP (1980) In vitro catenation and decatenation of DNA and a novel eucaryotic ATP-dependent topoisomerase. Cell 20(2):461-467 doi:10.1016/0092-8674(80)90632-7

Bandele OJ, Osheroff N (2008) (–)-Epigallocatechin Gallate, A Major Constituent of Green Tea, Poisons Human Type II Topoisomerases. Chemical Research in Toxicology 21(4):936-943 doi:10.1021/tx700434v

Barkai-Golan R (2008) Alternaria mycotoxins. In: Barkai-Golan R, Paster N (eds) Mycotoxins in fruits and vegetables. vol 1. Academic Press, Elsevier, p 185-203

Barthelmes HU, Niederberger E, Roth T, et al. (2001) Lycobetaine acts as a selective topoisomerase IIβ poison and inhibits the growth of human tumour cells. British Journal of Cancer 85(10):1585-1591 doi:10.1054/bjoc.2001.2142

Bergerat A, de Massy B, Gadelle D, Paul-Christophe V, et al. (1997) An atypical topoisomerase II from archaea with implications for meiotic recombination. Nature 386(6623):414-7 doi:http://dx.doi.org/10.1038/386414a0

Booth J, Boyland E, Sims P (1961) An enzyme from rat liver catalysing conjugations with glutathione. The Biochemical journal 79(3):516-24

Champoux JJ (1981) DNA is linked to the rat liver DNA nicking-closing enzyme by a phosphodiester bond to tyrosine. J Biol Chem 256(10):4805-4809

Champoux JJ (2001) DNA topoisomerases: structure, function, and mechanism. Annu Rev Biochem 70:369-413 doi:70/1/369 [pii]

10.1146/annurev.biochem.70.1.369

Champoux JJ, Dulbecco R (1972) An activity from mammalian cells that untwists superhelical DNA--a possible swivel for DNA replication (polyoma-ethidium bromide-mouse-embryo cells-dye binding assay). P Natl Acad Sci USA 69(1):143-146

Chen AY, Liu LF (1994) DNA topoisomerases: essential enzymes and lethal targets. Annu Rev Pharmacol Toxicol 34:191-218 doi:10.1146/annurev.pa.34.040194.001203

Chetsanga CJ, Lozon M, Makaroff C, Savage L (1981) Purification and characterization of Escherichia coli formamidopyrimidine-DNA glycosylase that excises damaged 7-methylguanine from deoxyribonucleic acid. Biochemistry 20(18):5201-5207

Cullinan SB, Gordan JD, Jin J, Harper JW, Diehl JA (2004) The Keap1-BTB protein is an adaptor that bridges Nrf2 to a Cul3-based E3 ligase: Oxidative stress sensing by a Cul3-Keap1 ligase. Molecular and cellular biology 24(19):8477-8486 doi:10.1128/MCB.24.19.8477-8486.2004

Depew RE, Liu LF, Wang JC (1978) Interaction between DNA and Escherichia coli protein omega. Formation of a complex between single-stranded DNA and omega protein. J Biol Chem 253(2):511-518

Di Monte D, Ross D, Bellomo G, Eklöw L, Orrenius S (1984) Alterations in intracellular thiol homeostasis during the metabolism of menadione by isolated rat hepatocytes. Archives of Biochemistry and Biophysics 235(2):334-342 doi:10.1016/0003-9861(84)90206-6

DiNardo S, Voelkel K, Sternglanz R (1984) DNA topoisomerase II mutant of Saccharomyces cerevisiae: Topoisomerase II is required for segregation of daughter molecules at the

termination of DNA replication. P Natl Acad Sci USA 81(9 I):2616-2620
Dinkova-Kostova AT, Holtzclaw WD, Cole RN, et al. (2002) Direct evidence that sulfhydryl groups of Keap1 are the sensors regulating induction of phase 2 enzymes that protect against carcinogens and oxidants. Proceedings of the National Academy of Sciences 99(18):11908-11913 doi:10.1073/pnas.172398899
Dinkova-Kostova AT, Massiah MA, Bozak RE, Hicks RJ, Talalay P (2001) Potency of Michael reaction acceptors as inducers of enzymes that protect against carcinogenesis depends on their reactivity with sulfhydryl groups. Proceedings of the National Academy of Sciences 98(6):3404-3409 doi:10.1073/pnas.051632198
Dong KC, Berger JM (2007) Structural basis for gate-DNA recognition and bending by type IIA topoisomerases. Nature 450(7173):1201-1205 doi:10.1038/nature06396
Dvorska JE, Surai PF, Speake BK, Sparks NHC (2001) Effect of the mycotoxin aurofusarin on the antioxidant composition and fatty acid profile of quail eggs. British Poultry Science 42(5):643-649 doi:10.1080/00071660120088470
Dvorska JE, Surai PF, Speake BK, Sparks NHC (2002) Antioxidant systems of the developing quail embryo are compromised by mycotoxin aurofusarin. Comparative Biochemistry and Physiology Part C: Toxicology & Pharmacology 131(2):197-205 doi:10.1016/s1532-0456(02)00006-6
EFSA (2011) Scientific Opinion on the risks for animal and public health related to the presence of Alternaria toxins in feed and food. EFSA Journal 9(10) doi:10.2903/j.efsa.2011.2407
EFSA (2016) Dietary exposure assessment to Alternaria toxins in the European population. EFSA Journal 14(12) doi:10.2903/j.efsa.2016.4654
Ernster L, Ljunggren M, Danielson L (1960) Purification and some properties of a highly dicumarol-sensitive liver diaphorase. Biochemical and Biophysical Research Communications 2(2):88-92 doi:http://dx.doi.org/10.1016/0006-291X(60)90193-5
Esteves-Souza A, Figueiredo DV, Esteves A, et al. (2007) Cytotoxic and DNA-topoisomerase effects of lapachol amine derivatives and interactions with DNA. Brazilian Journal of Medical and Biological Research 40(10):1399-1402 doi:10.1590/s0100-879x2006005000159
Ezekiel CN, Bandyopadhyay R, Sulyok M, Warth B, Krska R (2012) Fungal and bacterial metabolites in commercial poultry feed from Nigeria. Food Additives and Contaminants - Part A Chemistry, Analysis, Control, Exposure and Risk Assessment 29(8):1288-1299 doi:10.1080/19440049.2012.688878
Fehr M, Pahlke G, Fritz J, et al. (2009) Alternariol acts as a topoisomerase poison, preferentially affecting the IIα isoform. Molecular Nutrition & Food Research 53(4):441-451 doi:10.1002/mnfr.200700379
Fleck SC, Pfeiffer E, Podlech J, Metzler M (2014) Epoxide Reduction to an Alcohol: A Novel Metabolic Pathway for Perylene Quinone-TypeAlternariaMycotoxins in Mammalian Cells. Chemical Research in Toxicology 27(2):247-253 doi:10.1021/tx400366w
Fleming A (1929) On the Antibacterial Action of Cultures of a Penicillium, with Special Reference to their Use in the Isolation of B. influenzæ. British journal of experimental pathology 10(3):226-236
Fujii-Kuriyama Y, Imataka H, Sogawa K, Yasumoto K, Kikuchi Y (1992) Regulation of CYP1A1 expression. The FASEB Journal 6(2):706-710
Gellert M, Mizuuchi K, O'Dea MH, Nash HA (1976) DNA gyrase: an enzyme that introduces superhelical turns into DNA. Proc Natl Acad Sci U S A 73(11):3872-6
Goodman J, Hochstein P (1977) Generation of free radicals and lipid peroxidation by redox cycling of adriamycin and daunomycin. Biochemical and Biophysical Research Communications 77(2):797-803 doi:http://dx.doi.org/10.1016/S0006-291X(77)80048-X

Greenspan EM, Leiter J, Shear MJ (1950) Effect of alpha-peltatin, beta-peltatin, podophyllotoxin on lymphomas and other transplanted tumors. J Natl Cancer Inst 10(6):1295-1333

Holm C, Stearns T, Botstein D (1989) DNA topoisomerase II must act at mitosis to prevent nondisjunction and chromosome breakage. Molecular and cellular biology 9(1):159-168

Hong WK, Holland JF, Frei E (2010) Holland Frei cancer medicine

Itoh K, Chiba T, Takahashi S, et al. (1997) An Nrf2/small Maf heterodimer mediates the induction of phase II detoxifying enzyme genes through antioxidant response elements. Biochem Biophys Res Commun 236(2):313-22 doi:S0006291X97969436 [pii]

Itoh K, Igarashi K, Hayashi N, Nishizawa M, Yamamoto M (1995) Cloning and characterization of a novel erythroid cell-derived CNC family transcription factor heterodimerizing with the small Maf family proteins. Molecular and cellular biology 15(8):4184-4193

Itoh K, Wakabayashi N, Katoh Y, et al. (1999) Keap1 represses nuclear activation of antioxidant responsive elements by Nrf2 through binding to the amino-terminal Neh2 domain. Genes & Development 13(1):76-86 doi:10.1101/gad.13.1.76

Iyanagi T, Yamazaki I (1969) One-electron-transfer reactions in biochemical systems III. One-electron reduction of quinones by microsomal flavin enzymes. Biochimica et Biophysica Acta (BBA) - Bioenergetics 172(3):370-381 doi:http://dx.doi.org/10.1016/0005-2728(69)90133-9

Jarolim K, Wolters K, Woelflingseder L, et al. (2018) The secondary Fusarium metabolite aurofusarin induces oxidative stress, cytotoxicity and genotoxicity in human colon cells. Toxicol Lett 284:170-183 doi:10.1016/j.toxlet.2017.12.008

Jazwinski SM, Edelman GM (1984) Evidence for participation of a multiprotein complex in yeast DNA replication in vitro. J Biol Chem 259(11):6852-6857

Joseph P, Long Ii DJ, Klein-Szanto AJP, Jaiswal AK (2000) Role of NAD(P)H:quinone oxidoreductase 1 (DT diaphorase) in protection against quinone toxicity. Biochemical Pharmacology 60(2):207-214 doi:10.1016/S0006-2952(00)00321-X

Ju BG, Lunyak VV, Perissi V, et al. (2006) A topoisomerase IIβ-mediated dsDNA break required for regulated transcription. Science 312(5781):1798-1802 doi:10.1126/science.1127196

Kato Ji, Nishimura Y, Imamura R, Niki H, Hiraga S, Suzuki H (1990) New topoisomerase essential for chromosome segregation in E. coli. Cell 63(2):393-404 doi:10.1016/0092-8674(90)90172-b

Kaufmann SH (1998) Cell death induced by topoisomerase-targeted drugs: more questions than answers. Biochimica et Biophysica Acta (BBA) - Gene Structure and Expression 1400(1–3):195-211 doi:http://dx.doi.org/10.1016/S0167-4781(98)00136-5

Kensler TW, Wakabayashi N, Biswal S (2007) Cell survival responses to environmental stresses via the Keap1-Nrf2-ARE pathway Annu Rev Pharmacol. vol 47, p 89-116

Kim YR, Oh JE, Kim MS, et al. (2010) Oncogenic NRF2 mutations in squamous cell carcinomas of oesophagus and skin. Journal of Pathology 220(4):446-451 doi:10.1002/path.2653

Kobayashi A, Kang MI, Okawa H, et al. (2004) Oxidative stress sensor Keap1 functions as an adaptor for Cul3-based E3 ligase to regulate for proteasomal degradation of Nrf2. Molecular and cellular biology 24(16):7130-7139 doi:Doi 10.1128/Mcb.24.16.7130-7139.2004

Kucers A (1997) The use of antibiotics : a clinical review of antibacterial, antifungal, and antiviral drugs, 5th edn. Butterworth-Heinemann, Oxford ; Boston

Lang AJ, Mirski SEL, Cummings HJ, Yu Q, Gerlach JH, Cole SPC (1998) Structural

organization of the human TOP2A and TOP2B genes. Gene 221(2):255-266 doi:10.1016/s0378-1119(98)00468-5
Lepecq JB, Paoletti C (1967) A fluorescent complex between ethidium bromide and nucleic acids. J Mol Biol 27(1):87-106 doi:10.1016/0022-2836(67)90353-1
Lindsey Jr RH, Bromberg KD, Felix CA, Osheroff N (2004) 1,4-Benzoquinone is a topoisomerase II poison. Biochemistry 43(23):7563-7574 doi:10.1021/bi049756r
Liu LF, Liu C-C, Alberts BM (1980) Type II DNA topoisomerases: Enzymes that can unknot a topologically knotted DNA molecule via a reversible double-strand break. Cell 19(3):697-707 doi:http://dx.doi.org/10.1016/S0092-8674(80)80046-8
Lown JW (1983) The mechanism of action of quinone antibiotics. Molecular and Cellular Biochemistry 55(1):17-40 doi:10.1007/BF00229240
Lubet RA, Mayer RT, Cameron JW, et al. (1985) Dealkylation of pentoxyresorufin: A rapid and sensitive assay for measuring induction of cytochrome(s) P-450 by phenobarbital and other xenobiotics in the rat. Archives of Biochemistry and Biophysics 238(1):43-48 doi:10.1016/0003-9861(85)90138-9
Ma Q (2013) Role of Nrf2 in Oxidative Stress and Toxicity. Annu Rev Pharmacol 53(1):401-426 doi:10.1146/annurev-pharmtox-011112-140320
Markovits J, Linassier C, Fosse P, et al. (1989) Inhibitory effects of the tyrosine kinase inhibitor genistein on mammalian DNA topoisomerase II. Cancer Research 49(18):5111-5117
Martín JF, García-Estrada C, Zeilinger S (2014) Biosynthesis and molecular genetics of fungal secondary metabolites. Springer, New York
Matumba L, Sulyok M, Monjerezi M, Biswick T, Krska R (2015) Fungal metabolites diversity in maize and associated human dietary exposures relate to micro-climatic patterns in Malawi. World Mycotoxin Journal 8(3):269-282 doi:10.3920/wmj2014.1773
McMahon M, Itoh K, Yamamoto M, et al. (2001) The cap 'n' collar basic leucine zipper transcription factor Nrf2 (NF-E2 p45-related factor 2) controls both constitutive and inducible expression of intestinal detoxification and glutathione biosynthetic enzymes. Cancer Research 61(8):3299-3307
Meister A, Anderson ME (1983) Glutathione. Annu Rev Biochem 52:711-60 doi:10.1146/annurev.bi.52.070183.003431
Miceli MH, Lee SA (2011) Emerging moulds: epidemiological trends and antifungal resistance. Mycoses 54(6):e666-e678 doi:10.1111/j.1439-0507.2011.02032.x
Miller MG, Rodgers A, Cohen GM (1986) Mechanisms of toxicity of naphthoquinones to isolated hepatocytes. Biochemical Pharmacology 35(7):1177-1184 doi:http://dx.doi.org/10.1016/0006-2952(86)90157-7
Mizuuchi K, Fisher LM, O'Dea MH, Gellert M (1980) DNA gyrase action involves the introduction of transient double-strand breaks into DNA. P Natl Acad Sci USA 77(4 I):1847-1851
Moi P, Chan K, Asunis I, Cao A, Kan YW (1994) Isolation of Nf-E2-Related Factor-2 (Nrf2), a Nf-E2-Like Basic Leucine-Zipper Transcriptional Activator That Binds to the Tandem Nf-E2/Ap1 Repeat of the Beta-Globin Locus-Control Region. P Natl Acad Sci USA 91(21):9926-9930 doi:DOI 10.1073/pnas.91.21.9926
Nguyen T, Sherratt PJ, Huang HC, Yang CS, Pickett CB (2003) Increased protein stability as a mechanism that enhances Nrf2-mediated transcriptional activation of the antioxidant response element. Degradation of Nrf2 by the 26 S proteasome. J Biol Chem 278(7):4536-41 doi:10.1074/jbc.M207293200
O'Brien PJ (1991) Molecular mechanisms of quinone cytotoxicity. Chemico-Biological Interactions 80(1):1-41 doi:http://dx.doi.org/10.1016/0009-2797(91)90029-7
Patriarca A, Azcarate MP, Terminiello L, Fernández Pinto V (2007) Mycotoxin production by

Alternaria strains isolated from Argentinean wheat. International Journal of Food Microbiology 119(3):219-222 doi:10.1016/j.ijfoodmicro.2007.07.055
Patriarca A, Fernández Pinto V (2017) Prevalence of mycotoxins in foods and decontamination. Current Opinion in Food Science 14:50-60 doi:http://dx.doi.org/10.1016/j.cofs.2017.01.011
Pullman B (1986) A few considerations on quinones as antitumor agents. International Journal of Quantum Chemistry 30(13 S):95-105 doi:10.1002/qua.560300811
Radjendirane V, Joseph P, Lee YH, et al. (1998) Disruption of the DT diaphorase (NQO1) gene in mice leads to increased menadione toxicity. J Biol Chem 273(13):7382-7389 doi:10.1074/jbc.273.13.7382
Rattner JB (1996) Topoisomerase II alpha is associated with the mammalian centromere in a cell cycle- and species-specific manner and is required for proper centromere/kinetochore structure. The Journal of Cell Biology 134(5):1097-1107 doi:10.1083/jcb.134.5.1097
Rushmore TH, Morton MR, Pickett CB (1991) The Antioxidant Responsive Element - Activation by Oxidative Stress and Identification of the DNA Consensus Sequence Required for Functional-Activity. J Biol Chem 266(18):11632-11639
Russell R, Paterson RRM, Lima N (2016) Molecular biology of food and water borne mycotoxigenic and mycotic fungi. CRC Press,Taylor & Francis Group, Boca Raton
Sahai BM, Kaplan JG (1986) A quantitative decatenation assay for type II topoisomerases. Analytical Biochemistry 156(2):364-379 doi:10.1016/0003-2697(86)90267-8
Schafer FQ, Buettner GR (2001) Redox environment of the cell as viewed through the redox state of the glutathione disulfide/glutathione couple. Free Radical Biology and Medicine 30(11):1191-1212 doi:10.1016/s0891-5849(01)00480-4
Schwarz C, Tiessen C, Kreutzer M, Stark T, Hofmann T, Marko D (2012) Characterization of a genotoxic impact compound in Alternaria alternata infested rice as Altertoxin II. Arch Toxicol 86(12):1911-25 doi:10.1007/s00204-012-0958-4
Shen LL, Pernet AG (1985) Mechanism of inhibition of DNA gyrase by analogues of nalidixic acid: the target of the drugs is DNA. Proc Natl Acad Sci U S A 82(2):307-11
Shibata T, Kokubu A, Gotoh M, et al. (2008a) Genetic Alteration of Keap1 Confers Constitutive Nrf2 Activation and Resistance to Chemotherapy in Gallbladder Cancer. Gastroenterology 135(4):1358-1368.e4 doi:10.1053/j.gastro.2008.06.082
Shibata T, Ohta T, Tong KI, et al. (2008b) Cancer related mutations in NRF2 impair its recognition by Keap1-Cul3 E3 ligase and promote malignancy. Proceedings of the National Academy of Sciences 105(36):13568-13573 doi:10.1073/pnas.0806268105
Singh A, Misra V, Thimmulappa RK, et al. (2006) Dysfunctional KEAP1–NRF2 Interaction in Non-Small-Cell Lung Cancer. PLoS Medicine 3(10):e420 doi:10.1371/journal.pmed.0030420
Srinivas P, Gopinath G, Banerji A, Dinakar A, Srinivas G (2004) Plumbagin induces reactive oxygen species, which mediate apoptosis in human cervical cancer cells. Molecular Carcinogenesis 40(4):201-211 doi:10.1002/mc.20031
Stack ME, Prival MJ (1986) Mutagenicity of the Alternaria metabolites altertoxins I, II, and III. Appl Environ Microb 52(4):718-22
Sugino A, Higgins NP, Brown PO, Peebles CL, Cozzarelli NR (1978) Energy coupling in DNA gyrase and the mechanism of action of novobiocin. Proc Natl Acad Sci U S A 75(10):4838-42
Suttie JW (2009) Vitamin K in health and disease. CRC Press, Boca Raton
Taguchi K, Motohashi H, Yamamoto M (2011) Molecular mechanisms of the Keap1-Nrf2 pathway in stress response and cancer evolution. Genes to Cells 16(2):123-140 doi:10.1111/j.1365-2443.2010.01473.x
Tewey KM, Rowe TC, Yang L, Halligan BD, Liu LF (1984) Adriamycin-induced DNA

damage mediated by mammalian DNA topoisomerase II. Science 226(4673):466-468
Tiessen C, Ellmer D, Mikula H, et al. (2016) Impact of phase I metabolism on uptake, oxidative stress and genotoxicity of the emerging mycotoxin alternariol and its monomethyl ether in esophageal cells. Archives of Toxicology:1-14 doi:10.1007/s00204-016-1801-0
Tiessen C, Gehrke H, Kropat C, et al. (2013) Role of topoisomerase inhibition and DNA repair mechanisms in the genotoxicity of alternariol and altertoxin-II. World Mycotoxin Journal 6(3):233-244 doi:10.3920/wmj2013.1592
Toborek M, Hennig B (1994) Fatty acid-mediated effects on the glutathione redox cycle in cultured endothelial cells. American Journal of Clinical Nutrition 59(1):60-65
Vejdovszky K, Warth B, Sulyok M, Marko D (2016) Non-synergistic cytotoxic effects of Fusarium and Alternaria toxin combinations in Caco-2 cells. Toxicology Letters 241:1-8 doi:10.1016/j.toxlet.2015.10.024
Viegas J, Baum M (2017) Fungi and molds, First edition. edn. Rosen Central, New York
Wang R, An J, Ji F, Jiao H, Sun H, Zhou D (2008) Hypermethylation of the Keap1 gene in human lung cancer cell lines and lung cancer tissues. Biochemical and Biophysical Research Communications 373(1):151-154 doi:10.1016/j.bbrc.2008.06.004
Wild AC, Moinova HR, Mulcahy RT (1999) Regulation of gamma-glutamylcysteine synthetase subunit gene expression by the transcription factor Nrf2. J Biol Chem 274(47):33627-36
Wilson I, Wardman P, Lin T-S, Sartorelli AC (1987) Reactivity of thiols towards derivatives of 2- and 6-methyl-1,4-naphthoquinone bioreductive alkylating agents. Chemico-Biological Interactions 61(3):229-240 doi:http://dx.doi.org/10.1016/0009-2797(87)90003-2
Yang X, Li W, Prescott ED, Burden SJ, Wang JC (2000) DNA Topoisomerase IIβ and Neural Development. Science 287(5450):131
Yates MS, Kwak M-K, Egner PA, et al. (2006) Potent Protection against Aflatoxin-Induced Tumorigenesis through Induction of Nrf2-Regulated Pathways by the Triterpenoid 1-[2-Cyano-3-,12-Dioxooleana-1,9(11)-Dien-28-Oyl]Imidazole. Cancer Research 66(4):2488
Zhang DD, Hannink M (2003) Distinct cysteine residues in Keap1 are required for Keap1-dependent ubiquitination of Nrf2 and for stabilization of Nrf2 by chemopreventive agents and oxidative stress. Molecular and cellular biology 23(22):8137-51
Zhang Y, Talalay P, Cho CG, Posner GH (1992) A major inducer of anticarcinogenic protective enzymes from broccoli: Isolation and elucidation of structure. P Natl Acad Sci USA 89(6):2399-2403

8 List of abbreviations

ALS	Altensuin
AOH	Alternariol
AME	Alternariol mono metylether
ALP	Alterperylenol
ALN	Altersetin
ATX I/ II	Altertoxin I/ II
AURO	Aurofusarin

CHO	Chinese hamster ovary
CYP1A1	Cytochrome P450
DON	Deoxynivalenol
DNA	Deoxyribonucleic acid
EROD	Ethoxyresorufin-O-deethylase
FB1	Fumonisin B1
FC	Fusarin C
FPG	Formamidopyrmidine-DNA-glycosylase
γ-GCL	γ-glutamate cysteine ligase
GSH	Glutathion
HO-1	Heme oxygenase-1
Keap1	Kelch-like ECH-associated protein 1
ICE	*In vivo* complex of enzyme assay
MAC	Macrosporin
MON	Moniliformin
NAD(P)H	nicotinamide adenine dinucleotide (phosphate)
NQO1	NAD(P)H quinone dehydrogenase 1
Nrf2/ARE	Nuclear factor(erythroid-derived 2)-like 2–antioxidant responsive element
PYR	Pyrenophorol
q-PCR	Quantitative real-time polymerase chain reaction
ROS	reactive oxygen species
SRB	Sulforhodamine B
STTX III	Stemphyltoxin III
TEN	Tentoxin
Topo II	DNA-topoisomerase II
WST-1	Wotersulable tetrazolium salt

9 List of figures

Attachment: Publication 1

Arch Toxicol
DOI 10.1007/s00204-016-1726-7

MOLECULAR TOXICOLOGY

Activation of the Nrf2-ARE pathway by the *Alternaria alternata* mycotoxins altertoxin I and II

Katharina Jarolim[1] · Giorgia Del Favero[1] · Gudrun Pahlke[1] · Victoria Dostal[1] · Kristin Zimmermann[2] · Elke Heiss[2] · Doris Ellmer[3] · Timo D. Stark[3] · Thomas Hofmann[3] · Doris Marko[1]

Received: 20 August 2015 / Accepted: 27 April 2016

Abstract The mycotoxins altertoxin I and II (ATX I and II) are secondary metabolites produced by *Alternaria alternata* fungi and may occur as food and feed contaminants, especially after long storage periods. Although the toxic potential of altertoxins has been previously investigated, little is known about the pathways that play a role in their intracellular metabolism. In order to identify potential targets of ATX I and ATX II, the two toxins were tested for interaction with the nuclear factor erythroid-derived 2-like 2/antioxidant response element (Nrf2/ARE) pathway in mammalian cells. This pathway can be activated by various stressors resulting in the expression of enzymes important for metabolism and detoxification. In the present study, only ATX II triggered a concentration-dependent increase in Nrf2-ARE-dependent luciferase expression. Consistently, confocal microscopy revealed an ATX II-induced increase in Nrf2 signal in HT29 intestinal cells. In agreement with these data, ATX II induced the transcription of γ-glutamate cysteine ligase, the key enzyme in catalyzing GSH synthesis of the cells and which is regulated by Nrf2. Further investigations demonstrated that ATX II induced a concentration-dependent depletion of the cellular GSH levels after short incubation time (3 h) and an increase after longer incubation time (24 h). In conclusion, it was demonstrated that ATX II can interact at several levels of the Nrf2-ARE pathway in mammalian cells and that ATX I does not share the same mechanism of action.

Keywords *Alternaria alternata* · Altertoxin I (ATX I) · Altertoxin II (ATX II) · Nrf2 · Glutathione · Confocal/SIM microscopy

Introduction

The filamentous fungi of the genus *Alternaria* comprise more than 100 species; among these, *Alternaria alternata* is the most common one (Rotem 1994). *A. alternata* is a saprophytic field fungus which is abundant in the atmosphere, in soil and in seeds and has been reported to grow on a wide variety of food and feed items, including fruits like strawberries, blueberries, grapes and citrus fruits (Tournas and Katsoudas 2005), as well as tomatoes (Andersen and Frisvad 2004) and wheat (Müller and Korn 2013). *A. alternata* is known to produce a large number of secondary metabolites and many of these are generally recognized as mycotoxins. For this reason, *A. alternata* might represent a potential health risk for humans and animals, but, in spite of that, no regulatory limits have been introduced so far to define its presence in commercialized food and feed. In this respect, the European Food Safety Authority (EFSA) pointed out the need for further investigations to improve the knowledge about the toxicological profile of mycotoxins formed by *A. alternata* (EFSA 2011). These toxins can be grouped according to their chemical structure,

Electronic supplementary material The online version of this article (doi:10.1007/s00204-016-1726-7) contains supplementary material, which is available to authorized users.

✉ Doris Marko
doris.marko@univie.ac.at

[1] Department of Food Chemistry and Toxicology, Faculty of Chemistry, University of Vienna, Währinger Straße 38, 1090 Vienna, Austria

[2] Department of Pharmacognosy, Faculty of Life Sciences, University of Vienna, Althanstraße 14, 1090 Vienna, Austria

[3] Chair of Food Chemistry and Molecular Sensory Science, TU München, Lise-Meitner-Straße 34, 85354 Freising, Germany

Published online: 13 May 2016

such as the terpenoids, pyranones or quinones (Lou et al. 2013). Among these, the class of the perylene quinone-type mycotoxins comprises ATX I and ATX II (Fig. 1). These two compounds seem to have high potential to pose a major threat for human health due to their mutagenic and genotoxic properties (Schrader et al. 2001; Schwarz et al. 2012b; Stack and Prival 1986). Structurally, the two molecules differ only by means of the functional group in positions 7 and 8, where ATX I carries a hydroxyl group and ATX II an epoxide moiety. Even though minor, this structural difference seems to account for the diverse toxicological characteristics of the two compounds. In fact, both molecules have been described as mutagenic in *S. typhimurium* strains TA98, TA100, TA1537, TA102 and TA104, yet ATX I was reported to be less potent than ATX II (Schrader et al. 2001; Stack and Prival 1986). Similarly, this trend was confirmed for several other properties, such as: mutagenicity in V79 cells (Fleck et al. 2012; Schrader et al. 2006), ability to induce DNA strand breaks and formamidopyrimidine DNA glycosylase-sensitive sites in human cancer cell lines (Fleck et al. 2014; Schwarz et al. 2012b) or cytotoxicity in mammalian cell cultures (Boutin et al. 1989; Tiessen et al. 2013b). Although the toxicological impact of altertoxins has been investigated previously, studies dealing with the metabolic pathways of perylene quinone-type mycotoxins have been limited to the observations that ATX II can be reduced to ATX I by the colorectal adenocarcinoma cell line Caco2 and that ATX II can form adducts with GSH in a cell-free system (Fleck et al. 2014). Thus, many questions remain to be addressed in particular regarding the potential of ATX I and ATX II to induce and/or interact with phase II metabolic pathways. In this context, as a first step, we investigated whether altertoxins interact with the Nrf2-ARE signaling pathway. Nrf2-ARE pathway is a major route triggering the expression of a broad spectrum of phase II enzymes (Itoh et al. 1997). The transcription factor Nrf2 recognizes and binds to the 5′-flanking region of the ARE in the promoter region of target genes which encode for antioxidant proteins and enzymes (Rushmore et al. 1991). Under basal conditions, Nrf2 is negatively regulated by Kelch-like ECH-associated protein 1 (Keap1), which mediates the degradation of the transcription factor via its function as adaptor for the CRL3 class of cullin-RING-ligase E3 (Kobayashi et al. 2004). In oxidative stress conditions, Nrf2 is released from its repressor Keap1 and translocates from the cytosol to the nuclear compartment where it acts as a transcription factor (canonical activation pathway; Nguyen et al. 2009). As a result, Nrf2 plays a vital role in launching cellular response against stressors and inducing important defense systems like glutathione (GSH). Taking this as starting point, the aim of the present study was to investigate whether altertoxins ATX I and II could have an impact on several key steps of the Nrf2-ARE signaling pathway. The effect of the two mycotoxins was investigated for their potential to induce oxidative stress and cytotoxicity, for their effect on the NRF2/Keap1 homeostasis and, ultimately, on the direct effects on the γGCL and cellular GSH.

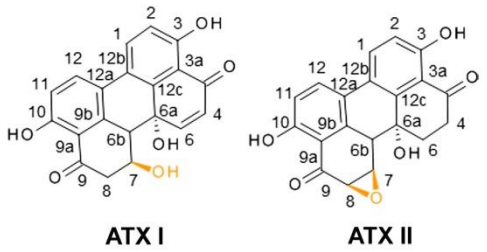

Fig. 1 Toxins structures. Chemical structures of the two perylene quinone-type *Alternaria* mycotoxins ATX I and ATX II

Results

Identification of ATX I and II from *A. alternata* infested rice

MS measurements of ATX I identified the toxin with an *m/z* in the (−) HRESIMS of 351.0868 $[M–H]^-$ (calculated for $C_{20}H_{15}O_6$, −0.3 ppm). The NMR data (^1H NMR and ^{13}C NMR) are in line with Hradil et al. (1989) and Stack et al. (1986) (Online Resource). ATX II was identified with an m/z of 349.0731 $[M–H]^-$ in the (−) qTOF-MS (calculated for $C_{20}H_{14}O_6$, −3,9 ppm). ATX I and ATX II were isolated from the inoculated rice cultures with purities of >96 and >97 %, respectively.

Effect of ATXs on the Nrf2-ARE pathway activation in the luciferase reporter gene assay

In order to investigate whether incubation with ATX I and ATX II can lead to Nrf2-activation, an ARE-dependent luciferase reporter gene assay was performed. In this system, binding of Nrf2 to the ARE promoter region leads to the expression of luciferase, whose activity can be measured by chemiluminescence. After 20 h of incubation, ATX I did not elicit Nrf2 activation in the reporter cells in any of the tested concentrations (Fig. 2). On the contrary, when cells were incubated with ATX II, the Nrf2 activity increased in a concentration-related manner. Incubation of the cells with 5 μM ATX II induced luciferase activity, indicative for activation of the Nrf2-ARE pathway, significantly (323 ± 35 % increase) in comparison with the solvent control (0.1 % EtOH). The luciferase signal measured in cells incubated with 5 μM ATX

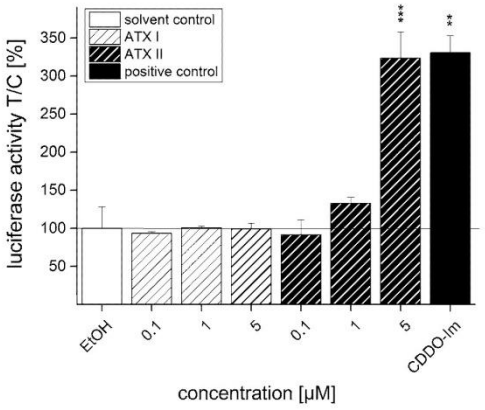

Fig. 2 Induction of ARE-dependent luciferase expression after 20 h of incubation with ATX I and ATX II in CHO cells. ARE-driven luciferase activity after 20 h of incubation with ATX I (*striped bars*, *white background*), ATX II (*striped bars*, *black background*) and 0.1 µM CDDO-Im (*positive control*, *black bar*) in serum-containing medium. Luciferase activity data are expressed as mean values ±SEM of at least three independent experiments, calculated to respective GFP luminescence, normalized to solvent control (EtOH). Significance levels refer to a comparison to solvent control (**$p < 0.01$, ***$p < 0.001$; $n = 3$ independent experiments performed in triplicate)

II reached values comparable to those of the positive control CDDO-Im (331 ± 23 %; Fig. 2). The measurement of the fluorescence of eGFP, which was used as reference for cellular density, showed a slight, though not significant, decrease in cells incubated with 5 µM ATX II (79 ± 19 %) in comparison with the of solvent control (Supplementary material, Fig S1).

Effect of ATXs on Nrf2 and Keap1 immunolocalization in HT29 cells

In order to further study the mechanisms sustaining the effects of ATXs on the Nrf2 pathway, additional immunofluorescence experiments were performed in HT29 cells. This model was previously used as representative of intestinal cells and it is particularly relevant for the study of food contaminants (Schwarz et al. 2012a; Tiessen et al. 2013b). In control conditions, the fluorescent signal of Nrf2 (red) appears to be similar to that of Keap1 (green; Fig. 3a). In cells incubated with CDDO-Im (1 h; positive controls), a tendency toward the increase in Nrf2 was visible, (Fig. 3b, f). After incubation with ATX I for 1 h (0.1, 1 and 5 µM; Fig. 3c–e), the signal of Nrf2 and Keap1 in HT29 cells was comparable to that of controls. In fact, quantification of the mean intensity of the fluorescence elicited by the antibodies recognizing Nrf2 and Keap1 presented minimal fluctuations. For instance, in cells incubated with 5 µM ATX I, the Nrf2 signal increase was only of 111 ± 4 % and for Keap1 of 117 ± 15 % (Fig. 3f). In contrast, 1 h of incubation with ATX II led to a concentration-dependent increase in Nrf2 fluorescence (Fig. 4c–f), which was significant at the highest tested concentration (202 ± 37 % increase for 5 µM ATX II; Fig. 4f). Evaluation of Keap1 signal in cells incubated with ATX II revealed only a tendency toward the increase, but no significant changes (163 ± 37 % increase for 5 µM ATX II; Fig. 4f). In order to better characterize the localization of Nrf2 after incubation with 5 µM ATX II, structured illumination microscopy (SIM) was also used. In fact, with this technique, it was possible to better visualize the presence of Nrf2 (red; Fig. 4g, h) inside the nuclear "shell" provided by lamin B (gray; Fig. 4g, h).

After 3 h of incubation, CDDO-Im did not seem to have an effect on Nrf2 and Keap1 in comparison with controls (Fig. 5a–c) and, in line with previous results, ATX I did not elicit any effect on the two proteins (Fig. 5a, d). Incubation of HT29 cells with ATX II for 3 h (Fig. 5a, e) triggered an increase in Nrf2 and Keap1 fluorescence, which was confirmed by image analysis with significantly higher signal intensities for both Nrf2 and Keap1 (5 µM ATX II; Fig. 5a, e).

Moreover, in order to attempt to characterize the effect of our experiments on the relative distribution of Nrf2 and Keap1 in the nuclear and in the cytosolic compartments, an additional evaluation of the images was also performed. The mean intensity of fluorescence signals of Nrf2 and Keap1 in the selected areas (nuclei and cytosol) was used to express the corresponding Nrf2/Keap1 ratio signals. After 1 h of incubation with 5 µM ATX II, the cytosolic Nrf2/Keap1 ratio was significantly elevated in comparison with the solvent control EtOH, whereas no significant difference in the nuclear compartment was observed (Fig. 6a). After a longer incubation time (3 h), a significant increase in the cytosolic Nrf2/Keap1 ratio was observed for the positive control CDDO-Im. In addition, both CDDO-Im and 5 µM ATX II triggered in HT29 cells a significant increase in the Nrf2/Keap1 ratio in the nuclear compartment (Fig. 6b).

Impact of ATXs on transcription levels of γGCL and Nrf2 in HT29 cells

In order to verify whether in HT29 cells the effect of ATX II on Nrf2 activation and translocation could be further linked to an altered expression of ARE-dependent genes, the relative transcription of Nrf2 and γGCL was measured by qPCR. The gene transcription relative to the solvent control (0.1 % EtOH) of γGCL and Nrf2 was investigated after 3 h (Fig. 7a) and 24 h (Fig. 7b) of incubation with ATX II (0.1, 1 and 5 µM). 0.5 µM CDDO-Im and tBHQ (200 µM) were included as positive controls. After 3 h, a significant increase in γGCL

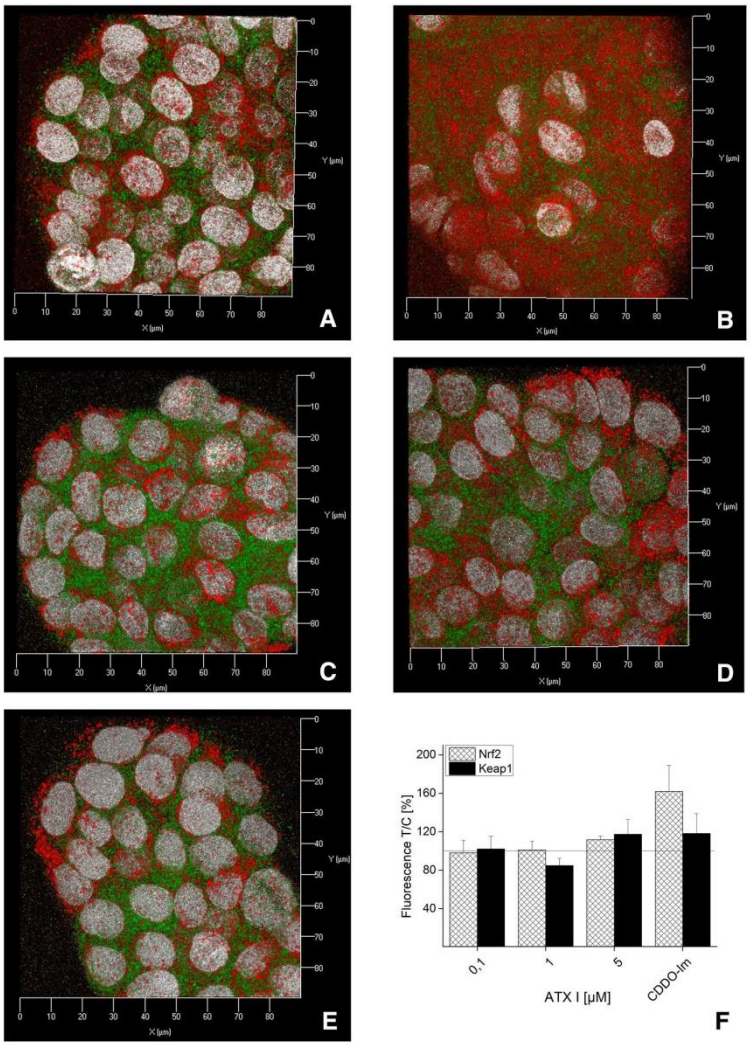

Fig. 3 Immunofluorescence localization of Nrf2 and Keap1 after 1 h of incubation with ATX I in HT29 cells. Representative images of immunolocalization of Nrf2 (*red*), Keap-1 (*green*) and lamin B (*gray*) after incubation with EtOH (solvent control, **a**), 0.5 µM CDDO-Im (**b**), ATX I 0.1 µM (**c**), 1 µM (**d**), 5 µM (**e**). *Axes x* 0–90 µm, *y* 0–90 µm. **f** Quantification of Nrf2 (*patterned bars*) and Keap1 (*black bars*) signals in cells incubated with ATX I (0.1, 1 and 5 µM) and CDDO-Im (0.5 µM). Mean values of fluorescence in the optical fields are expressed as percentage of solvent controls ±SEM ($n = 3$–6 independent experiments) (color figure online)

mRNA was measured in cells incubated with CDDO-Im and tBHQ. Consistently, 1 and 5 µM ATX II also increased the relative gene transcription of γGCL of 2.7 ± 0.3 and 3.6 ± 0.5-folds, respectively. In cells incubated with ATX II, Nrf2 mRNA also showed a concentration-dependent tendency toward increase, even if not significant (Fig. 7a). After 24 h of incubation with ATX II, the trend was reversed, showing a significant decrease in both γGCL and Nrf2 at 5 µM (Fig. 7b).

Impact of ATXs on mitochondrial activity in HT29 cells in the WST-1 assay

After 24 h of incubation with ATX II, the relative gene transcription of both Nrf2 and γGCL was decreased; since this behavior could potentially indicate cytotoxicity, the impact of the toxin on cellular viability was investigated. The cytotoxic potential of ATX II was determined with the colorimetric water-soluble tetrazolium salt-1 assay

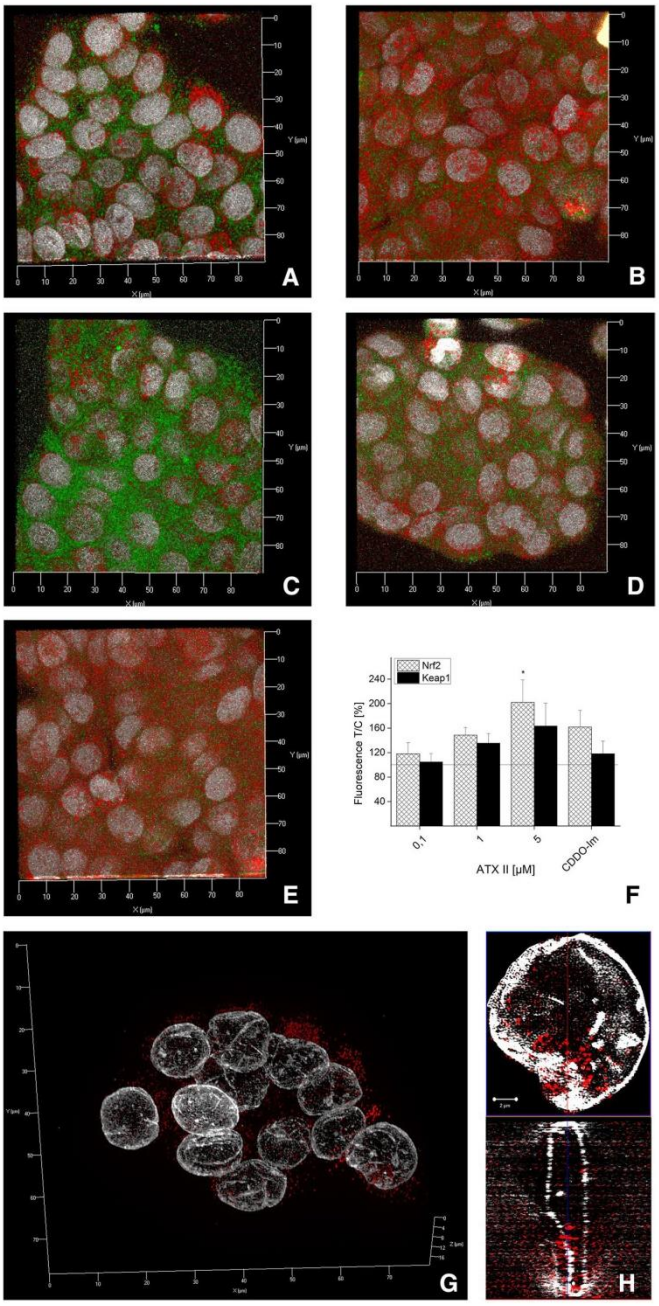

Fig. 4 Immunofluorescence localization of Nrf2 and Keap1 after 1 h of incubation with ATX II in HT29 cells. Representative images of immunolocalization of Nrf2 (*red*), Keap-1 (*green*) and lamin B (*gray*) after incubation with EtOH (solvent control, **a**), 0.5 µM CDDO-Im (**b**), 0.1 µM ATX II (**c**), 1 µM ATX II (**d**), 5 µM ATX II (**e**). *Axes x* 0–90 µm, *y* 0–90 µm. **f** Quantification of Nrf2 (*patterned bars*) and Keap1 (*black bars*) signals in cells incubated with ATX II (0.1, 1 and 5 µM) and CDDO-Im (0.5 µM). Mean values of fluorescence in the optical fields are expressed as percentage of solvent controls ±SEM ($n = 3$–6 independent experiments; significance levels indicated as *asterisk* refer the comparison with 0.1 µM ATX II, $^*p < 0.05$). SIM 3D image of Nrf2 (*red*) and lamin B (*gray*) after incubation with 5 µM ATX II (**g**; *axes x* 0–80 µm, *y* 0–80 µm, *z* 0–20 µm) and representative cross section of one of the nuclei (**h**; *scale bar* 2 µm) (color figure online)

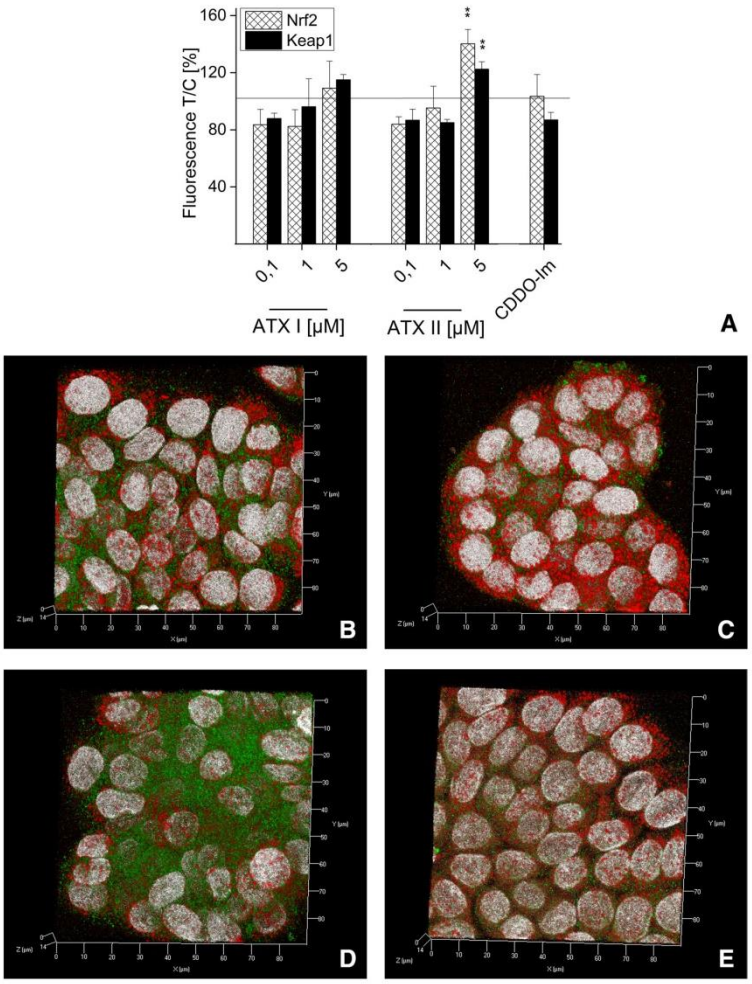

Fig. 5 Immunofluorescence localization of Nrf2 and Keap1 after 3 h of incubation with ATX I and ATX II in HT29 cells. Quantification of Nrf2 (*patterned bars*) and Keap1 signals (*black bars*) in cells incubated with ATX I, ATX II and CDDO-Im (**a**). Representative images of immunolocalization of Nrf2 (*red*), Keap1 (*green*) and lamin B (*gray*) after incubation with 0.1 % EtOH (solvent control, **b**), 0.5 µM CDDO-Im (**c**) 5 µM ATX I (**d**), 5 µM ATX II (**e**). *Axes x* 0–90 µm, *y* 0–90 µm, *z* 0–14 µm. Mean values of fluorescence in the optical fields are expressed as percentage of solvent controls ±SEM ($n = 3$ independent experiments). Significance levels are calculated comparing signal intensity values normalized to solvent control (0.1 % EtOH) and *asterisk* refers to the comparison with 0.1 µM ATX II (**$p < 0.01$) (color figure online)

(WST-1) and ATX I was added for comparison. After 24 h incubation, ATX I did not reduce significantly the mitochondrial activity of the intestinal cells in any of the used concentrations (0.1, 1 and 5 µM), although a slight decrease for the two higher concentrations was observable (88 ± 6 % in case of 1 µM ATX I and 89 ± 6 % for 5 µM ATX I; Fig. 8). In contrast, ATX II showed a clear cytotoxic effect at the highest concentration tested (5 µM), reducing the mitochondrial activity significantly to 31 ± 8 %. From these data, an EC_{50}-value for ATX II was calculated of 2.26 µM.

Influence of ATX II on cellular tGSH and GSSG levels in HT29 cells

In order to verify whether the effects observed on the gene transcription levels of γGCL induced by ATX II were mirrored in the actual levels of GSH, the concentrations of both tGSH (composed of GSH and GSSG) and GSSG were measured in HT29 cells after 1, 3 and 24 h of incubation with the mycotoxin (0.1, 1 and 5 µM). A concentration-dependent decrease in the tGSH was detected after 1 h of incubation with ATX II, and at 5 µM the tGSH levels were

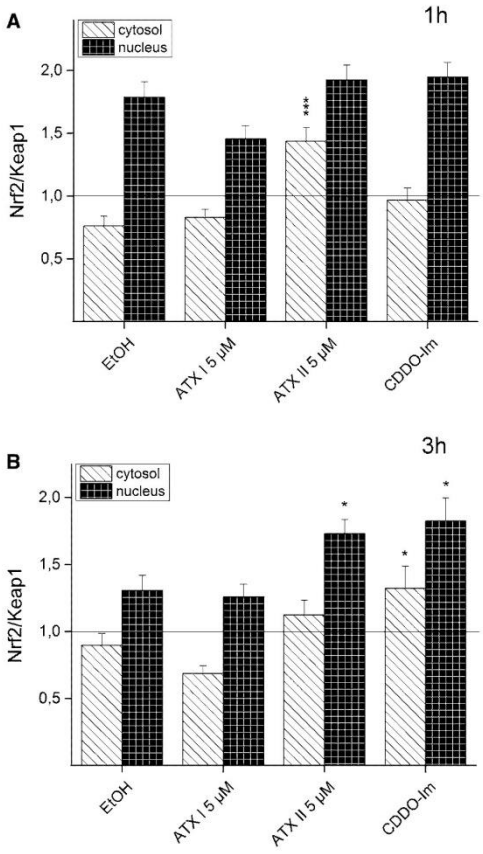

Fig. 6 Influence of the incubation with ATX I and ATX II on the Nrf2/Keap1 ratio in HT29 cells. Nrf2/Keap1 fluorescence signal ratio were measured in the cytosolic (*striped bars*, *white background*) and nuclear (*patterned bars*, *black background*) compartments of HT29 cells. Results describe the incubation of HT29 cells with 0.1 % EtOH (solvent control), 5 µM ATX I, 5 µM ATX II and 0.5 µM CDDO-Im for 1 h (**a**) and 3 h (**b**). Mean values of fluorescence of Nrf2 and Keap1 for every compartment are expressed as ratio ±SEM. Significance levels indicated as *asterisk* refer the comparison with solvent control (EtOH; $^{*}p < 0.05$, $^{***}p < 0.001$; $n = 18$ optical fields randomly selected from three independent experiments)

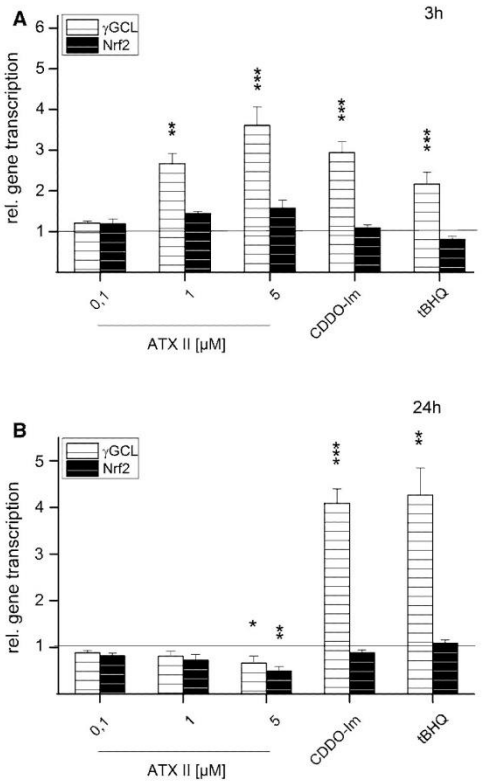

Fig. 7 Concentration- and time-dependent effect of ATX II on gene expression of γGCL and Nrf2 in HT29 cells. Impact of ATX II on relative gene transcription of phase 2 enzyme γGCL (*white background*) and transcription factor Nrf2 (*black background*) in HT29 cells after 3 h (**a**) and 24 h (**b**). 0.1 % EtOH served as solvent control, 0.5 µM CDDO-Im and 200 µM tBHQ as positive controls. Depicted are mean $2^{-\Delta\Delta C_T}$ ±SEM as fold transcription of 3–5 independent experiments compared to solvent control. Significance levels indicated as *asterisk* refer to comparison with solvent control (EtOH; $^{*}p < 0.05$, $^{**}p < 0.01$, $^{***}p < 0.001$)

significantly lower in comparison with the solvent control (Fig. 9a). After 3 h, this effect was reversed, showing a significant increase in the cellular tGSH level at 5 µM ATX II (Fig. 9a). Incubation of HT29 cells for 24 h led to a further rise of tGSH, significantly elevated already at the concentration of 1 µM and above. In parallel with the response of tGSH, the levels of GSSG showed a tendency toward a slight decrease after 1 h of incubation with ATX II (5 µM) and increased significantly, in line with above-mentioned results, after 3 and 24 h (Fig. 9b).

Effect of ATX II on reactive oxygen species formation in HT29 cells

In order to clarify whether the observed ATX II-mediated activation of the Nrf2-ARE pathway could be related also to oxidative stress, the potential of ATX II to induce ROS formation was investigated in HT29 cells using the dichlorofluorescein (DCF) assay. In this system, after 1 h of incubation, the fluorescence increased significantly

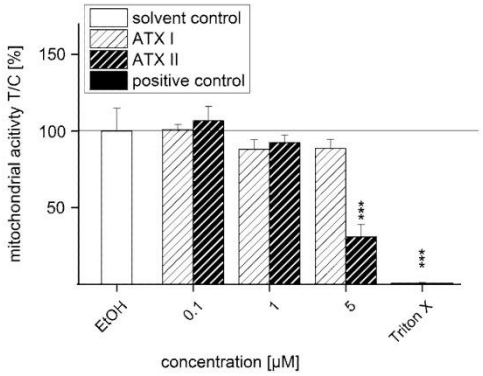

Fig. 8 Cytotoxicity of ATX I and ATX II after 24 h of incubation in HT29 cells in the WST-1 assay. Mitochondrial activity of HT29 cells was measured after 24 h of incubation with ATX I (*striped bars, white background*) and ATX II (*striped bars, black background*) with the WST-1 assay. 0.1 % EtOH was used as solvent control and Triton X (0.1 %) as positive control. Data are expressed as mean values ±SEM of three independent experiments normalized to solvent control. Significance levels refer to a comparison to solvent control (EtOH; $***p < 0.001$; $n = 3$ independent experiments performed in triplicate)

(150 ± 5 %) for cells exposed to 5 µM ATX II (Fig. 10). The positive control 200 µM H_2O_2 led to a significant increase in signal intensity to 174 ± 3 % (Fig. 10).

Discussion

The perylene quinone-type mycotoxins ATX I and ATX II, predominately produced by the saprophytic mold *Alternata alternata* (Lou et al. 2013), have been investigated for their toxicological importance with regard to their cytotoxic (Boutin et al. 1989; Fleck et al. 2012; Tiessen et al. 2013a), genotoxic (Fleck et al. 2012; Schwarz et al. 2012b) as well as mutagenic potential (Fleck et al. 2012; Stack and Prival 1986). However, studies focusing on the cellular metabolism and detoxification of these mycotoxins are relatively limited. In the present work, we investigated whether ATX I and ATX II interact with one of the major signaling pathways involved in phase II metabolism, the Nrf2-ARE pathway. The epoxide residue of ATX II, which is missing in ATX I (Fig. 1), confers sulfhydryl reactivity to the first, making ATX II a potential inducer of the Nrf2 transcription factor, which, in turn, is known to regulate the expression of a broad spectrum of phase II enzymes (Dinkova-Kostova et al. 2001; Itoh et al. 1997). In accordance with this mechanism, incubation with 5 µM ATX II for 20 h elicited a marked increase in Nrf2-ARE-dependent transcribed

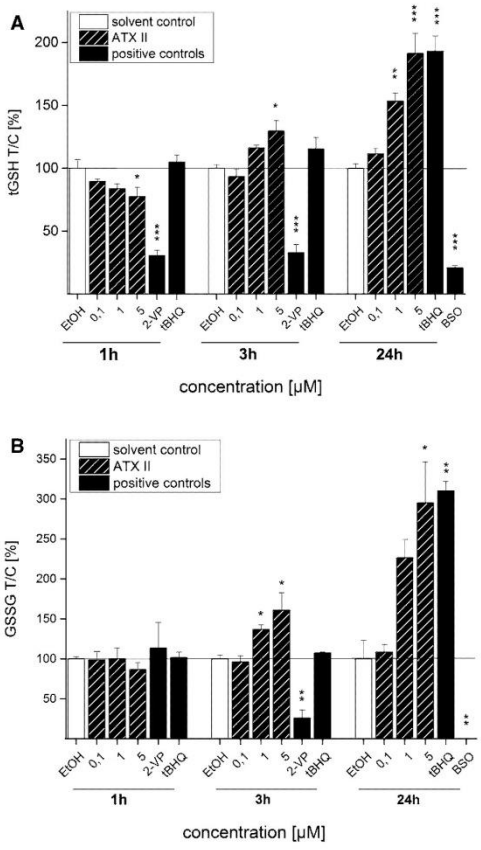

Fig. 9 Concentration- and time-dependent effect of ATX II on tGSH and GSSG levels in HT29 cells. tGSH (**a**) and GSSG (**b**) content in HT29 cells after 1, 3 and 24 h of incubation with ATX II. 0.1 % EtOH was used as solvent control and 0.01 % 2-VP, 200 µM tBHQ and 1 mM BSO as positive controls. Depicted data are mean values ±SEM of 3–5 independent experiments normalized to solvent control. Significance levels indicated as *asterisk* refer to a comparison to solvent control (EtOH; $*p < 0.05$, $**p < 0.01$, $***p < 0.001$)

luciferase activity in the reporter gene assay, whereas incubation with ATX I had no effect on Nrf2 activation (Fig. 2).

Since the human exposure to mycotoxins is limited mainly to oral uptake, the subsequent investigations were conducted in the colon adenocarcinoma cell line HT29. In these cells, the effect of ATX I and ATX II on the transcription factor Nrf2 was studied with immunofluorescence and confocal microscopy after 1 and 3 h of incubation. These short incubation periods were chosen on the basis of previous studies that have demonstrated how

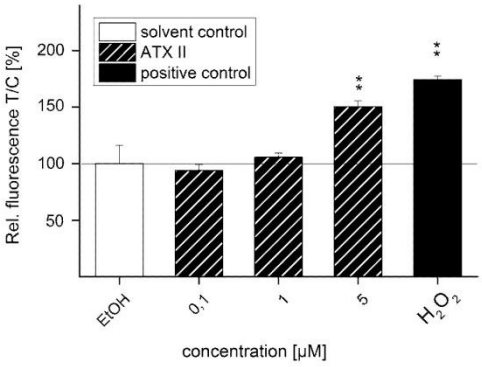

Fig. 10 Oxidative potential of ATX II after 1 h of incubation in HT29 cells measured with the DCF assay. Fluorescence of DCF was measured after 1 h of incubation with ATX II in HT29 cells. 0.1 % EtOH was used as solvent control and 200 µM H_2O_2 as positive control. Depicted data are mean values ±SEM of three independent experiments performed in pentaplicates. Significance levels indicated as *asterisk* refer to a comparison to solvent control (EtOH; $^{**}p < 0.01$)

Nrf2-ARE-dependent gene transcripts could be measured already after 3 h in this cell line (Boettler et al. 2011). For ATX I, no increase of in the Nrf2 signal was observed in any of our experimental conditions (Figs. 3, 5). On the contrary, a significant increase in Nrf2 immunolocalization was already observable after 1 h of incubation with ATX II (5 µM; Fig. 4) and was still detectable after 3 h (Fig. 5). To investigate the distribution of Nrf2 in the cellular compartments in more detail, its localization was also monitored with the help of SIM technique. As shown in Fig. 4, after 1 h of incubation with 5 µM ATX II, Nrf2 is clearly localized in the cellular cytoplasm, as well as, inside the nucleus (Fig. 4g, h). In addition to the effect on the Nrf2, ATX II also triggered an increase in the Keap1 signal (3 h incubation; Fig. 5). A similar effect was previously reported for the food contaminant deoxynivalenol (Katika et al. 2014), suggesting that Keap1 could also be an important target for the mechanism of action of mycotoxins. The synthetic triterpenoid CDDO-Im, even if it is a potent Nrf2-inducer in the luciferase assay (Fig. 2), did not trigger a significant increase in the Nrf2 signal in the microscopy experiments (Figs. 3, 4, 5). This difference can be probably explained by a distinct sensitivity and/or kinetics of Nrf2 activation triggered by CDDO-Im in comparison with ATX II in the two experimental systems. Moreover, previous studies already documented that the time dependency of CDDO-Im-mediated Nrf2 induction may vary between 0.5 up to 8 h of incubation in human leukemia cells (Liby 2005). As previously mentioned, Nrf2 is mainly located and repressed in the cytoplasm by Keap1 in its inactive state, so it was decided to present the immunolocalization data also as Nrf2/Keap1 signal ratios. Indeed, this more detailed analysis of the distribution of Nrf2 relative to Keap1 revealed a significant increase in the Nrf2/Keap1 ratios after 3 h of incubation with CDDO-Im in the cytosolic and the nuclear compartment in comparison with solvent controls (Fig. 6b). Interestingly, also ATX II led to a significantly elevated cytosolic Nrf2/Keap1 ratio already after 1 h of incubation (Fig. 6a), followed by a significant increase in the ratio in the nuclear compartment after 3 h (Fig. 6b). Intriguingly, this interpretation of the fluorescent signals could mirror a time-dependent increase in Nrf2 relative to Keap1 and its subsequent translocation from the cytoplasm into the nucleus.

As mentioned earlier, activation of Nrf2-ARE pathway triggers a signaling cascade which leads to the expression of, among others, genes that are associated with phase II metabolism. Consistently, 3 h of incubation with ATX II (1 and 5 µM) led to an increase in the gene transcription of phase II enzyme γGCL in HT29 cells, while no impact was observable on the amount of Nrf2 transcripts (Fig. 7a). The same pattern was observed for the positive controls CDDO-Im and tBHQ and was previously described also by Boettler et al. (2011). In particular, Boettler and co-workers described how chlorogenic acid is able to increase nuclear Nrf2 and the transcription of γGCL mRNA without directly altering the gene transcription of Nrf2. Overall, these data seem to suggest that the effect of ATX II and CDDO-Im in our experimental system could be sustained by a post-transcriptional mechanism, possibly targeting Nrf2 degradation rather than inducing a transcriptional change. This mechanism has been postulated in earlier publications as well, since it was described that Nrf2-inducers could act on the protein level, stabilizing Nrf2 and enhancing its activation, rather than interacting at the transcriptional level (Nguyen et al. 2003; Stewart 2002). After 24 h incubation with ATX II, the relative transcript levels of both γGCL and Nrf2 were comparable to that of the solvent control or even significantly lowered (5 µM ATX II Fig. 7b). To elucidate whether this reduction could be related to the onset of cytotoxic effects, the cytotoxicity of ATX II was investigated after 24 h with the WST-1 assay in HT29 cells. In line with previous findings, ATX II significantly reduced the activity of mitochondrial dehydrogenases with an EC_{50} of 2.26 µM (Fig. 8).

In order to give an overview of the ATX II-mediated Nrf2 activation from the nuclear translocation to the increase in the final enzymatic product, the impact of the mycotoxin on GSH and GSSG levels was also analyzed in HT29 cells. Incubation with ATX II for 3 h led to an increase in cellular tGSH (GSH + GSSG) and GSSG content (Fig. 9), which was in agreement with the time

response of Nrf2 activation observed with confocal microscopy and qPCR. The ATX II-induced increase in tGSH and GSSG amount was still measurable after 24 h, whereas the gene transcription of γGCL was no longer elevated after that incubation time. On the contrary, after the short-term incubation of 1 h with ATX II, the cellular tGSH and GSSG levels decreased significantly. This reduction could indicate a potential consumption of GSH in the course of cellular defense mechanisms against toxic effects induced by ATX II, as, for instance, oxidative stress. In agreement with this hypothesis, the DCF assay indicated that ATX II triggers the formation of ROS in intestinal cells after 1 h of incubation (5 µM, Fig. 10). In case of ATX II-induced oxidative stress, the cellular depletion of GSH should go along with an increase in oxidized GSSG, which is then mirrored in a shift of the corresponding GSSG/GSH ratio (Nemeth and Boda 1989). Calculations of these respective GSSG/GSH values did not reveal any changes in cells incubated with ATX II, the ratios remained comparable to that of the solvent control. Based on this result, the consumption of GSH by ATX II-induced oxidative effects seemed less likely. Intriguingly, ATX II was previously reported to form adducts with GSH in a cell-free system (Fleck et al. 2014). Taking this observation into account, our data suggest that the prevailing effect of ATX II-induced reduction in GSH levels could be attributed to the formation of aforementioned GSH adducts, rather than pro-oxidative effects.

Overall, the present study demonstrates that the *A. alternata* mycotoxin ATX II may have an impact at several levels of the Nrf2 signaling pathway and that this impact is particularly relevant in intestinal cells. These findings open new insights into the comprehension of the toxicity of perylene quinone-type mycotoxins. In fact, even though it is commonly accepted that activation of the Nrf2 pathway is usually related to a reduction in the toxicity of the inducing compound, the interpretation of the presented data is probably more complex. Although induction of GSH is normally associated with a more efficient formation of detoxification products, this mechanism does not seem to play a major role for ATX II. In fact, previous studies demonstrated that a depletion of GSH in V79 cells prior to incubation with ATX II barely has any effect on the genotoxicity of the toxin (Fleck et al. 2014). In addition, activation of the Nrf2 pathway has also been described as a source of detrimental effects in cancer promotion (Singh et al. 2006). In this light, the possible involvement of Nrf2-ARE activation in carcinogenesis has also to be kept in mind when considering the genotoxic and mutagenic effects of ATX II (Schwarz et al. 2012b; Stack et al. 1986). Moreover, the observed Nrf2-ARE mediated induction of phase II response triggered by ATX II may, potentially, also enhance the health risk associated with the ingestion of food contaminated with other mycotoxins. In fact, since *Alternaria* spp. do not only produce altertoxins, but rather toxin mixtures, the phase I and II activating ability of ATX II may contribute to the intracellular formation of mycotoxin metabolites which may result in a further increase in overall toxicity of *Alternaria* fungi (Pahlke et al. 2016). In conclusion, the effects of ATX II on the Nrf2-ARE pathway seem to open new prospective in the study and the toxicological characterization of the emerging mycotoxins ATX I and ATX II.

Materials and methods

Fungi cultivation and toxin isolation

For the isolation of altertoxins (ATXs), rice was inoculated with the *A. alternata* strain DSM62010 and cultivated to obtain a toxin-containing ethyl acetate extract as previously described (Schwarz et al. 2012a). Briefly, ATX I was purified from the extract by the group of Thomas Hofmann, chair of Food Chemistry and Molecular Sensory Science at the University of Technology, Munich, Germany. The ethyl acetate extract was fractionated with solid-phase extraction; thus, extract aliquots (300 mg each) were dissolved in MeOH/H_2O (90/10, v/v; 5 ml) and then eluted onto the top of a C18 ec cartridge (1 g, Chromabond, Macherey–Nagel, Düren, Germany) preconditioned with MeOH, followed by H_2O. Fractionation was performed by flushing the column with decreasing polarity using different MeOH/H_2O ratios: MeOH/H_2O (30/70, v/v; 20 ml; fraction S1), MeOH/H_2O (50/50, v/v; 20 mL; fraction S2), MeOH/H_2O (70/30, v/v; 20 ml; fraction S3), MeOH/H_2O (90/10, v/v; 20 mL; fraction S4), followed by MeOH/H_2O (90/10, v/v; 20 ml; fraction S5), and methanol (40 ml; fraction S6). The fractions S1–S6 were collected and concentrated in a vacuum and freeze-dried. ATX I was isolated from fraction 4 by means of HPLC. Fraction S4 was dissolved in aqueous MeCN (1 ml, 50 %) and was chromatographically fractionated on a preparative HPLC system (PrepStar, Varian, Darmstadt, Germany) consisting of two HPLC-pumps (Model SD-1), a two wavelength UV detector (Prostar 325), fraction collector (Model 701) and equipped with a C-18 column (ThermoHypersil ODS, 10 × 250 mm, 5 µm; Kleinostheim, Germany) as the stationary phase. Monitoring the effluent (4.2 ml/min) at 350 nm, chromatography was performed starting with a mixture (58/42, v/v) of aqueous HCOOH (0.1 % in H_2O) and MeCN, the MeCN content was increased to 50 % within 20 min, followed by column washing and reequilibration. Individual fractions were collected, concentrated under reduced pressure (40 °C) and freeze-dried in duplicate. ATX I was then repurified using the HPLC and column mentioned above and the following gradient. Monitoring the effluent (4.2 ml/min) at 350 nm,

chromatography was performed starting with a mixture (80/20, v/v) of aqueous HCOOH (0.1 % in H2O) and MeCN; the MeCN content was increased to 45 % within 16 min and to 70 % within 4 min, followed by column washing and reequilibration. Individual fractions were collected, concentrated under reduced pressure (40 °C) and freeze-dried in duplicate, yielding ATX I (in high purity (>97 % HPLC–UV, 270 nm).

ATX II was isolated at the Department of Food Chemistry and Toxicology (University of Vienna) from the ethyl acetate extract obtained from *Alternaria*-infested rice with semi-preparative HPLC and verified by MS measurements on the ESI-Q-TOF MS (maXis classic, Bruker Corporation, MA, USA) as previously described (Schwarz et al. 2012b).

Cell culture

Chinese hamster ovary cell line CHO-K1 cell line was purchased from ATCC (VA, USA), stably transfected with an expression vector for the *Photinus pyralis* luciferase driven by the ARE of murine GSTA1 gene (pGL4.22[luc2CP/Puro]) and an expression vector for enhanced green fluorescent protein (eGFP; pEGF-N1; ClonTech, CA, USA). CHO cells were cultivated in complete DMEM (10 % FCS, 1 % P/S) supplemented with 1 % L-glutamine (L-glu; 584 mg/ml) and 0.08 % puromycin (4 µg/ml). Human colon adenocarcinoma cell line HT29 was purchased from ATCC. HT29 cells were cultivated in DMEM supplemented with 10 % fetal calf serum (FCS) and 1 % penicillin/streptomycin (P/S, 50 U/ml), referred to as complete DMEM. Cell culture media and supplements were purchased from GIBCO Invitrogen (Karlsruhe, Germany), Lonza Group Ltd (Basel, Switzerland), Sigma-Aldrich Chemie GmbH (Munich, Germany) and Sarstedt AG&Co (Nuembrecht, Germany). Cell lines were cultivated and incubated in humidified incubators at 37 °C and 5 % CO_2 and routinely tested for the absence of mycoplasma contamination.

Nrf2 luciferase reporter gene assay

Nrf2 activation was measured in CHO cells carrying an ARE-dependent luciferase expressing plasmid and an expression vector for eGFP. 60 000 cells/100 µl complete medium supplemented with 1 % L-glu were seeded in 96-well plates and allowed to settle for 4 h. Cells were incubated with the respective concentrations of ATX I and ATX II with a final EtOH concentration of 0.1 % for 20 h. 0.1 % EtOH was used as solvent control and 0.1 µM 1[2-cyano-3,12-dioxooleana-1,9(11)-dien-28-oyl]imidazolide (CDDO-Im), a synthetic triterpenoid which activates the Nrf2-ARE pathway (Liby 2005), served as positive control. Afterward cells were washed with pre-warmed PBS and the plates were stored at −80 °C for at least 1 h. Subsequently 50 µl lysis buffer (no. E3791, Promega, Madison) was added and the cell lysates were transferred into a dark 96-well plate. Luciferase activity was measured with the TECAN GeniosPro plate reader. ATP (5 in 20 mM tricine) and luciferin (1 in 20 mM tricine) were auto-injected, and luminescence and eGFP-derived fluorescence signals were recorded for each well. Luminescence was normalized to the respective fluorescence of the eGFP value to account for eventual cytotoxicity. Each compound was tested in a triplicate with a minimum of three independent experiments.

Immunocytochemistry and microscopy

For immunocytochemical analysis cells were seeded in multi-well microscopy slides (Falcon). After 72 h, cells were incubated with the respective toxin concentrations and CDDO-Im (0.5 µM) was used as positive control. At the end of the incubation (1 or 3 h), the cells were washed with pre-warmed PBS and fixed with 3.7 % formaldehyde for 15 min. The cells were then washed with PBS, and slides were stored at 4 °C prior to staining. Cells were permeabilized with 0.2 % triton X for 10 min, washed and blocked with PBS-BSA (1 %, 1 h, RT), the primary antibodies added and the slides incubated for 2 h (RT). Primary antibodies were purchased from Santa Cruz Biotechnology (Heidelberg, Germany) and used according to the specification of the supplier (1:1000 dilution): anti-lamin B goat polyclonal antibody (sc-6216), anti-Nrf2 rabbit polyclonal antibody (sc-722), anti-Keap1 mouse monoclonal antibody (sc-365626). After removal of the primary antibodies, fluorescent-labeled secondary antibodies were added and slides incubated in a dark humidified chamber for 1.5 h. For our study, Alexa Fluor 568 Donkey Anti-Rabbit (A10042), Alexa Fluor 647 Donkey Anti Goat (A-21447) and Alexa Fluor 488 Donkey Anti-Mouse (A-21202) antibodies were used (dilution 1:1500, Life Technologies). The slides were then washed and post-fixed with 3.7 % formaldehyde (10 min, RT); at the end of the post-fixation, 100 mM glycine was used to mask reactive sites and slides were mounted and sealed with Roti-Mount FluoCare (Roth, Graz, Austria). Images were acquired with a Confocal LSM Zeiss 710 equipped with ELYRA PS. 1 system. Structured illumination microscopy (SIM) images were acquired with Plan Apochromat 100×/1.46 oil objective, zoom 2, confocal images with a Plan Apochromat 63X/1.4 oil objective, zoom 1.5. Images were acquired from at least three different cell preparations for the analysis of Nrf2 and Keap1 signals and, for each cell preparation, at least three different optical fields were acquired, resulting in at least nine images for each experimental condition. Images were acquired to allow complete 3D reconstruction of the whole cells and Nrf2 and Keap1 quantification derived

from the evaluation of the mean fluorescent signal intensity expressed as percentage of negative control (solvent, EtOH 0.1 %, Figs. 3, 4, 5). Mean intensity of the signals was derived from the raw data of the images with the software Zeiss ZEN 2012 SP1. The evaluation of the Nrf2 and Keap1 signals was performed in a central section of the 3D reconstruction, with the nuclear structure provided by lamin B as reference. During the selection of the optical fields and of the image analysis, the Nrf2 acquisition channel was initially disabled in order to avoid any bias. In order to ensure the comparability of the signals, the acquisition of all the experimental conditions (ATX I and ATX II 0.1, 1, 5 µM, positive and negative controls) of the same biological replicate was performed the same day, maintaining constant laser parameters (power, digital gain), as well as background levels. For the estimation of the nuclear and cytosolic ratio of the Nrf2/Keap1 signals (Mean intensity of signal of Nrf2 channel/Mean intensity of signal of Keap1 channel; Fig. 6), nuclei and cytosolic areas were randomly selected in the optical fields. The quantification was performed in at least two different areas of each compartment (nuclear or cytosolic) for every image, resulting in at least 18 different areas analyzed for each experimental condition.

RNA isolation and measurement of transcription levels of γGCL and Nrf2 with qPCR

For the qPCR experiments, 800,000 (3 h incubation) and 500,000 (24 h incubation) HT29 cells were seeded in Petri dishes (Ø = 6 cm) and allowed to grow for 48 h. Subsequently, cells were incubated with 0.1, 1 and 5 µM ATX II and the solvent control EtOH (0.1 %) for 3 and 24 h in complete medium. CDDO-Im and pro-oxidant butylhydroquinone (tBHQ), which inhibits GSH synthesis and activates the Nrf2-ARE pathway (Huang et al. 2000), served as positive control. Subsequently, total RNA was isolated (RNeasy® Mini Kit, Qiagen, Hilden, Germany) and reverse transcribed into cDNA (QuantiTect® Reverse Transcription Kit, Qiagen, Hilden, Germany). Real-time PCR was performed with the StepOne Plus™ Instrument (Life Technologies) using QuantiTect SYBR Green PCR Master Mix and Primer Assays: HS_GCLC_1_SG, HS_NFE2L2_1_SG, HS_ACTB_1_SG (Qiagen Hilden, Germany). Transcript levels normalized to levels of the endogenous control gene β-actin were quantified using the $\Delta\Delta C_T$ method as PCR efficiencies of target and control gene have been found comparable.

WST-1 assay

Cytotoxic properties of ATX I and ATX II were investigated with the WST-1 assay (Roche, Basel, Switzerland). Briefly, 7 500 HT29 cells were seeded in 96-well plates and allowed to grow for 48 h at 37 °C and 5 % CO_2 in a humidified incubator. Cells were incubated with 100 µl of complete medium, containing the respective toxin concentration in 0.1 % EtOH. The detergent Triton X (0.01 %) was used as positive control for cell permeabilization and subsequent cell death by necrosis (Borenfreund and Puerner 1985). Cells were washed after the incubation period of 24 h and WST-1 dye was added in serum-free medium. After 45 min the absorption at 450 nm was measured, values were normalized to respective control. The EC_{50} was calculated with OriginPro 9.1 with dose–response fitting.

Measurement of cellular tGSH and GSSG

Concentrations of tGSH and GSSG in HT29 cells were measured according to Tietze (1969) and Schwarz et al. (2012b). Briefly, HT29 cells were seeded in Petri dishes (Ø = 10 cm) and allowed to grow for 48 or 72 h. Incubations took place for 1, 3 and 24 h with respective ATX II concentrations. 200 µM tBHQ was used as positive control for all three incubation times, 0.01 % 2-VP only for the 1 and 3 h periods due to its cytotoxicity, for the 24 h incubation, buthionine sulfoximine (BSO) was taken. For measurement of GSSG, 20 µl of 0.01 % 2-VP and 100 µl of 50 % triethanolamine (TEA) were added to 500 µl cell suspension and shaken for 1 h at 1300 rpm and 26 °C. 150 µl of cell suspension and 20 µl of GSSG standard solutions were mixed with 180 µl GSSG reaction mix composed of 154 µl A/B buffer [23.1 µl buffer A (125 mM KH_2PO_4, 8 mM EDTA) and 130.9 µl buffer B (125 mM K_2HPO_4, 8 mM EDTA)], 2 µl 6 mM 5,5′-dithiobis-(2-nitrobenzoic acid) (DTNB) in A/B buffer, 4 µl of 20 mM NADPH and 2 µl of GSH reductase (GR, 50 U/ml). GSH and GSSG samples were shaken for 30 s and then measured spectrophotometrically at 405 nm. The tGSH and GSSG values were referred to the respective protein contents, which were measured colorimetrically with the bicinchoninic acid (BCA) Protein Assay Kit purchased from Life Technologies (Thermo Scientific, MA, USA) and normalized to solvent control.

Dichlorofluorescein assay

The influence of ATX II on the redox status of HT29 cells was measured with the DCF assay according to Keston and Brandt (1965). In this assay, 20,000 HT29 cells per well were seeded in 200 µl of serum-containing medium in a black 96-well plate and allowed to grow for 48 h. Afterward each well was washed with 37 °C PBS and incubated with 100 µl of dichlorofluorescein diacetate (DCF-DA) for 30 min at 37 °C. Subsequently, cells were washed with 37 °C PBS and incubated with the respective ATX II concentrations in a final EtOH concentration of 0.1 %, which

also served as solvent control and 200 µM H_2O_2 was used as positive control. Phenol red-free DMEM was used for the incubations. The fluorescence was measured (excitation at 485 nm, emission at 528 nm) after 1 h and the values were normalized to solvent control.

Statistical evaluation

All data are presented as the mean ± SEM. The data were tested for normal distribution with the Shapiro–Wilk test. The statistical significances for single concentrations (positive controls) were compared with the Student's two-sample t test. Concentration ranges were evaluated for significant effects with the one-way analysis of variance (ANOVA), and in case of a significant difference of $p < 0.05$, post hoc Fisher's least significant difference test was performed. Generally, raw data were used, but if the inter-experimental variances were too high, significances were calculated using the data normalized to controls. In this case, significances of samples were calculated compared to the lowest compound concentration used, where no effect was observed (0.1 µM ATX I or ATX II, respectively), since comparison to the 100 % controls was mathematically not feasible.

Acknowledgments Open access funding provided by University of Vienna. The authors are grateful to Eva Attakpah from the Department for Food Chemistry and Toxicology at the University of Vienna for her technical support. The authors acknowledge the support of "BioProMotion" Bioactivity and Metabolism grant from the University of Vienna, Austria to Kristin Zimmermann.

Compliance with ethical standards

Conflict of interest The authors declare that they have no conflict of interest.

References

Andersen B, Frisvad JC (2004) Natural occurrence of fungi and fungal metabolites in moldy tomatoes. J Agric Food Chem 52(25):7507–7513. doi:10.1021/jf048727k

Boettler U, Sommerfeld K, Volz N et al (2011) Coffee constituents as modulators of Nrf2 nuclear translocation and ARE (EpRE)-dependent gene expression. J Nutr Biochem 22(5):426–440. doi:10.1016/j.jnutbio.2010.03.011

Borenfreund E, Puerner JA (1985) Toxicity determined in vitro by morphological alterations and neutral red absorption. Toxicol Lett 24(2–3):119–124. doi:10.1016/0378-4274(85)90046-3

Boutin BK, Peeler JT, Twedt RM (1989) Effects of purified altertoxins I, II, and III in the metabolic communication V79 system. J Toxicol Environ Health 26(1):75–81. doi:10.1080/15287398909531234

Dinkova-Kostova AT, Massiah MA, Bozak RE, Hicks RJ, Talalay P (2001) Potency of Michael reaction acceptors as inducers of enzymes that protect against carcinogenesis depends on their reactivity with sulfhydryl groups. Proc Natl Acad Sci 98(6):3404–3409. doi:10.1073/pnas.051632198

EFSA (2011) Scientific Opinion on the risks for animal and public health related to the presence of Alternaria toxins in feed and food. EFSA J 9(11):2407. doi:10.2903/j.efsa.2011.2407

Fleck SC, Burkhardt B, Pfeiffer E, Metzler M (2012) Alternaria toxins: altertoxin II is a much stronger mutagen and DNA strand breaking mycotoxin than alternariol and its methyl ether in cultured mammalian cells. Toxicol Lett 214(1):27–32. doi:10.1016/j.toxlet.2012.08.003

Fleck SC, Pfeiffer E, Podlech J, Metzler M (2014) Epoxide reduction to an alcohol: a novel metabolic pathway for perylene quinone-type Alternaria mycotoxins in mammalian cells. Chem Res Toxicol 27(2):247–253. doi:10.1021/tx400366w

Hradil CM, Hallock YF, Clardy J, Kenfield DS, Strobel G (1989) Phytotoxins from Alternaria cassiae. Phytochemistry 28(1):73–75. doi:10.1016/0031-9422(89)85011-3

Huang HC, Nguyen T, Pickett CB (2000) Regulation of the antioxidant response element by protein kinase C-mediated phosphorylation of NF-E2-related factor 2. Proc Natl Acad Sci 97(23):12475–12480. doi:10.1073/pnas.220418997

Itoh K, Chiba T, Takahashi S et al (1997) An Nrf2/small Maf heterodimer mediates the induction of phase II detoxifying enzyme genes through antioxidant response elements. Biochem Biophys Res Commun 236(2):313–322. doi:10.1006/bbrc.1997.6943

Katika MR, Hendriksen PJM, Van Loveren H, Peijnenburg AACM (2014) Characterization of the modes of action of deoxynivalenol (DON) in the human Jurkat T-cell line. J Immunotoxicol 12(3):206–216. doi:10.3109/1547691x.2014.925995

Keston AS, Brandt R (1965) The fluorometric analysis of ultramicro quantities of hydrogen peroxide. Anal Biochem 11(1):1–5

Kobayashi A, Kang MI, Okawa H et al (2004) Oxidative stress sensor Keap1 functions as an adaptor for Cul3-based E3 ligase to regulate for proteasomal degradation of Nrf2. Mol Cell Biol 24(16):7130–7139. doi:10.1128/Mcb.24.16.7130-7139.2004

Liby K (2005) The synthetic triterpenoids, CDDO and CDDO-imidazolide, are potent inducers of heme oxygenase-1 and Nrf2-ARE signaling. Cancer Res 65(11):4789–4798. doi:10.1158/0008-5472.can-04-4539

Lou J, Fu L, Peng Y, Zhou L (2013) Metabolites from Alternaria fungi and their bioactivities. Molecules 18(5):5891–5935. doi:10.3390/molecules18055891

Müller MEH, Korn U (2013) Alternaria mycotoxins in wheat—a 10 years survey in the Northeast of Germany. Food Control 34(1):191–197. doi:10.1016/j.foodcont.2013.04.018

Nemeth I, Boda D (1989) The ratio of oxidized/reduced glutathione as an index of oxidative stress in various experimental models of shock syndrome. Biomed Biochim Acta 48(2–3):S53–S57

Nguyen T, Sherratt PJ, Huang HC, Yang CS, Pickett CB (2003) Increased protein stability as a mechanism that enhances Nrf2-mediated transcriptional activation of the antioxidant response element. Degradation of Nrf2 by the 26 S proteasome. J Biol Chem 278(7):4536–4541. doi:10.1074/jbc.M207293200

Nguyen T, Nioi P, Pickett CB (2009) The Nrf2-antioxidant response element signaling pathway and its activation by oxidative stress. J Biol Chem 284(20):13291–13295. doi:10.1074/jbc.R900010200

Pahlke G, Tiessen C, Domnanich K et al (2016) Impact of Alternaria toxins on CYP1A1 expression in different human tumor cells

and relevance for genotoxicity. Toxicol Lett 240(1):93–104. doi:10.1016/j.toxlet.2015.10.003

Rotem J (ed) (1994) The genus Alternaria: biology, epidemiology and pathogenicity. The American Phytopathological Society, St. Paul

Rushmore TH, Morton MR, Pickett CB (1991) The Antioxidant responsive element—activation by oxidative stress and identification of the DNA consensus sequence required for functional-activity. J Biol Chem 266(18):11632–11639

Schrader TJ, Cherry W, Soper K, Langlois I, Vijay HM (2001) Examination of *Alternaria alternata* mutagenicity and effects of nitrosylation using the Ames Salmonella test. Teratog Carcinog Mutagen 21(4):261–274. doi:10.1002/tcm.1014

Schrader TJ, Cherry W, Soper K, Langlois I (2006) Further examination of the effects of nitrosylation on *Alternaria alternata* mycotoxin mutagenicity in vitro. Mutat Res Genet Toxicol Environ Mutagen 606(1–2):61–71. doi:10.1016/j.mrgentox.2006.02.008

Schwarz C, Kreutzer M, Marko D (2012a) Minor contribution of alternariol, alternariol monomethyl ether and tenuazonic acid to the genotoxic properties of extracts from *Alternaria alternata* infested rice. Toxicol Lett 214(1):46–52. doi:10.1016/j.toxlet.2012.08.002

Schwarz C, Tiessen C, Kreutzer M, Stark T, Hofmann T, Marko D (2012b) Characterization of a genotoxic impact compound in *Alternaria alternata* infested rice as Altertoxin II. Arch Toxicol 86(12):1911–1925. doi:10.1007/s00204-012-0958-4

Singh A, Misra V, Thimmulappa RK et al (2006) Dysfunctional KEAP1–NRF2 Interaction in Non-Small-Cell Lung Cancer. PLoS Medicine 3(10):e420. doi:10.1371/journal.pmed.0030420

Stack ME, Prival MJ (1986) Mutagenicity of the Alternaria metabolites altertoxins I, II, and III. Appl Environ Microb 52(4):718–722

Stack ME, Mazzola EP, Page SW et al (1986) Mutagenic Perylenequinone Metabolites of *Alternaria alternata*: altertoxins I, II, and III. J Nat Prod 49(5):866–871. doi:10.1021/np50047a017

Stewart D (2002) Degradation of transcription factor Nrf2 via the ubiquitin-proteasome pathway and stabilization by cadmium. J Biol Chem 278(4):2396–2402. doi:10.1074/jbc.M209195200

Tiessen C, Fehr M, Schwarz C et al (2013a) Modulation of the cellular redox status by the Alternaria toxins alternariol and alternariol monomethyl ether. Toxicol Lett 216(1):23–30. doi:10.1016/j.toxlet.2012.11.005

Tiessen C, Gehrke H, Kropat C et al (2013b) Role of topoisomerase inhibition and DNA repair mechanisms in the genotoxicity of alternariol and altertoxin-II. World Mycotoxin J 6(3):233–244. doi:10.3920/wmj2013.1592

Tietze F (1969) Enzymic method for quantitative determination of nanogram amounts of total and oxidized glutathione: applications to mammalian blood and other tissues. Anal Biochem 27(3):502–522

Tournas VH, Katsoudas E (2005) Mould and yeast flora in fresh berries, grapes and citrus fruits. Int J Food Microbiol 105(1):11–17. doi:10.1016/j.ijfoodmicro.2005.05.002

Attachment: Publication 2

Arch Toxicol
DOI 10.1007/s00204-016-1855-z

BIOLOGICS

Dual effectiveness of *Alternaria* but not *Fusarium* mycotoxins against human topoisomerase II and bacterial gyrase

Katharina Jarolim[1] · Giorgia Del Favero[1] · Doris Ellmer[2] · Timo D. Stark[2] · Thomas Hofmann[2] · Michael Sulyok[3] · Hans-Ulrich Humpf[4] · Doris Marko[1]

Received: 8 July 2016 / Accepted: 15 September 2016

Abstract Type II DNA-topoisomerases (topo II) play a crucial role in the maintenance of DNA topology. Previously, fungi of the *Alternaria* genus were found to produce mycotoxins that target human topo II. These results implied the question why a fungus should produce secondary metabolites that target a human enzyme. In the current work, the homology between human topo II and its bacterial equivalent, gyrase, served as basis to study a potential dual inhibition of both enzymes by mycotoxins. A total of 15 secondary metabolites produced by fungi of the genera *Alternaria* and *Fusarium* were assessed for their impact on topo II of human and bacterial origin in the decatenation and the supercoiling assay, respectively. In line with the theory of dual topo II inhibition, six of the tested *Alternaria* mycotoxins were active against both enzymes, the dibenzo-α-pyrones alternariol (AOH) and alternariol monomethyl ether (AME), as well as the perylene-quinones altertoxin I (ATX I) and II (ATX II), alterperylenol (ALP) and stemphyltoxin III (STTX III). The *Alternaria* metabolites altersetin (ALN), macrosporin (MAC), altenusine (ALS) and pyrenophorol (PYR) impaired the function of human topo II, but did not show any effect on gyrase. The potency to inhibit topo II activity declined in the row STTX III (initial inhibitory concentration 10 μM) > AOH (25 μM) = AME (25 μM) = ALS (25 μM) = ATX II (25 μM) > ALN (50 μM) = ATX I (50 μM) > ALP (75 μM) = PYR (75 μM) > MAC (150 μM). Inhibition of gyrase activity was most pronounced for AOH and AME (initial inhibitory concentration 10 μM) followed by ATX II (25 μM) > ATX I = ALP = STTX III (50 μM). In contrast, none of the investigated *Fusarium* mycotoxins deoxynivalenol (DON), fumonisin B1, fusarin C and moniliformin, as well as the *Alternaria* metabolite tentoxin, had any impact on the activity of neither human nor bacterial topo II.

Keywords Topoisomerase II · Gyrase · Mycotoxins · *Alternaria* · *Fusarium*

Introduction

DNA-topoisomerases are essential enzymes that play a fundamental role in the maintenance of cellular DNA topology, i.e., the integrity of DNA during replication or chromosomal segregation (Champoux and Dulbecco 1972; DiNardo et al. 1984). According to their respective catalytic mechanism of action, they are divided into type I and type II topoisomerases (Liu et al. 1980). The dimeric topoisomerase (topo) II acts as decatenase, introducing transient double-strand breaks into the DNA substrate, allowing the passage of an intact DNA double-strand and resealing the break afterward (Hsieh and Brutlag 1980; Liu et al. 1980). While a wanted effect in cancer therapy, the functional disturbance of human topo II by food constituents may imply severe adverse effects (McClendon and Osheroff 2007).

Electronic supplementary material The online version of this article (doi:10.1007/s00204-016-1855-z) contains supplementary material, which is available to authorized users.

✉ Doris Marko
doris.marko@univie.ac.at

[1] Department of Food Chemistry and Toxicology, Faculty of Chemistry, University of Vienna, 1090 Vienna, Austria

[2] Chair of Food Chemistry and Molecular Sensory Science, Technical University of Munich, 85354 Freising, Germany

[3] Department IFA-Tulln, University of Natural Resources and Life Sciences Vienna (BOKU), 3430 Tulln, Austria

[4] Institute of Food Chemistry, Westfälische Wilhelms-Universität Münster, 48149 Münster, Germany

Published online: 28 September 2016

In previous studies, three secondary metabolites produced by food-contaminating fungi of the genus *Alternaria,* the dibenzo-α-pyrones AOH and AME, as well as the perylene-quinone ATX II, were found to inhibit the activity of human topo II in vitro (Fehr et al. 2009; Tiessen et al. 2013). Based on these results, the question arose what might prompt a mold to produce secondary metabolites that target human enzymes. Since a fungus faces a variety of microorganisms within its habitat, against which it must compete, the formation of toxic secondary metabolites that are detrimental to potential predators is discussed as defense method to ensure proper growth and propagation (Magan and Aldred 2007). The production of antibiotics is a mechanism of antibacterial defense that has been observed for many genera of fungi imperfecti, the most prominent being *Aspergillus* and *Penicillium* spp. (Lancini et al. 1995). A common target for antibiotic pharmaceuticals is gyrase, a bacterial topo II (Alt et al. 2011; Gellert et al. 1976b). Since gyrase shares a high degree of homology with human topo II, the previously observed interaction between *Alternaria* mycotoxins and human topo II was taken as indication of a potential dual inhibition. To consider this question, 15 secondary metabolites produced by *Alternaria* and *Fusarium* fungi were investigated for their effect on the activity of topo II of both human and bacterial origin. These molds grow as endophytes on host plants worldwide, contaminating a variety of food and feed (Kharwar et al. 2014; Placinta et al. 1999). The two fungi genera synthesize chemically very diverse secondary metabolites, as can be seen with an exemplarily selection in Fig. 1. Some of the tested *Alternaria* mycotoxins share structural features, for instance the perylene-quinone-type toxins ATX I, ATX II, ALP and STTX III (Fig. 1a), which differ by an epoxy group and/or a double bond. The dibenzo-α-pyrones AOH

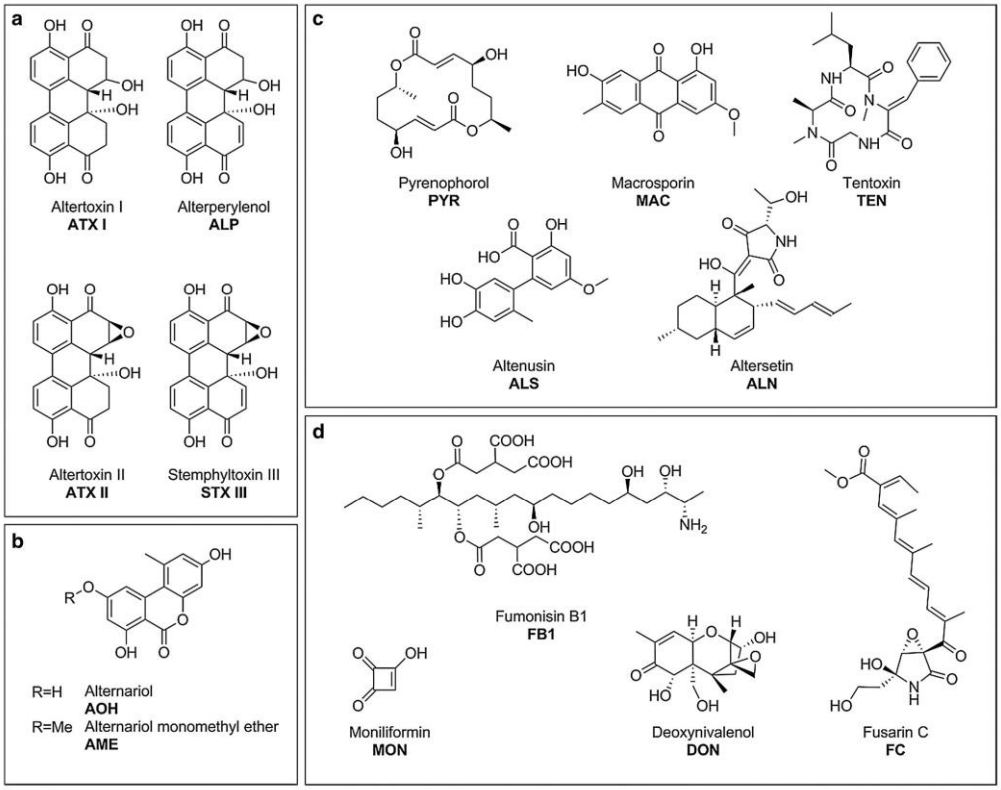

Fig. 1 Chemical structures of secondary metabolites produced by *Alternaria* and *Fusarium* fungi. Molecules are grouped according to structure and producing organisms in **a** perylene-quinone-type, **b** dibenzo-α-pyrones both from *Alternaria* and **c** other *Alternaria* mycotoxins, **d** four secondary metabolites produced by *Fusarium* spp

and AME (Fig. 1b), also produced by *Alternaria* fungi, distinguish themselves only by a methyl group. The further *Alternaria* metabolites that were assessed in this study constitute a chemically heterogeneous group, composed of the macrodiolide PYR, the anthraquinone MAC, the tetrapeptide TEN, the tetramic acid derivative ALN and the biphenyl ALS (Fig. 1c). The investigated *Fusarium* metabolites include the trichothecene DON, the polyketide FB1, which is characterized by an eicosane backbone, the sesquiterpenoid FC and the semiquadric acid MON (Fig. 1d). In the present work, these 15 secondary fungal metabolites were investigated for their potential interference with type II topoisomerases of human and bacterial origin in cell-free experimental setups. Since most of the selected perylenequinones are not commercially available, these compounds were isolated from rice inoculated with *Alternaria alternata* cultures.

Experimental procedures

Cell culture and fungus cultivation

The human colon adenocarcinoma cell line HT29 and the *Alternaria alternata* strain DSM 62010 were obtained from the German Collection of Microorganisms and Cell Cultures GmbH (DSMZ, Braunschweig, Germany). Cells were cultured in Dulbecco's modified Eagle medium (DMEM; GIBCO Invitrogen, Karlsruhe, Germany) supplemented with 10 % FBS and 1 % P/S and maintained in incubators at 37 °C and 5 % CO_2. Cultivation of the *Alternaria* strains was performed on moist, autoclaved rice, as described previously (Schwarz et al. 2012b).

Isolation and identification of *Alternaria* perylene-quinone-type mycotoxins from inoculated rice cultures

Due to lack of commercially available ATX I, ATX II, ALP and STTX III, the toxins were isolated from *Alternaria*-infested rice. Ethyl acetate extracts were prepared after 21 days of incubation from rice which was inoculated with *Alternaria alternata* strain DSM 62010 as described in Schwarz et al. (2012a). Fractionation of the ethyl acetate extracts by solid-phase extraction (SPE) and isolation of the toxins with HPLC were conducted according to Jarolim et al. (2016). For isolation individual fractions were collected, concentrated under reduced pressure (40 °C), and freeze-dried in duplicate, yielding ATX II and STTX III in high purities (>97 % HPLC–UV, 270 nm). ATX I and ALP were re-purified using the HPLC system and column mentioned in Jarolim et al. (2016) and the following gradient. Monitoring the effluent (4.2 ml/min) at 350 nm, chromatography was performed starting with a mixture (80/20, v/v) of aqueous formic acid (0.1 % in H_2O) and MeCN, the MeCN content was increased to 45 % within 16 min and to 70 % within 4 min, followed by column washing and re-equilibration. Individual fractions were collected, concentrated under reduced pressure (40 °C), and freeze-dried in duplicate, yielding ATX I and ALP (>97 % HPLC–UV, 270 nm).

Aliquots of the isolated fractions were analyzed by means of UPLC–TOF–MS^e on a Waters Synapt G2-S HDMS mass spectrometer (Waters, Manchester, UK) coupled to an Acquity UPLC core system (Waters, Milford, MA, USA) equipped with a 2 × 150 mm, 1.7 µm, BEH C18 column (Waters, Manchester, UK) consisting of a binary solvent manager, sample manager and column oven. Operated with a flow rate of 0.4 ml/min at 50 °C, the following gradient was used for chromatography: Starting with a mixture (10/90, v/v) of aqueous formic acid (0.1 % in H_2O) and MeCN (0.1 % formic acid), the MeCN content was increased to 100 % within 4 min and, then, kept constant for 0.5 min. Scan time for the MS^e method (centroid) was set to 0.1 s. Analyses were performed in the negative ESI and the high-resolution mode using the following ion source parameters: capillary voltage −2.5 kV, sampling cone 30 V, source offset 20 V, source temperature 150 °C, desolvation temperature 450 °C, cone gas 30 l/h, nebuliser 6.5 bar and desolvation gas 850 l/h. Data processing was performed by using MassLynx 4.1 SCN 9.16 (Waters, Manchester, UK) and the elemental composition tool for determining the accurate mass. All data were lock mass corrected on the pentapeptide leucine enkephaline (Tyr-Gly-Gly-Phe-Leu, *m/z* 554.2615, $[M–H]^-$) in a solution (1 ng/µl) of MeCN/0.1 % formic acid (1/1, v/v). Scan time for the lock mass was set to 0.3 s, an interval of 15 s and 3 scans to average with a mass window of ±0.3 Da. Calibration of the Synapt G2-S in the range from *m/z* 50 to 1200 was performed using a solution of sodium formiate (5 mmol/l) in 2-propanol/H_2O (9/1, v/v). The UPLC and Synapt G2-S systems were operated with MassLynx™ software (Waters).

All 1D and 2D NMR measurements (^1H, ^1H-^1H-gCOSY, gHSQC, gHMBC and ^{13}C) were performed on an Avance III 500 MHz spectrometer with a CTCI probe (Bruker, Rheinstetten, Germany).

ATX I was identified by UPLC-ESI-TOF-MS and NMR as previously described in Jarolim et al. (2016). The structure of the isolated ATX II was described in detail by Schwarz et al. (2012b). ATX II was identified with an *m/z* of 349.0714 ($[M–H]^-$, calculated for $C_{20}H_{13}O_6$, 349.0712, +0.6 ppm) in the (–) HRESIMS. Data of the ^1H NMR and ^{13}C NMR of ALP and STTX III are summarized in the supplementary information (Tables S2–S5) and were in line to Hradil et al. (1989); and Stack and Prival (1986). ALP was

identified with an *m/z* of 349.0714 ([M-H]$^-$, calculated for $C_{20}H_{13}O_6$, 349.0712, +0.6 ppm) in the (–) HRESIMS *m/z*. ^{1}H NMR and ^{13}C NMR data are summarized in appendix and in line to Hradil et al. (1989); and Okuno et al. (1983). STTX III was identified with an *m/z* of 347.0557 ([M–H]$^-$, calculated for $C_{20}H_{11}O_6$, 347.0556, +0.3 ppm) in the (–) HRESIMS. ^{1}H NMR and ^{13}C NMR data of ALP and STTX III are summarized in the electronic supplementary information (Tables S1–S5) and were in line to Stack and Mazzola (1989).

Secondary metabolites from *Alternaria* and *Fusarium* spp.

The *Alternaria* dibenzo-α-pyrones AOH and AME and the *Fusarium* trichothecene DON were bought from Sigma–Aldrich (MI, USA). Macrosporin, tentoxin, altenusin and pyrenophorol were obtained from Enzo Life Sciences (Lausen, Switzerland). Altersetin was purchased from AnalytiCon Discovery GmbH (Potsdam, Germany). FB_1 and FC were isolated from *Fusarium verticillioides* MRC 826 and *Fusarium verticillioides* MRC 0712 as described in the literature (Hübner et al. 2012; Kleigrewe et al. 2011). MON was synthesized according to Lohrey et al. (2011).

Decatenation assay

The interference of the tested secondary fungal metabolites with human topoisomerase II α was determined using the decatenation assay. Briefly, this assay is based on the measurement of the ability of topo II α enzyme to decatenate a fragment of catenated kDNA. The topo II poison and anticancer drug etoposide was used as positive control (Ross et al. 1984). A gel with 1 % agarose (w/v) was prepared using tris–acetate-EDTA (TAE) puffer containing 20 mM tris, 1 mM EDTA and 9.6 mM acetic acid. The reaction mixture with a final volume of 20 µl contained 0.5 U human topoisomerase II α, 200 ng kDNA, the test substance with a solvent concentration of 5 % EtOH (in case of perylene-quinones due to better stability) or DMSO and complete Topo II Assay Buffer from TopoGEN. The solution was allowed to react for 1 h at 37 °C, and the reaction was stopped on ice by adding loading buffer (25 % glycerol, 0.125 % bromphenolblue) with 5 % N-lauroylsarkosin. For dyeing of DNA bands, the gel was incubated for 20 min with 10 mg/l ethidium bromide solution. For quantification purposes, the fluorescence intensities of the decatenated kDNA bands at the lower end of the gels were used. The fluorescence signal was detected with the ImageQuant LAS-4000 (GE Healthcare Life Sciences, Buckinghamshire, England). Catenated DNA was quantified using Fujifilm Image Gauge software (Fujifilm Medical Systems USA, Inc., Connecticut, USA). For quantification the fluorescence intensities were normalized to solvent control (=100 %).

Gyrase supercoiling assay

The secondary metabolites were tested for their potential impact on the activity of the bacterial topo II gyrase with the gyrase supercoiling assay, where the difference in mobility between relaxed and supercoiled closed circular pUC19 was used (Gellert et al. 1976a). Gyrase from *E. coli* and relaxed 2686-bp-long puUC19 were purchased from New England Biolabs (Frankfurt am Main, Germany). A gel with 1 % agarose (w/v) was prepared using tris-acetat-EDTA (TAE) puffer containing 20 mM Tris, 1 mM EDTA and 9.6 mM acetic acid. Reaction mixture for determination of gyrase inhibition with a final volume of 20 µl contained 0.5 U gyrase, 250 ng pUC19, 35 mM Tris HCl (pH 7.5), 24 mM KCl, 4 mM $MgCl_2$, 2 mM DTT, 1.75 mM ATP, 5 mM spermidine, 0.1 mg/ml BSA and 6.5 % glycerol. The solution was allowed to react for 60 min at 37 °C, and the reaction was stopped on ice by adding loading buffer (25 % glycerol, 0.125 % bromphenolblue) with 5 % *N*-lauroylsarkosin. For dyeing of DNA bands, the gel was incubated for 20 min with 10 mg/l ethidium bromide solution. The fluorescence signal was detected with the ImageQuant LAS-4000 (GE Healthcare Life Sciences, Buckinghamshire, England). Catenated DNA was quantified using Fujifilm Image Gauge software (Fujifilm Medical Systems USA, Inc., Connecticut, USA). Activity of gyrase was assessed according to mobility shifts in the DNA pattern on the gel. Relaxed pUC19 demonstrated a lower migrating distance in the gel compared to the supercoiled analogue which was generated in case of active gyrase. The aminocoumarin antibiotic novobiocin (50 µM) was used as positive control (Gellert et al. 1976b). Quantification of the DNA bands via fluorescence intensity, as performed in the decatenation assay, was not applicable for this method because of the high degree of band multiplicity, presumably due to topoisomeres. Hence, the quantification was done by evaluating the observed initial inhibitory concentrations on the gels of at least three independent experiments and an average initial inhibitory concentration was calculated.

Results

Assessment of the impact of selected secondary metabolites from *Alternaria* and *Fusarium* spp. on the activity of human topo II α

The effect of 15 secondary metabolites of *Alternaria* and *Fusarium* fungi on the activity of human topo II α was evaluated with the decatenation assay (Table 1). Incubation

Table 1 Effect of *Alternaria* and *Fusarium* toxins of the activity of type IIA topoisomerases human topo II α and bacterial gyrase

	Initial inhibitory conc. (μM)	
	h topo II α	Gyrase
Alternaria spp.		
Perylene chinones		
ATX I	++	+++
ATX II	++++	++++
ALP	++	+++
STTX III	+++++	+++
Dibenzo-α-pyrones		
AOH	++++[a]	+++++
AME	++++[a]	+++++
Others		
ALN	+++	–
ALS	++++	–
PYR	+++	–
MAC	–	–
TEN	–	–
Fusarium spp.		
FB1	–	–
FC	–	–
MON	–	–
DON	–	–

Effects of mycotoxins on human recombinant topo II α (h topo II α) and bacterial gyrase based on at least three independent experiments (initial inhibition at: 10 μM (+++++), 25 μM (++++), 50 μM (+++), 75 μM (++) and 150 μM (+); no inhibition up to 150 μM (–))

[a] Fehr et al. (2009)

of human topo II α and kDNA for 1 h in the presence of all four *Alternaria* perylene-quinone-type mycotoxins decreased the activity of the enzyme in a concentration-dependent manner (Fig. 2). ATX I led to a significant decrease at 50 μM and was thus a weaker inhibitor than ATX II, for which an initial inhibitory concentration of 25 μM was observed. ALP, which showed the weakest impact on topo II α of the four compounds, significantly decreased topo II α activity at 75 μM. The most potent inhibitor in the decatenation assay was STTX III with an initial inhibitory concentration of 10 μM. Of the further five *Alternaria* metabolites tested in this assay, ALN, MAC, ALS, PYR (Fig. 3) and TEN (Fig. 4), the first four also showed inhibitory effects on human topo II α. Among these, ALS had the highest potency to suppress topo II-mediated decatenation with an initial inhibitory concentration of 25 μM, thus comparable to ATX II. According to the initial inhibitory concentrations in the decatenation assay, the potency for topo II inhibition declined in the row STTX III (10 μM) > ALS (25 μM) = ATX II (25 μM) > ALN (50 μM) = ATX I (50 μM) > ALP (75 μM) = PYR (75 μM) > MAC (150 μM). Of the four *Fusarium* metabolites that were examined, FB1, MON, DON and FC, none was tested positive for inhibition of the decatenating activity of topo II α up to a concentration of 150 μM (Fig. 4).

Assessment of the impact of selected secondary metabolites from *Alternaria* and *Fusarium* spp. on the activity of bacterial gyrase

In order to evaluate if the effects on human topo II were reflected with respect to interference with the bacterial homologue, the impact of the substances on gyrase from *E. coli* was measured with the gyrase supercoiling assay. This gel-based assay allows an estimation of a substance's inhibitory potential by assessing the migration of the plasmid pUC19, which is converted from the relaxed topoisomere to the more condensed and thus faster migrating supercoiled form by active gyrase. In Fig. 5 four exemplary gels are depicted of the three active *Alternaria* metabolites ATX I, AOH and AME, which reduced the supercoiling activity of gyrase to different extents, as well as the *Fusarium* mycotoin FB1, which did not show any targeting of gyrase. All four perylene-quinones, ATX I, ATX II, ALP and STTX III, impaired the activity of the enzyme (Fig. 6a). None of the other tested compounds, neither *Alternaria* nor *Fusarium* metabolites, had any effect on the activity of gyrase (Fig. 6b, c). Lane 1 of each gel represents the relaxed DNA plasmid, pUC19, without addition of enzyme or toxin, in lane 2 the respective solvent (DMSO) and gyrase were added. Lanes 3–8 and 3–19 show the addition of the tested compounds in a concentration range from 1 μM to 100 μM. Novobiocin (50 μM) was used as positive control (Figs. 5, lane 9, 6, lane 15). The conversion from the initially relaxed DNA plasmid to the supercoiled form catalyzed by gyrase can be seen when comparing lanes 1 (without gyrase) and 2 (with gyrase). With increasing concentrations of each of the active toxins, ATX I, ATX II, ALP, STTX III, AOH or AME, a shift from the supercoiled plasmid to the relaxed form was observable, indicative for an inhibition of the supercoiling activity of gyrase. The most pronounced inhibitory effects on gyrase activity were observed for the dibenzo-α-pyrones, AOH and AME (initial inhibitory concentrations of 10 μM), followed by the altertoxin ATX II (25 μM) and ATX I, ALP and STTX III (50 μM; Table 1).

Discussion

Topo II plays an important role in the maintenance and alteration of the topological structure of DNA in the course of cellular processes like replication or chromosomal segregation. Due to its involvement in this broad range of

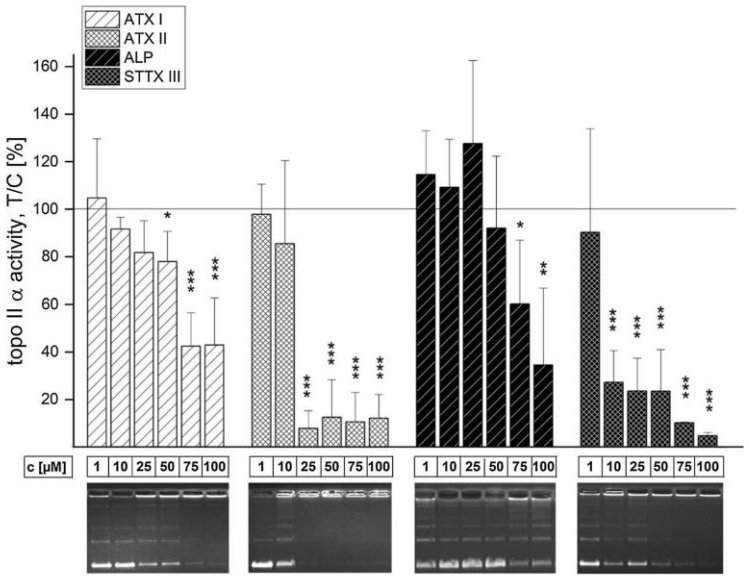

Fig. 2 Impact of *Alternaria* mycotoxins ATX I, ATX II, ALP and STTX III on the activity of human topo II α in the decatenation assay. Depicted are the fluorescence intensities of the catenated kDNA, normalized to solvent control (5 % EtOH) and representative gels. Bars refer to mean values ± standard deviation of at least three independent experiments. Significance levels refer to comparison with the respective smallest concentration of each substance ***$p < 0.001$, **$p < 0.01$, *$p < 0.5$)

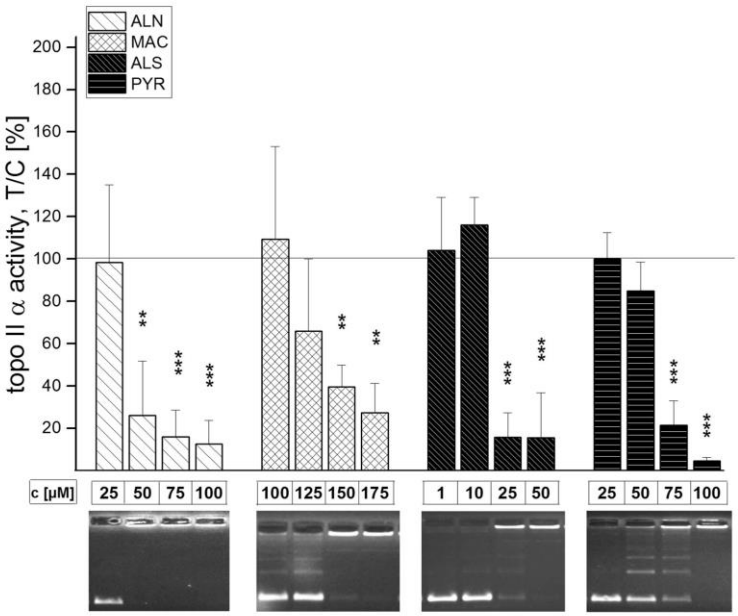

Fig. 3 Impact of *Alternaria* mycotoxins ALN, MAC, ALS and PYR on the activity of human topo II α in the decatenation assay. Depicted are the fluorescence intensities of the catenated kDNA, normalized to solvent control (5 % EtOH) and representative gels. Bars refer to mean values ± standard deviations of at least three independent experiments. Significance levels refer to comparison with the respective smallest concentration of each substance ***$p < 0.001$, **$p < 0.01$, *$p < 0.5$)

vital biological processes, compounds that interfere with the proper function of the enzyme pose a potential health threat. Previously three mycotoxins produced by the endophytic mold of the genus *Alternaria*, the perylenequinone derivative ATX II and the dibenzo-α-pyrones AOH and AME, have been described to affect the function of

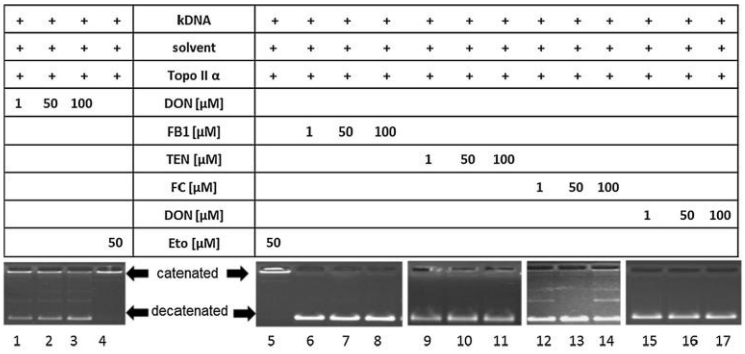

Fig. 4 Impact of secondary metabolites of *Fusarium* spp. on the activity of human topo II α in the decatenation assay. Depicted are representative gels of DON (*lanes 1–3*), FB1 (*lanes 6–8*), TEN (lanes 9–11), FC (*lanes 12–14*) and MON (*lanes 15–17*) with concentrations of 1, 50 and 100 µM each. Etoposide (50 µM) served as positive control (*lanes 4, 5*)

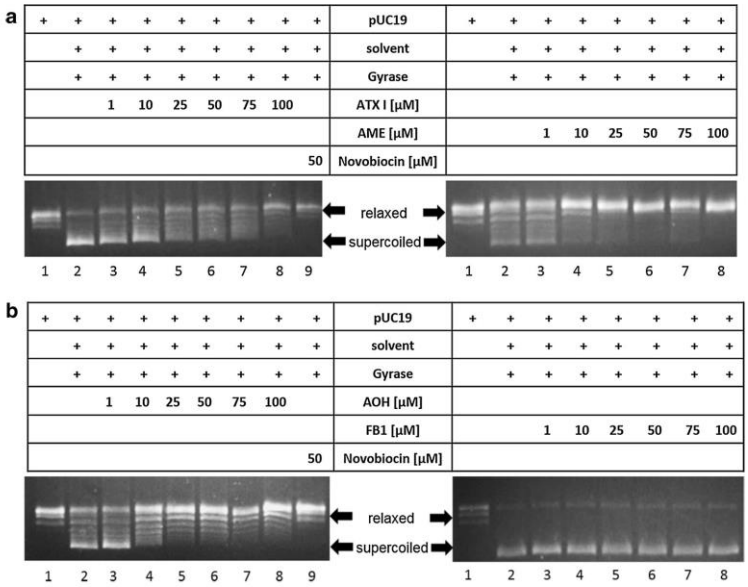

Fig. 5 Impact of secondary metabolites produced by *Alternaria* and *Fusarium* fungi on bacterial gyrase. Effect of **a** *Alternaria* perylene-quinone-type mycotoxin ATX I and dibenzo-α-pyrone AME and of **b** *Alternaria* mycotoxin AOH and *Fusarium* mycotoxin FB1 on the supercoiling activity of bacterial gyrase. *Lane 1* relaxed pUC19 without gyrase, *lane 2* addition of 0.5 U gyrase, *lanes 3–8* gyrase and toxins in the concentration range 1–100 µM in solvent (5 %), *lane 9* gyrase and novobiocin as positive control

human topo II (Fehr et al. 2009; Tiessen et al. 2013). These results opened a wider research field focused on the effect of fungal secondary metabolites on this important enzyme family. In the present work, 15 secondary metabolites, 11 of which are produced by *Alternaria* spp. and 4 by *Fusarium* spp., were investigated for their effects on human topo II α (Fig. 1). Except for TEN, all the secondary *Alternaria* metabolites inhibited the activity of human topo II α in the decatenation assay in a concentration range between 1 and 150 µM (Figs. 2, 3, 4). Within these ten topo II-targeting metabolites, no correlation between structural characteristics and inhibition potential was observable, except for the *Alternaria* perylene-quinone derivatives. Of the four assessed compounds that belong to this class, ATX II and STTX III revealed the most pronounced impact on the activity of human topo II α. Both mycotoxins contain an epoxide group, whereas their structural analogues ATX I and ALP, weaker inhibitors, lack this moiety (Fig. 1a). The correlation between the presence of an epoxide and, as a consequence thereof, an enhancement of the respective inhibitory potential was restricted to human topo II α within the perylene-quinones, since the activity of bacterial gyrase was reduced most effectively by the altertoxins ATX I and ATX II, with the same potency. Interestingly, the

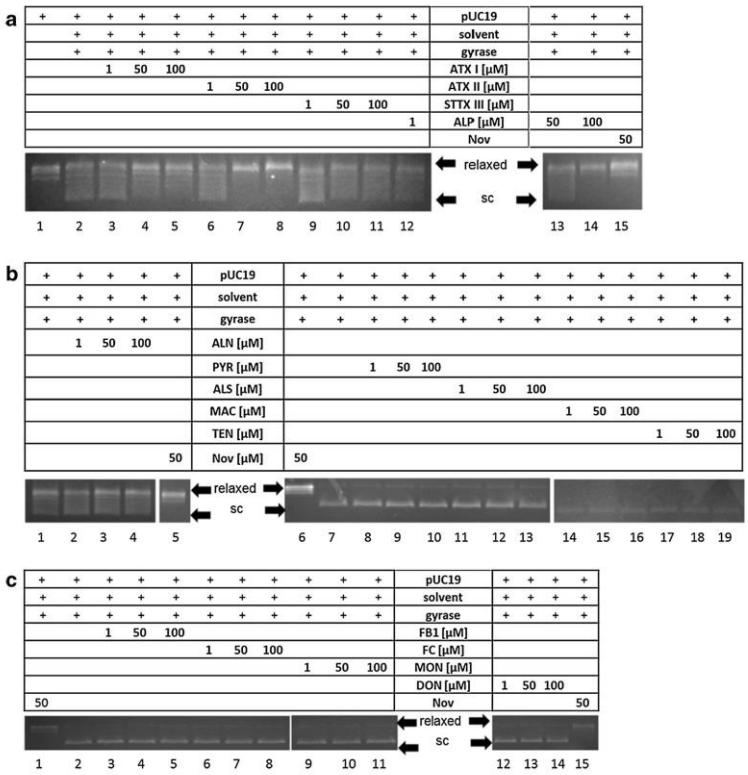

Fig. 6 Impact of secondary metabolites produced by *Alternaria* and *Fusarium* fungi on bacterial gyrase. **a** The perylene-quinone derivatives ATX I (*lanes 3–5*), ATX II (*lanes 6–8*), ALP (*lanes 9–11*) and STTX III (*lanes 12–14*), **b** *Alternaria* metabolites ALN (*lanes 2–4*), PYR (*lanes 8–10*), ALS (*lanes 11–13*), MAC (*lanes 14–16*) and TEN (*lanes 17–19*). In **c** gels of FB1 (*lanes 3–5*), FC (*lanes 6–8*), MON (*lanes 9–11*) and DON (*lanes 12–14*) are depicted. Novobiocin (50 µM) was used as positive control

Fusarium mycotoxin DON, also equipped with an epoxy moiety (Fig. 1d), did not show any impact on either human nor bacterial enzyme, possibly due to steric hindrance of the epoxide. Comparison of the two benzo-α-dipyrones, AOH and AME, which are structurally alike except for the additional methyl group in case of AME, showed that this moiety did not affect the inhibitory potency toward topo II (Fig. 1b). In line with these findings, AOH was previously described not only to suppress topo II activity under cell-free conditions but also to act as a topo II poison in intact cells, stabilizing the covalent topo-II-DNA intermediate (Fehr et al. 2009). In contrast, ATX II, also potent under cell-free conditions, did not affect the intracellular levels of the covalent topo-II-DNA intermediate, indicating a function as a catalytic inhibitor (Tiessen et al. 2013).

The impact on the activity of human topo II α, which was observed for 10 out of 15 tested secondary metabolites from *Alternaria* spp. in the decatenation assay, raised the question whether this mechanism was restricted to compounds produced by this genus. As an initial orientating study, considering the amount of known mycotoxins, four *Fusarium* metabolites out of different structural classes (FB1, MON, DON and FC; Fig. 1d) were examined for their effect on human topo II α. Of note, none of the tested *Fusarium* metabolites showed any interference with the enzyme (Fig. 4). Thus, the inhibition of topo II α seemed to be restricted to the secondary metabolites produced by *Alternaria* spp.

The present results indicated a common effect of inhibition of topo II by the tested secondary metabolites produced by *Alternaria* spp. Since topo II is an enzyme family ubiquitous not only in mammals, but plays a vital role in prokaryotes as well, the targeting of topo II by the secondary fungal metabolites may be based on a potential dual inhibition of the human enzyme and its bacterial homologue (Champoux 2001; McClendon and Osheroff 2007). In general, the biosynthesis of substances which interfere with cellular targets of potential predators, that are essential for survival in the food chain, is a mechanism that was described for other fungi imperfecti, as for instance the production of antibiotics by *Penicillium* or *Aspergillus* spp. (Lancini et al. 1995). Indeed, the bacterial topo II, gyrase,

is a target of many classes of pharmaceutical antibiotics (Gellert et al. 1976b). In line with this theory, investigations of the impact of the tested secondary metabolites on gyrase from *E. coli* revealed that some of the tested secondary metabolites showed an effect on both the human and bacterial topo II, while other substances were only active against the human enzyme (Table 1). The compounds that suppressed both the human and the bacterial analogue were the perylene-quinone-type mycotoxins and the dibenzo-α-pyrones from *Alternaria* spp. These results support our theory that the impairment of the function of human topo II by secondary fungal metabolites may be attributed to the high degree of homology between human and bacterial enzyme. This implies that gyrase probably constitutes the main target of *Alternaria* spp., but their secondary metabolites affect human topo II as well. Such a dual targeting of topoisomerases was reported for other compounds, for instance the coumarin novobiocin, which targets mammalian as well as prokaryotic topo II (Larsen et al. 2003). Furthermore, several novel quinolone derivatives were shown to be active against both bacterial gyrase and its homolog, also of bacterial origin, the tetrameric topoisomerase IV (Mitton-Fry et al. 2013).

To the best of our knowledge, so far no data about the antibacterial activity of the perylene-quinones or the dibenzo-α-pyrones tested in this study have been published. On the contrary, antibiotic effects were described for some of the metabolites that inhibited human topo II α but not gyrase, to which ALN, ALS, PYR and MAC belong (Fig. 2; Table 1). Antibiotic properties of ALN toward gram-positive bacteria were reported previously, while gram-negative ones, among which *E. coli* are counted, were not affected (Schobert and Schlenk 2008). Furthermore, bacteria possess a second topo II aside from gyrase, topoisomerase IV, which also represents a target of antibiotics (Kato et al. 1990; Khodursky et al. 1995). Although gyrase and topo IV share a high degree of homology, antibacterial agents differ in their sensitivity toward the two enzymes (Hooper 1999; Pommier et al. 2010; Takei et al. 2001). Hence, it is possible to speculate that the compounds that did not affect gyrase, but were active against human topo II, may potentially target topo IV. This specificity for topo IV was also reported for the glycosylated flavonoid quercetin (Bernard et al. 1997). ALS, which inhibited human topo II but not gyrase, might also target topo IV, since the substance was previously reported to decrease the growth of a spectrum of pathogenic bacteria (Kjer et al. 2009).

Only one of the *Alternaria* metabolites, the phytotoxin TEN, and all 4 tested *Fusarium* compounds did not reveal an inhibitory potency against either human or bacterial topo II (Halloin et al. 1970). Interestingly, antibacterial characteristics were described for DON in *Streptococcus agalactaie*, but not *E. coli* (Ali-Vehmas et al. 1998). Presumably the mechanism of action behind the reported antibacterial characteristics was not topo II-related. Generally, the impairment of topo II seemed to be limited to the secondary metabolites from *Alternaria* spp. that were tested in this study, whereas the *Fusarium* mycotoxins did not show any effect on this enzyme, neither on the human nor on the bacterial one.

In conclusion, 10 out of 15 secondary metabolites produced by *Alternaria* spp., evaluated for their impact on human topo II in the present work, revealed an inhibitory potential. Additionally, the perylene-quinone derivatives and the dibenzo-α-pyrones were also active against the bacterial homologue, gyrase, which indicated a dual inhibition of human as well as bacterial topo II. In contrast, none of the tested *Fusarium* metabolites revealed any interference with either human topo II or gyrase. With respect to food safety, interference with topo II apparently has to be considered as a potential genotoxic mechanism for a broader spectrum of *Alternaria* metabolites. On the other hand, in medicinal chemistry, topo II inhibition is a well-used drug effect in cancer therapy. Moreover, targeting of bacterial gyrase is a promising feature toward the identification of novel antibiotic structures. Considering the broad spectrum of secondary metabolites formed by *Alternaria* spp. and the already identified structures with activity toward human topo II and bacterial gyrase, it is likely to speculate that *Alternaria* secondary metabolites might represent a promising pool for the identification of compounds with pharmaceutical potency.

Acknowledgments Open access funding provided by University of Vienna. The authors thank Hannes Puntscher for the technical support.

References

Ali-Vehmas T, Rizzo A, Westermarck T, Atroshi F (1998) Measurement of antibacterial activities of T-2 toxin, deoxynivalenol, ochratoxin A, aflatoxin B1 and fumonisin B1 using microtitration tray-based turbidimetric techniques. J Vet Med Ser A Physiol Pathol Clin Med 45(8):453–458. doi:10.1111/j.1439-0442.1998.tb00848.x

Alt S, Mitchenall LA, Maxwell A, Heide L (2011) Inhibition of DNA gyrase and DNA topoisomerase IV of *Staphylococcus aureus* and *Escherichia coli* by aminocoumarin antibiotics. J Antimicrob Chemother 66(9):2061–2069. doi:10.1093/jac/dkr247

Bernard FX, Sablé S, Cameron B, Provost J, Desnottes JF, Crouzet J, Blanche F (1997) Glycosylated flavones as selective inhibitors of topoisomerase IV. Antimicrob Agents Chemother 41(5):992–998

Champoux JJ (2001) DNA topoisomerases: structure, function, and mechanism. Annu Rev Biochem 70:369–413. doi:10.1146/annurev.biochem.70.1.369

Champoux JJ, Dulbecco R (1972) An activity from mammalian cells that untwists superhelical DNA—a possible swivel for DNA replication (polyoma-ethidium bromide-mouse-embryo cells–dye binding assay). Proc Natl Acad Sci USA 69(1):143–146

DiNardo S, Voelkel K, Sternglanz R (1984) DNA topoisomerase II mutant of *Saccharomyces cerevisiae*: topoisomerase II is required for segregation of daughter molecules at the termination of DNA replication. Proc Natl Acad Sci USA 81(9I):2616–2620

Fehr M, Pahlke G, Fritz J, Christensen MO, Boege F, Altemoeller M, Podlech M, Marko D (2009) Alternariol acts as a topoisomerase poison, preferentially affecting the IIα isoform. Mol Nutr Food Res 53(4):441–451. doi:10.1002/mnfr.200700379

Gellert M, Mizuuchi K, O'Dea MH, Nash HA (1976a) DNA gyrase: an enzyme that introduces superhelical turns into DNA. Proc Natl Acad Sci USA 73(11):3872–3876

Gellert M, O'Dea MH, Itoh T, Tomizawa J (1976b) Novobiocin and coumermycin inhibit DNA supercoiling catalyzed by DNA gyrase. Proc Natl Acad Sci USA 73(12):4474–4478

Halloin JM, De Zoeten GA, Walker JC (1970) The effects of tentoxin on chlorophyll synthesis and plastid structure in cucumber and cabbage. Plant Physiol 45(3):310–314. doi:10.1104/pp.45.3.310

Hooper DC (1999) Mode of action of fluoroquinolones. Drugs 58(Suppl 2):6–10. doi:10.2165/00003495-199958002-00002

Hradil CM, Hallock YF, Clardy J, Kenfield DS, Strobel G (1989) Phytotoxins from *Alternaria cassiae*. Phytochemistry 28(1):73–75. doi:10.1016/0031-9422(89)85011-3

Hsieh TS, Brutlag D (1980) ATP-dependent DNA topoisomerase from D. melanogaster reversibly catenates duplex DNA rings. Cell 21(1):115–125. doi:10.1016/0092-8674(80)90119-1

Hübner F, Harrer H, Fraske A, Kneifel S, Humpf H-U (2012) Large scale purification of B-type fumonisins using centrifugal partition chromatography (CPC). Mycotoxin Res 28(1):37–43. doi:10.1007/s12550-011-0114-7

Jarolim K, Del Favero G, Pahlke G et al (2016) Activation of the Nrf2-ARE pathway by the *Alternaria alternata* mycotoxins altertoxin I and II. Arch Toxicol. doi:10.1007/s00204-016-1726-7

Kato J, Nishimura Y, Imamura R, Niki H, Hiraga S, Suzuki H (1990) New topoisomerase essential for chromosome segregation in *E. coli*. Cell 63(2):393–404. doi:10.1016/0092-8674(90)90172-b

Kharwar RN, Upadhyay RS, Dubey NK, Raghuwanshi R (2014) Microbial diversity and biotechnology in food security. Springer, Varanasi

Khodursky AB, Zechiedrich EL, Cozzarelli NR (1995) Topoisomerase IV is a target of quinolones in *Escherichia coli*. Proc Natl Acad Sci USA 92(25):11801–11805. doi:10.1073/pnas.92.25.11801

Kjer J, Wray V, Edrada-Ebel R, Ebel R, Pretsch A, Lin W, Proksch P (2009) Xanalteric acids I and II and related phenolic compounds from an endophytic *Alternaria* sp. Isolated from the mangrove plant *Sonneratia alba*. J Nat Prod 72(11):2053–2057. doi:10.1021/np900417g

Kleigrewe K, Söhnel A-C, Humpf H-U (2011) A new high-performance liquid chromatography-tandem mass spectrometry method based on dispersive solid phase extraction for the determination of the mycotoxin fusarin C in corn ears and processed corn samples. J Agric Food Chem 59(19):10470–10476. doi:10.1021/jf2026814

Lancini G, Parenti F, Gallo GG (1995) Antibiotics: a multidisciplinary approach. Springer, New York

Larsen AK, Escargueil AE, Skladanowski A (2003) Catalytic topoisomerase II inhibitors in cancer therapy. Pharmacol Ther 99(2):167–181. doi:10.1016/s0163-7258(03)00058-5

Liu LF, Liu C-C, Alberts BM (1980) Type II DNA topoisomerases: enzymes that can unknot a topologically knotted DNA molecule via a reversible double-strand break. Cell 19(3):697–707. doi:10.1016/S0092-8674(80)80046-8

Lohrey L, Murata T, Uemura D, Humpf HU (2011) Synthesis of isotopically labeled fusarium mycotoxin 13C 2-moniliformin [1-hydroxycyclobut-1-ene-3,4-dione]. Synlett 15:2242–2244. doi:10.1055/s-0030-1261189

Magan N, Aldred D (2007) Why do fungi produce mycotoxins? In: Dijksterhuis J, Samson A (eds) Food mycology: a multifaceted approach to fungi and food. CRC Press, New York

McClendon AK, Osheroff N (2007) DNA topoisomerase II, genotoxicity, and cancer. Mutat Res 623(1–2):83–97. doi:10.1016/j.mrfmmm.2007.06.009

Mitton-Fry MJ, Brickner SJ, Hamel JC et al (2013) Novel quinoline derivatives as inhibitors of bacterial DNA gyrase and topoisomerase IV. Bioorg Med Chem Lett 23(10):2955–2961. doi:10.1016/j.bmcl.2013.03.047

Okuno T, Natsume I, Sawai K, Sawamura K, Furusaki A, Matsumoto T (1983) Structure of antifungal and phytotoxic pigments produced by alternaria sps. Tetrahedron Lett 24(50):5653–5656. doi:10.1016/s0040-4039(00)94165-0

Placinta CM, D'Mello JPF, Macdonald AMC (1999) A review of worldwide contamination of cereal grains and animal feed with Fusarium mycotoxins. Anim Feed Sci Technol 78(1–2):21–37. doi:10.1016/s0377-8401(98)00278-8

Pommier Y, Leo E, Zhang H, Marchand C (2010) DNA topoisomerases and their poisoning by anticancer and antibacterial drugs. Chem Biol 17(5):421–433. doi:10.1016/j.chembiol.2010.04.012

Ross W, Rowe T, Glisson B, Yalowich J, Liu L (1984) Role of topoisomerase II in mediating epipodophyllotoxin-induced DNA cleavage. Cancer Res 44(12 I):5857–5860

Schobert R, Schlenk A (2008) Tetramic and tetronic acids: an update on new derivatives and biological aspects. Bioorg Med Chem 16(8):4203–4221. doi:10.1016/j.bmc.2008.02.069

Schwarz C, Kreutzer M, Marko D (2012a) Minor contribution of alternariol, alternariol monomethyl ether and tenuazonic acid to the genotoxic properties of extracts from *Alternaria alternata* infested rice. Toxicol Lett 214(1):46–52. doi:10.1016/j.toxlet.2012.08.002

Schwarz C, Tiessen C, Kreutzer M, Stark T, Hofmann T, Marko D (2012b) Characterization of a genotoxic impact compound in *Alternaria alternata* infested rice as Altertoxin II. Arch Toxicol 86(12):1911–1925. doi:10.1007/s00204-012-0958-4

Stack ME, Mazzola EP (1989) Stemphyltoxin III from *Altenaria alternata*. J Nat Prod 52(2):426–427. doi:10.1021/np50062a042

Stack ME, Prival MJ (1986) Mutagenicity of the Alternaria metabolites altertoxins I, II, and III. Appl Environ Microb 52(4):718–722

Takei M, Fukuda H, Kishii R, Hosaka M (2001) Target Preference of 15 quinolones against *Staphylococcus aureus*, based on antibacterial activities and target inhibition. Antimicrob Agents Chemother 45(12):3544–3547. doi:10.1128/aac.45.12.3544-3547.2001

Tiessen C, Gehrke H, Kropat C, Schwarz C, Baechler S, Fehr M, Pahlke G, Marko D (2013) Role of topoisomerase inhibition and DNA repair mechanisms in the genotoxicity of alternariol and altertoxin-II. World Mycotoxin J 6(3):233–244. doi:10.3920/wmj2013.1592

Attachment: Publication 3

Toxicology Letters 284 (2018) 170–183

Contents lists available at ScienceDirect

Toxicology Letters

journal homepage: www.elsevier.com/locate/toxlet

The secondary *Fusarium* metabolite aurofusarin induces oxidative stress, cytotoxicity and genotoxicity in human colon cells

Katharina Jarolim[a], Konstantin Wolters[a], Lydia Woelflingseder[a], Gudrun Pahlke[a], Julia Beisl[a], Hannes Puntscher[a], Dominik Braun[a], Michael Sulyok[b], Benedikt Warth[a], Doris Marko[a,*]

[a] University of Vienna, Faculty of Chemistry, Department of Food Chemistry and Toxicology, Währinger Straße 38, 1090 Vienna, Austria
[b] University of Natural Resources and Life Sciences Vienna (BOKU), Department IFA-Tulln, 3430 Tulln, Austria

GRAPHICAL ABSTRACT

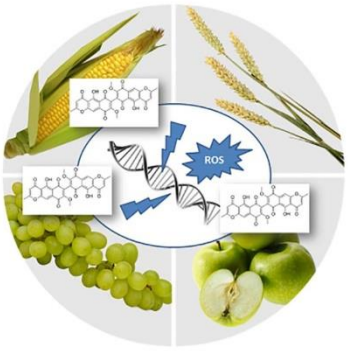

ARTICLE INFO

Keywords:
Mycotoxin
Aurofusarin
Food safety
Cytotoxicity
Genotoxicity
Reactive oxygen species

ABSTRACT

Aurofusarin (AURO), a dimeric naphthoquinone, is produced by *Fusarium* fungi. Although frequently found in food and feed, toxicological studies are limited. Hence, the *in vitro* toxicity of AURO was investigated in the colon adenocarcinoma cell line HT29 and the non-tumorigenic colon cells HCEC-1CT. Cytotoxic effects were found at concentrations ≥1 μM by evaluating mitochondrial activity (WST-1) and cellular proliferation (sulforhodamine B assay). 10 μM of AURO induced a decrease of cells in the S-phase, measured by flow cytometry. Confocal microscopy revealed AURO-mediated increase of intracellular p53 protein. In accordance, DNA-damage was seen in the comet assay (≥1 μM) together with enhanced levels of formamidopyrimidine-DNA-glycosylase (fpg)-sensitive sites, indicative for oxidative stress. An increase of intracellular reactive oxygen species was observed in the dichlorofluorescein (DCF) assay (≥5 μM). The GSSG/GSH ratio was elevated, but no impact on redox-sensitive Nrf2-dependent genes (Nrf2, γ-GCL, NQO1) was found at the gene expression level. However, induction of cytochrome P450 monooxygenase (CYP) 1A1 was measured at the gene expression and protein level. In conclusion, these *in vitro* data suggest that, when co-occurring, AURO might be considered as a potential contributor to the overall toxicity of respective *Fusarium* mycotoxin mixtures.

* Corresponding author.
E-mail address: doris.marko@univie.ac.at (D. Marko).

https://doi.org/10.1016/j.toxlet.2017.12.008
Received 27 June 2017; Received in revised form 22 November 2017; Accepted 11 December 2017
Available online 14 December 2017
0378-4274/

1. Introduction

Fungi of the genus *Fusarium* are ubiquitously occurring molds that grow on a variety of cereal crops, and cause the plant diseases ear rot and head blight which can result in severe losses of crop yield (Bottalico and Perrone, 2002). Different *Fusarium* species produce a variety of secondary metabolites, many of which are described to induce adverse effects in humans and animals, therefore classified as mycotoxins. For the most common *Fusarium* mycotoxins such as the trichothecenes, zearalenone and the fumonisins, the toxicological effects are well known and thus legal maximum limits have been established in the European Union (European Commission, 2006; JECFA, 2011). However, besides these well-investigated mycotoxins, *Fusarium* spp. produce further secondary metabolites, for which the toxicological potential has not been characterized yet. These contaminants are thus not classified as mycotoxins, although they may constitute a potential issue for health and consumer safety. One of the *Fusarium* metabolites that have not been elucidated yet with regard to toxicological potential is AURO, a coloring pigment that was originally isolated from the mycelium of *Fusarium culmorum* strains in 1937, long before the first mycotoxins were described in the 1960's (Ashley et al., 1937). Subsequent elucidation of the chemical structure revealed that the molecule is a dimeric naphthoquinone (Fig. 1) (Baker and Roberts 1966; Shibata et al., 1966). Although naphthoquinones and their derivatives have been associated with adverse effects such as cytotoxicity, genotoxicity and oxidative stress (Demma et al., 2009; Frydman et al., 1997; Srinivas et al., 2004; Thor et al., 1982), studies on the toxicological impact of AURO are still very limited. The metabolite was shown to interfere with antioxidants and fatty acids in eggs and embryos of quails (Dvorska et al., 2001, 2002). Moreover, AURO was found to negatively affect the growth performance of red tilapia (Tola et al., 2015) and to be cytotoxic in mammalian cells (Uhlig et al., 2006; Vejdovszky et al., 2016).

AURO is produced by a variety of *Fusarium* spp. and is therefore frequently found in food and feed from different climatic regions. Some examples include maize from Malawi or Italy, in which concentrations up to 2046 µg/kg were reported (Blandino et al., 2015; Matumba et al., 2015). In Nigerian poultry feed and fonio millet AURO contaminations up to 10200 and 7280 µg/kg were detected, respectively (Ezekiel et al., 2012a,b). The metabolite was also found in samples from temperate climate regions in central and northern European countries including barley, oats and wheat from Norway or grapes from Slovakia (Mikušová et al., 2013; Uhlig et al., 2013). Thus, a toxicological characterization of the contaminant may contribute to the knowledge of potential health risks associated with the unintended dietary intake of *Fusarium* infested foodstuff.

In the present study, the impact of AURO on several endpoints of toxicological relevance was examined in order to elucidate the toxicological relevance of the frequently found secondary metabolite, using the adenocarcinoma cell line HT29 and the extended primary cell line HCEC-1CT. The conducted experiments investigated cytotoxicity, genotoxicity, oxidative stress and the potential effect on genes involved in the cellular redox environment, interference with topoisomerase II and the glutathione system, as well as potential DNA intercalation. Furthermore, an LC–MS/MS method was developed and applied to comprehensively characterize the compound's stability.

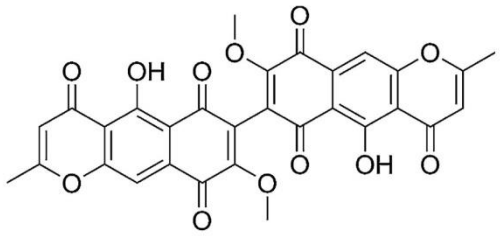

Aurofusarin

Fig. 1. Chemical structure of AURO.

2. Methods

2.1. Chemicals

Aurofusarin was purchased from Biovitica with a purity of 97.5% (Bioviotica Naturstoffe GmbH, Dransfeld, Germany). The substance was dissolved in dimethylsulfoxide (DMSO) to yield a stock solution of 1 mM, ultrasonicated for 5 min, aliquoted and stored at −20 °C. A new stock solution was prepared every 2 months.

2.2. Cell culture

HT29 human colon adenocarcinoma cells were purchased from the German Collection of Microorganisms and Cell Cultures (DSMZ, Braunschweig, Germany). Cells were cultivated in Dulbecco's Modified Eagle Medium, supplemented with 10% inactivated fetal calf serum and 1% penicillin/streptomycin (50 U/ml; referred to as complete medium). HCEC-1CT cells were kindly provided by Prof. Jerry W. Shay (UT Southwestern Medical Center, Dallas, TX, USA) and cultured in a basal medium obtained from Dulbecco's Modified Eagle Medium (high glucose) supplemented with 2% 10X medium 199, 2% cosmic calf serum, 20 mM HEPES, 50 µg/ml gentamicin, 10 µl/ml insulin-transferrin-selenium-G supplement, 20 ng/ml recombinant human EGF and 1 µg/ml hydrocortisone. Media and supplements were purchased from Invitrogen Life Technologies (Karlsruhe, Germany). Cells were cultivated at 37 °C and 5% CO_2 in a humidified incubator and routinely tested for mycoplasma contamination. AURO was dissolved in DMSO and incubated in complete medium with a final DMSO concentration of 1%.

2.3. Stability assessment

We evaluated the stability of AURO in DMSO, which is the typical solvent in cell culture assays and in an acetonitrile (ACN)/water mixture, which is frequently used for analytical purpose. Due to its limited solubility in other solvents AURO was initially dissolved in 100% DMSO to yield a concentration of 1 mM corresponding to 553.4 mg/l. This stock solution was diluted to a concentration of 0.18 mM or 100 mg/l in either 30% ACN or 100% DMSO and subsequently stored in triplicates. All samples were kept in amber vials, except those intended to investigate the influence of light exposure, for which clear vials were used. Control samples for each solvent were kept as references at −80 °C immediately after preparation, without further treatment. AURO samples containing 30% ACN as solvent were stored for 1 d, 3 d, 7 d, 14 d and 56 d under the following conditions: −20 °C, 4 °C, room temperature (RT, on average 22.8 °C) and 37 °C. To investigate the influence of exposure to light, ACN samples were also stored at RT for the same time intervals in common glass vials in the lab. Furthermore, the solvents ACN and DMSO were compared for their potential impact on AURO stability after storage for 14 d and 56 d at −20 °C. In order to determine the stability of AURO in cell culture medium, additional AURO samples in DMEM, containing 10% FCS, 1% P/S and 1% DMSO, were kept for 3 d at 37 °C. Moreover, the impact of ultrasonication (US, 15 min) and of three freezing and thawing cycles at −20 °C (FT) on AURO concentration was tested. The respective vials were stored at −80 °C until the day of measurement, for 14 d. All storage conditions were tested in triplicate. Samples were measured using the LC–MS/MS method described below and results were expressed as mean values ± SD, relative to the solvent reference.

Attachment: Publication 3

2.4. Liquid chromatography tandem mass spectrometry

For measurement of the stability testing samples, a sensitive and specific LC–MS/MS method was developed. A Thermo TSQ Vantage LC–MS/MS triple quadrupole system (Thermo, San Jose, CA, USA) coupled to a Dionex D3000 UHPLC system was utilized and operated in the positive ionization mode. For chromatographic separation a Kinetex Biphenyl column (3.0 × 150 mm, Phenomenex, Torrance, CA, US) equipped with a 2.6 µm particle size and a SecurityGuard ULTRA pre-column (Phenomenex) was used. Gradient elution was performed at 40 °C and a flow rate of 0.4 ml/min within 14 min. Eluent A (H_2O/ACN; 90/10) and eluent B (ACN) both contained 0.1% formic acid. After an initial time period of 1.0 min at 100% A, the percentage of B was raised to 50% until minute 2.0. Then, eluent B was raised to 95% until minute 8.0 followed by a hold-time of 2.0 min and subsequent 4.0 min column re-equilibration at 100% A. A volume of 5 µl was injected. AURO eluted after 7.03 min. Electrospray (ESI) MS/MS was performed in selected reaction monitoring (SRM). The two transitions m/z 571.1 $[M+H]^+ \rightarrow$ 485.2/429.1 with the corresponding collision energies of 37/58 eV were monitored for AURO. The S-lens was set to 179. MS/MS parameters were optimized via direct infusion of the reference standards. Quantification of all analytes for which reference standards were available was done by external calibration curves (1/x weighted). Nitrogen was used as drying and argon as collision gas. The parameters of the ion source were as follows: Source temperature 300 °C, capillary voltage 3000 V, collision gas pressure 1.5 mTorr, sheath gas pressure 50 au, ion sweep gas pressure 0 au, aux gas pressure 30 au, capillary temperature 300 °C. Data acquisition was performed using the Xcalibur software (version 3.1) and the quantitative evaluation was done using TraceFinder (version 3.3).

2.5. Mitochondrial activity

The mitochondrial activity of HT29 and HCEC-1CT cells was evaluated by the water soluble tetrazolium salt-1 assay (WST-1; Roche Applied Science, Basel, Switzerland). For 1 h incubations 20,000 HT29 or 1,500 HCEC-1CT cells were seeded whereas for a 24 h incubation 7,500 HT29 or 1,000 HCEC-1CT cells were used in 96 well plates in complete medium and allowed to attach and grow for 48 h. This was followed by incubations with AURO for 1 h and 24 h in complete medium at final concentrations of 0.01, 0.1, 1, 5 and 10 µM. DMSO (1%; v/v) was used as solvent control and 0.1% triton x-100 as a positive control. The assay was performed according to the manufacturer's protocol (Cell Proliferation Reagent WST-1, Roche, Basel, Switzerland). Extinction was measured at 450 and 650 nm with the plate reader (Victor V3 14200; Perkin Elmer Inc, Massachusetts, USA).

2.6. Cellular proliferation

The proliferation of HT29 cells was tested with the sulforhodamine B assay (Skehan et al., 1990). 6,500, 3,000 or 1,000 HT29 cells or 1,500, 1,000 or 750 HCEC-1CT cells were seeded for incubation times of 24 h, 48 h and 72 h, respectively, in 96 well plates in complete medium and allowed to grow for 48 h. Cells were incubated with AURO concentrations of 0.01, 0.1, 1, 5 and 10 µM in complete medium at a final DMSO concentration of 1% which was used as solvent control. Cells were seeded in technical triplicates. The assay was performed according to manufacturer's protocol (Sigma Aldrich, Merck,Vienna, Austria). Absorption was measured at 570 nm with a plate reader (Victor V3 14200; Perkin Elmer Inc, Massachusetts, USA). A blank (medium and 1% DMSO without cells) was distracted from the values of the wells containing cells. All values were normalized to solvent control 1% DMSO.

2.7. Cell cycle analysis

The cell cycle analysis was performed using Guava Cell Cycle Reagent (Merck Millipore, Darmstadt, Germany). Preparation and fixation were performed according to manufacturer's recommendations. Shortly, HT29 and HCEC-1CT cells were seeded at densities of 30,000 and 10,000 cells per well in 24 well plates respectively and allowed to grow for 72 h prior to a 24 h incubation. HT29 cells were harvested using trypsin (Sigma-Aldrich, Missouri, USA), HCEC-1CT cells with accutase (Sigma-Aldrich, Missouri, USA). The cells were washed with PBS and centrifuged, followed by the fixation in ice-cold ethanol. After removing the ethanol in another washing step, cells were stained with Guava Cell Cycle Reagent for 30 min and a total of 5,000 cells was measured immediately by flow cytometry using a Millipore Guava EasyCyte 5 (Merck Millipore, Darmstadt, Germany). Data analysis was carried out with ModFit LT 5.0 software using the synchronization wizard with a G_2/G_1 ratio of 1.9 and a trapezoid S-phase shape.

2.8. Immunocytochemical staining and microscopic assessment of p53, γ-H2AX and cellular morphology

The activity of p53 as a marker of DNA-damage, the phosphorylation of H2AX, indicative of DNA double strand breaks, as well as the overall morphological changes in HT29 and HCEC-1CT cells were evaluated by immunocytochemical stainings and analysis by confocal microscopy (Burma et al., 2001; Kastan et al., 1991). For this purpose, cells were seeded in 8 well microscopy slides (Falcon, Corning, USA). After 48 h, cells were incubated for 1, 3 and 24 h with 5 and 10 µM AURO and additionally, 50 µM Etoposide was used as positive control. At the end of the incubation period, incubation solutions were removed; cells were washed with pre-warmed PBS and fixed with 3.7% formaldehyde for 20 min. Subsequently, cells were rinsed twice with PBS and stored prior to staining at 4 °C. Cells were permeabilized for 30 min using 0.2% triton x-100, washed once with PBS and blocked for 90 min at RT using 10% normal goat serum. Then the primary antibodies were added and incubated for 14 h at 4 °C. Primary antibodies were purchased from Abcam (Cambridge, UK) and Santa Cruz Biotechnology (Heidelberg, Germany) and used according to the specification of the supplier: anti-histone H2A.X (phosphor S139) rabbit monoclonal antibody (ab195189; dilution 1:200) and anti-p53 (FL-393) rabbit polyclonal antibody (sc-6243; dilution 1:50). After removal of the primary antibodies, cells were rinsed once with 0.05% triton x-100 and further incubated using a fluorescence-labeled secondary antibody and Alexa Fluor 488 Phalloidin for 1.5 h. In this study Alexa Fluor 568 Donkey Anti-Rabbit (A10042) antibody was used in a 1:350 dilution for p53 stainings on both cells lines. Alexa Fluor 488 Phalloidin was incubated on HT29 cells in a 1:200 dilution and on HCEC-1CT cells in a 1:400 dilution (Life Technologies, Karlsruhe, Germany). The slides were then washed several times with 0.05% triton x-100 and PBS and post-fixed with 3.7% formaldehyde (15 min, RT). Afterwards a 100 mM glycine solution was used to mask reactive sites and slides were mounted and sealed with Roti-Mount FluorCare DAPI (Roth, Graz, Austria). Images were acquired using a Confocal LSM Zeiss 710 equipped with ELYRA PS. 1 system. For the acquisition of the confocal images a Plan Apochromat 100 × /1.46 oil objective was used and for each cell preparation, at least three different optical fields were acquired. In order to ensure the comparability of the fluorescence signals the acquisition of each incubation time point, cell line and staining was performed the same day, maintaining constant laser parameters (power, digital gain).

2.9. DNA integrity

The genotoxic potential of AURO in HT29 cells was assessed by single cell gel electrophoresis, also called comet assay (Collins, 2004). For this purpose, 150,000 cells were seeded in petri dishes (Ø = 3.5 cm) in complete medium and allowed to grow for 48 h. Cells were incubated

with AURO concentrations 0.01, 0.1, 1, 5 and 10 μM in complete medium and at a final DMSO concentration of 1% for 1 h which was used as solvent control. The comet assay was performed as described before by Schwarz et al. (2012a,b). Briefly, the cells were detached by trypsin, counted and tested for viability with the trypan blue exclusion test. Cells with a viability > 80% were used for the assay. Cells (30.000) were embedded in 0.8% low melting agarose on microscopy slides and lysed. For each sample an additional slide was incubated with formamidopyrimidine-DNA-glycosylase (fpg) for 20 min. Subsequently, electrophoresis was conducted, followed by neutralization in a Tris/HCl buffer (pH 7.5). Before microscopic analysis the slides were stained with ethidium bromide. Tail intensities of 100 cells per slide were analyzed with the Comet Assay IV software (Perceptive Instruments, England) on a fluorescence microscope (Axioskop A1, Zeiss, Germany). After analysis, the mean value of 100 counted cells was calculated.

2.10. Formation of reactive oxygen species

The amount of reactive oxygen species produced in HT29 cells after incubation with AURO was assessed with the dichlorofluorescein (DCF) assay. This method takes advantage of the intracellular oxidation of the non-fluorescent 2′,7′-dihydrodichlorofluorescin to the fluorescent dye DCF after cellular uptake and de-esterification of 2′, 7′-dichlorofluorescin diactetate (Wang and Joseph, 1999). For this assay, 20,000 HT29 cells were seeded in 96 well plate and allowed to grow for 48 h. The cells were incubated with AURO concentrations of 0.01, 0.1, 1, 5 and 10 μM in complete medium with a final DMSO concentration of 1%. DMSO (1%) was used as solvent control and 50 μM H_2O_2 as positive control. DCF was measured at 495 nm excitation and 529 nm emission. A blank (medium and 1% DMSO without cells) was distracted from the values of the wells containing cells. All values were normalized to solvent control (1% DMSO).

2.11. GSH and GSSG level

The GSH and GSSG levels were measured in HT29 cells after 1 h, 3 h and 24 h of incubation with AURO at concentrations of 0.01, 0.1, 1, 5 and 10 μM according to Tietze (1969). Cells were seeded in petri dishes (Ø = 10 cm) and allowed to grow for 48 h, 1.6×10^6 cells for 1 h and 3 h incubations and 1.2×10^6 cells for the 24 h incubation experiments. Cells were incubated with AURO concentrations 0.01, 0.1, 1, 5 and 10 μM in complete medium and 1% final DMSO concentration. 1%. DMSO was used as solvent control, 200 μM *tert*-butylhydroquinone (tBHQ) as positive control for all incubation times, 0.01% 2-vinylpyridine (2-VP) for the short term (1 h and 3 h) and 1 mM buthionine sulfoximine (BSO) for the 24 h incubation, due to cytotoxicity of the former after 24 h of incubation. Cells were detached, centrifuged (4 °C, 420 x *g*, 10 min) and the pellet was resuspended in 370 μl buffer (23 mM KH_2PO_4, 107 mM K_2HPO_4, 8 mM EDTA, pH 7.5). Protein levels were determined with the bicinchoninic acid kit (Sigma) after precipitation with 10% sulfosalicylic acid (SSA) on ice, followed by centrifugation (4 °C, 20819 x *g*, 10 min). Measurement of tGSH and GSSG levels was performed as described by Jarolim et al. (2016b). The levels of tGSH and GSSG were normalized to the respective cellular protein amount measured by using the bicinchoninic acid assay (Smith et al., 1985), according to the manufacturer's protocol (Bicinchoninic acid solution, Sigma-Aldrich, Missouri, USA).

2.12. Activity of human topoisomerase II α

The activity of human topoisomerase II α (topo II α) was assessed with the gel-based, cell-free decatenation assay, as described before by Jarolim et al. (2016a). Briefly, AURO was incubated with human topo II α (TopoGEN) and kDNA (TopoGEN) in buffer (Tris-HCl, pH 8, 120 mM KCl, 10 mM $MgCl_2$, 0.5 mM ATP, 0.5 mM dithiothreitol) with a final DMSO concentration of 5% for 1 h at 37 °C. Tested AURO concentrations were 0.01, 0.1, 1, 5 and 10 μM. DMSO (5%) was used as solvent control and etoposide (250 μM) as positive control. The enzyme reaction was stopped by adding 5 μl of loading buffer (0.0025% bromophenol blue, 25% glycerol, 5% sarkosyl) and the suspension was loaded onto a 1% agarose gel to conduct electrophoresis at 250 V for 2 h. The gel was stained with ethidium bromide and detection of fluorescence was performed with ImageQuant LAS 4000 (GE Healthcare Europe GmbH, Uppsala, Sweden). Values were normalized to the solvent control which was set to 100%.

2.13. Analysis of stabilized topoisomerase II-DNA cleavage complex

The stabilization of the topo II-DNA complex, the so called cleavage complex, was investigated by the *in vivo* complex on enzyme (ICE) assay in HT29 cells as described by Fehr et al. (2009). For this purpose, 5×10^6 cells were seeded in petri dishes (Ø = 15 cm) and allowed to grow for 72 h. Cells were incubated with AURO concentrations of 0.1, 1, 5 and 10 μM in complete medium and a final DMSO concentration of 1% for 1 h. DMSO (1%) was used as solvent control and etoposide (50 μM) as positive control. After incubation, cells were washed with PBS, trypsinized and the cell suspension was homogenized by repeatedly drawning through a syringe (20 times), to ensure access to the nuclear DNA. The cell lysates were then loaded on top of a cesium chloride gradient and centrifuged at 100 000 x *g* for 22–24 h (Beckman Coulter, Krefeld, Germany). After centrifugation, fractions of 300 μl were taken and blotted onto a nitrocellulose membrane, which was incubated with 5% of milk powder in order to block unspecific binding sites and incubated with primary anti topo II α antibody (rabbit, H-286, sc-13059; Santa Cruz Biotechnology, Inc., Texas, USA) overnight at 4 °C. The membrane was incubated with secondary anti-rabbit antibody (goat anti-rabbit IgG-HRP, sc-2004; Santa Cruz Biotechnology) for 2 h and detected with chemoluminescent detection reagent according to the manufacturer's protocol (Amersham ECL Western Blotting Detection Reagent, GE Healthcare Life Sciences, Uppsala, Sweden) by using the ImageQuant LAS 4000 (GE Healthcare Life Sciences).

2.14. DNA intercalation

The potential DNA intercalation efficiency of AURO was estimated by assessing the fluorescence of DNA intercalator ethidium bromide in calf thymus DNA after incubation with AURO. In case of intercalation into the double strand, the fluorescence of ethidium bromide is reduced due to its replacement by the molecule (Morgan et al., 1979). For this purpose, 0.96 μg DNA from calf thymus (Bio Chemika) in 100 μl buffer (9.3 mM NaCl, 2 mM sodium acetate, 0.1 mM EDTA; pH 7) were mixed with 20 μM ethidium bromide and AURO or the positive control (3 μM actinomycin D (AD)) with a final solvent concentration of 1% DMSO. DMSO (1%) was used as solvent control and the tested AURO concentrations were 0.01, 0.1, 1, 5 and 10 μM. The fluorescence was measured using the Cytation 3 imaging reader (excitation = 544 nm, emission = 590 nm; BioTek, Winooski, USA) and the Gen5 data analysis software. Fluorescence values of samples without DNA were subtracted from samples containing DNA and normalized to solvent control (= 100%).

2.15. Gene transcription levels of Nrf2, γGCL, NQO1 and CYP1A1 with quantitative real time (qRT) PCR

0.8×10^6 and 0.6×10^6 HT29 cells were seeded in petri dishes (Ø = 3.5 cm) and allowed to grow for 48 h. Cells were incubated with AURO in the concentrations 0.01, 0.1, 1, 5 and 10 μM in complete medium and a final DMSO concentration of 1%. DMSO (1%) was used as solvent control, tBHQ (200 μM) as positive control. Total RNA was isolated (RNeasy® Mini Kit, Qiagen Hilden, Germany) after 3 h and 24 h incubations of HT29 with AURO concentrations of 0.01, 0.1, 1, 5 and

10 µM and reverse transcribed into cDNA according to the manufacturer's instructions (QuantiTect® Reverse Transcription Kit, Qiagen Hilden, Germany). Real time PCR was performed with the StepOne Plus™ Instrument (Life Technologies) using QuantiTect SYBR Green PCR Master Mix and Primer Assays: Hs_NQO-1_1_SG, Hs_NFE2L2_1_SG, Hs_CGCL_1_SG, Hs_CYP1A1_1_SG, Hs_ACTB_SG and Hs_GAPDH_2_SG (Qiagen Hilden, Germany) following the recommended PCR protocol. Transcript levels normalized to the mean value of mRNA levels from the endogenous control genes β-actin and GAPDH were quantified using the ΔΔCT method as PCR efficiencies of target and control genes have been found comparable.

2.16. Activity of CYP1A1

The activity of phase I enzyme CYP1A1 in HT29 cells following incubation with AURO was measured using the EROD assay (Donato et al., 1993). Utilizing this method, the intracellular conversion of ethoxyresorufin to fluorescent resorufin is assessed photometrically. Cells (50,000) were seeded in 500 µl of complete medium in a 24 well plate and allowed to grow for 48 h. Thereafter, cells were incubated with 0.01, 0.1, 1, 5 and 10 µM AURO in complete medium at a final DMSO concentration of 1% for 24 h which was used as solvent control. Benzo-(a)-pyrene (BaP; 1 µM) was used as positive control in this assay. Cells were washed with PBS and incubated with 500 µl of colorless DMEM with 10 µM dicumarol and 10 µM 7-ethoxyresorufin for 30 min 75 µl of the supernatant was added to 200 µl ethanol and measured at excitation = 535 nm and emission = 595 nm. The amount of resorufin of the samples was calculated from a resorufin standard curve. The 24 well plate was frozen at −80 °C in order to determine the protein content by the method of Bradford (1976) following the manufacturer's protocol (Roti®-Nanoquant, Carl Roth GmbH + Co. KG, Karlsruhe, Germany).

2.17. Statistical evaluation

Statistical calculations were performed using OriginPro2016 software (OriginLab Corp., Massachusetts, USA). Statistical significances between solvent control and/or a concentration range of AURO were calculated with one-way ANOVA and Fisher's posthoc test, statistical differences between a single positive control and solvent control/no effect level (lowest applied concentration) were performed with two-sample *t*-test.

3. Results

3.1. Stability assessment

Results of the stability evaluation are reported in Fig. 2a and b, an exemplary LC–MS/MS chromatogram is depicted in the Supplementary material (Fig. S1 in the online version at DOI: 10.1016/j.toxlet.2017.12.008). The tested solvents were 30% ACN, which is a routinely used solvent in LC–MS procedures and in 100% DMSO, which is frequently used to dissolve substances that are tested in cell culture experiments. The concentration of AURO in 30% ACN did not decline notably after storage at −20 °C for up to 56 d with the lowest value of 86 ± 25% relative to the reference control after 7 d, followed by 87 ± 22% after 14 d and 117 ± 18% after 56 d (Fig. 2b). In contrast, temperatures above −20 °C induced a rapid decrease of the integrity of AURO. Storage at 4 °C led to a reduction to 71 ± 20% of the reference after 7 d, while after 14 d at 4 °C the intact AURO accounted for less than half of the initial concentration (37 ± 10%), and after 56 d only 19 ± 6% of the substance remained (Fig. 2b). A further increase of storage temperature to RT led to a decrease of AURO to 40 ± 28% of reference already after 1 d, when the samples were not exposed to light during storage. When kept in clear vials under light exposure, only 2 ± 2% were measurable after 1 d. Apparently UV radiation had a more

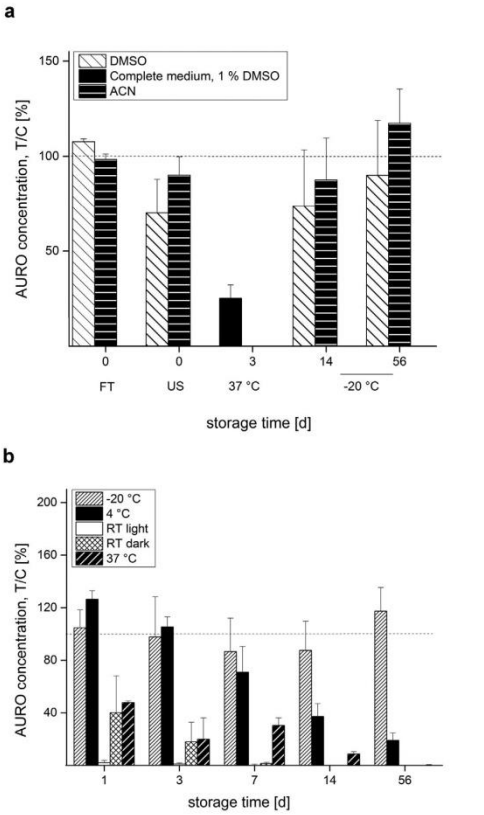

Fig. 2. Stability of AURO after different storage times and conditions. In a) a comparison of the stability of AURO in 100% DMSO (white bars, striped) and in 30% ACN (black bars, horizontal striped) is depicted. Tested conditions were three repeated times of freezing and thawing (FT), 6 min of ultrasonication (US), 3 days in complete culture medium with 1% DMSO at 37 °C (black bars). b) The short- and long-term stability of AURO was measured in 30% ACN after 1, 3, 7, 14 and 56 days. Samples were stored at −20 °C (white bars, striped), 4 °C (black bars), room temperature in transparent vials (RT light, white bars), room temperature in amber vials (RT dark, white bars, patterned) and at 37 °C (black bars, striped).

pronounced effect on the stability of AURO than elevated temperatures, since storage in 30% ACN at 37 °C led to a comparably weaker disintegration of AURO after 1 d, with 48 ± 1% of the initial concentration remaining. Comparison of 30% ACN, which is routinely used as solvent in analytical assays, and 100% DMSO, a solvent frequently applied in cell culture experiments, showed that AURO apparently was stable in both solvents at −20 °C (Fig. 2a). The high standard deviations in the results might be explained by the fact that all samples were measured in a randomized order. The analysis of all samples lasted about 32 h; during that time the vials were stored in the autosampler which was operated at 15 °C. This temperature was not tested in these experiments. However, based on the instability of AURO at RT after 1 d already, it seems likely that samples which have been analyzed later during the LC–MS/MS sequence might have undergone some breakdown until analysis. Therefore, operation at 4 °C is recommended for future experiments. The concentration of AURO in complete medium with 1% DMSO after storage at 37 °C for 3 d was comparable to that observed with pure solvent under the same conditions (25 ± 7% in

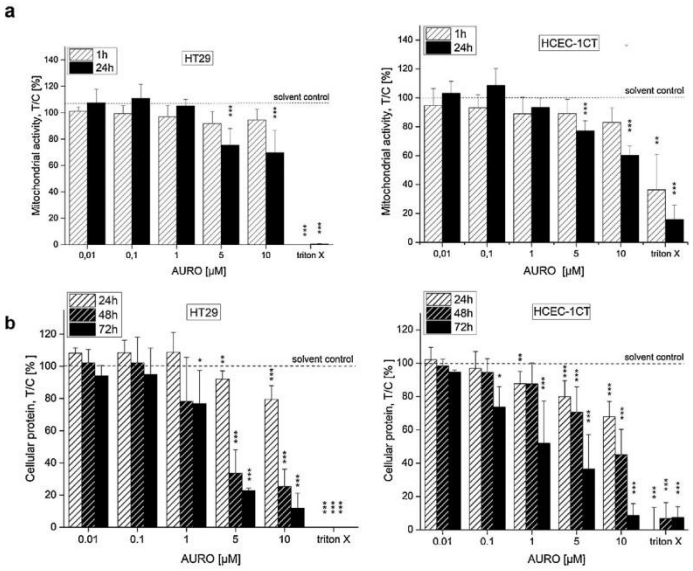

Fig. 3. Cytotoxic effects of AURO in HT29 and in HCEC-1CT cells. a) Impact of AURO on mitochondrial activity in the WST-1 assay after 1 h (white bars, striped) and 24 h (black bars) of incubation. b) Cellular proliferation, measured by the SRB assay, after 24 h (white bars, black striped), 48 h (black bars, white striped) and 72 h (black bars) of incubation. 1% DMSO served as solvent control (dotted line), 1% triton X as positive control. Results are depicted as mean ± SD of 4 independent experiments, significances refer to comparison with 0.01 µM AURO ($^{*}p < 0.05$, $^{**}p < 0.01$, $^{***}p < 0.001$).

medium (Fig. 2a) and 20 ± 16% in ACN (Fig. 2b)) indicating no higher stability in complex matrix. Freezing the vials at −20 °C and thawing them in three cycles had no mentionable impact on AURO stability in either DMSO or 30% ACN (108 ± 2% and 98 ± 3%, respectively). US for 15 min, which might be required to solve AURO completely in organic solvent, decreased its content to 90 ± 10% when dissolved in 30% ACN, while 100% DMSO as solvent led to a reduction of AURO concentration after US to 70 ± 18% of reference control.

3.2. Mitochondrial activity

The activity of mitochondrial oxidoreductases was measured in HT29 and HCEC-1CT cells by the WST-1 assay after 1 h and 24 h of incubation. In this test system, AURO induced significant reductions of mitochondrial activities in both cell lines after 24 h of 5 µM, compared to solvent control 1% DMSO (to 76 ± 12% for HT29 and 77 ± 7% for HCEC-1CT) and 10 µM (to 70 ± 17% for HT29 and 60 ± 6% for HCEC-1CT; Fig. 3a).

3.3. Cellular proliferation

The cellular viability was assessed in HT29 and HCEC-1CT using the SRB assay after 24 h, 48 h and 72 h incubation (Fig. 3b). In HCEC-1CT, 0.1 µM of AURO for 72 h led to a significant reduction to 74 ± 12% of solvent control (1% DMSO), while in HT29 72 h of incubation with 1 µM of AURO significantly reduced cellular proliferation to 77 ± 21%. In both HT29 and HCEC-1CT, 5 and 10 µM AURO significantly decreased the cellular proliferation after all three incubation times, with the lowest value measured after 72 h of 10 µM AURO, leaving 12 ± 9% of proliferating HT29 cells and only 7 ± 7% of HCEC-1CT.

3.4. Cell cycle analysis

The cell cycle distribution after 24 h of incubation with 5 and 10 µM AURO was assessed in HT29 and HCEC-1CT cells (Fig. 4). Compared to solvent control (1% DMSO), a decrease of cells in S-phase was observed after incubation with 10 µM AURO in HT29 cells, which appeared to be more sensitive to AURO, since no change was seen in HCEC-1CT after 24 h incubation with AURO (Fig. 4c). Quantification of the cell cycle distribution showed that the decline of HT29 cells in the S-phase was significantly lowered, compared to solvent control (1% DMSO; Fig. 5a), while no significant changes of cell cycle distribution were observed in HCEC-1CT (Fig. 5b). A slight, but not significant, increase of HT29 cells in the G_2/M-phase after incubation with 10 µM AURO was observable as well (Fig. 5a).

3.5. Immunocytochemical staining and microscopic assessment of p53, γ-H2AXand cellular morphology

In order to evaluate the role of p53 in AURO-induced toxicity, HT29 and HCEC-1CT cells were fixed and immunostained after 3 and 24 h of incubation, since an induction of p53 has been reported already in different cell systems after similar incubation times (Grandela et al., 2008; Karawajew et al., 2017). In HT29 cells both AURO concentrations (5 and 10 µM) resulted, in comparison to the solvent control (1% DMSO), in a pronounced increase of the p53 fluorescence signal (*red*) after 3 h of incubation (Fig. 6a). HCEC-1CT cells instead didn't show specific differences in p53 expression after 3 h AURO treatment (Fig. 6b). After 24 h of incubation 10 µM AURO led in both cell lines to an induction of the p53 signal (Fig. 6c and d). 50 µM etoposide was used as positive control.

DNA damage in the form of double-strand breaks is always followed by the phosphorylation of the histone H2AX. Therefore γ-H2AX is indicative for double-strand breaks and its visualization and detection allows the evaluation of DNA damage (Kuo and Yang, 2008). Incubation with 5 and 10 µM AURO for 1 h did not increase the fluorescent signal of γ-H2AX (*red)* in HT29 or HCEC-1CT cells (Fig. 7a and b).

Additionally, f-actin was stained using a fluorescently labeled phalloidin to determine morphological changes caused by AURO-induced toxicity. In HT29 cells only a slight effect on the filamentous actin network could be determined after 3 h of incubation caused by 10 µM AURO (Fig. 6a), whereas in the case of HCEC-1CT substantial morphological changes were observed after AURO treatment. In HCEC-

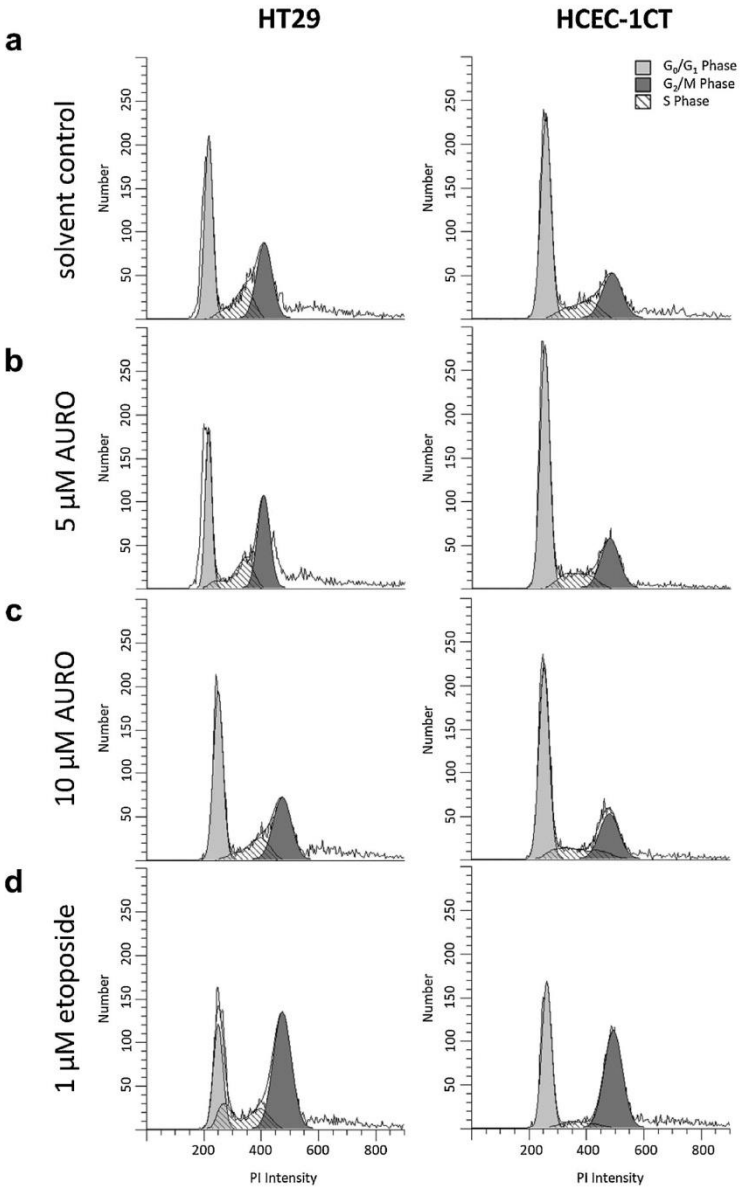

Fig. 4. Histograms of the cell cycle analysis of HT29 and HCEC-1CT cells, measured by flow cytometry. Depicted is the cell cycle distribution between G_0/G_1- (light grey), S- (white, black striped) and G_2/M-phase (dark grey) after incubation with a) solvent control (1% DMSO), b) 5 µM AURO, c) 10 µM AURO and d) positive control (1 µM etoposide).

1CT cells a loss of filamentous fine structure of the actin cytoskeleton is observed already after 3 h together with nuclear condensation and the occurrence of kidney shaped nuclei, effects which were even more pronounced after 24 h incubation (Fig. 6b and d).

3.6. DNA integrity

The genotoxic impact of AURO after 1 h was investigated in the comet assay. The solvent control DMSO (1%) showed a tail intensity of 3.3 ± 1%, which was significantly increased to 6.3 ± 2%, after incubation with 1 µM of AURO (Fig. 8, striped, white bars). Incubation with higher AURO concentrations (5 µM and 10 µM) induced tail intensities of 4.8 ± 0.9% and 5.3 ± 1%, respectively. Addition of the base excision repair enzyme fpg, which translates specific DNA lesions to DNA breaks (Chetsanga et al., 1981), induced significantly elevated DNA damage already at 0.1 µM (6.3 ± 2.4% as compared to

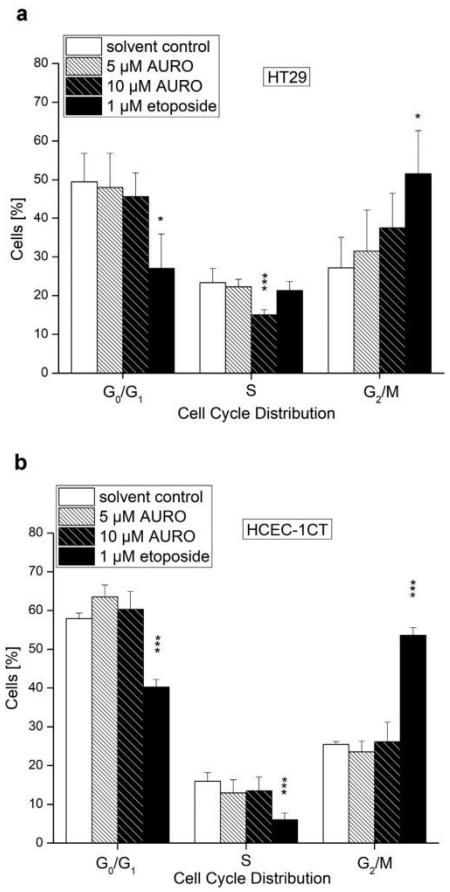

Fig. 5. Quantification of cell cycle distribution of HT29 and HCEC-1CT cells, measured by flow cytometry. The cell cycle distribution after 24 h of incubation with solvent control (1% DMSO), 5 and 10 µM AURO and positive control (1 µM etoposide) was measured in a) HT29 and b) HCEC-1CT cells. Results are depicted as mean ± SD of 4 independent experiments, significances refer to comparison with solvent control ($^{*}p < 0.05$, $^{***}p < 0.001$).

4.5 ± 1.4% in case of 1% DMSO with fpg; Fig. 8, striped, black bars). Furthermore, comparison of the tail intensities of the cells treated with fpg and those without the enzyme revealed, that the observed DNA damage was significantly elevated at the same AURO concentration when fpg was added. Accordingly, 0.1 µM AURO induced significantly higher tail intensity when fpg was applied than without the enzyme (6.3 ± 2.4% vs 4 ± 1.1%). This significant difference upon addition of fpg was observed up to a concentration of 10 µM.

3.7. Formation of reactive oxygen species

The intracellular onset of oxidative stress was evaluated by the DCF assay after incubation times of 1 h, 2 h and 3 h. The higher AURO concentrations (5 and 10 µM) significantly induced the formation of reactive oxygen species (ROS) after all incubation periods, with ROS levels approximately 30% higher than the solvent control (Fig. 9).

3.8. GSH and GSSG level

The intracellular tGSH level was altered after 3 h of incubation with 0.01 µM and 1 µM AURO and led to a significant decrease of tGSH from 53 ± 2% nmol tGSH/mg protein to 49 ± 2% and 50 ± 2%, respectively (Fig. 10a). Incubations with higher concentrations AURO (5 and 10 µM) for 3 h did not mediate significant changes of tGSH. After 1 h of incubation no changes of tGSH levels were observed in the applied concentration range (0.01–10 µM). However, an incubation period of 24 h, at concentrations of 5 and 10 µM AURO, induced a significant decrease of intracellular tGSH from 54 ± 4 nmol tGSH/mg protein, when incubated with 1% DMSO (solvent control), to 39 ± 3 for 5 µM and 32 ± 2 nmol tGSH/mg protein for 10 µM AURO. The levels of oxidized GSSG were not altered after 1 h of incubation at any concentration. While 3 h incubation with 5 and 10 µM AURO led to significant increases from 0.44 ± 0.05 nmol GSSG/mg protein in case of incubation with 1% DMSO to 0.51 ± 0.06 nmol GSSG/mg protein for 5 µM and 0.6 ± 0.05 nmol GSSG/mg protein for 10 µM AURO, respectively (Fig. 10b). After incubation for 24 h, the GSSG levels remained elevated, although not reaching significance, comparable to the values after 3 h of incubation, from 0.43 ± 0.05 nmol GSSG/mg protein of solvent control to 0.52 ± 0.12 for 5 µM and 0.6 ± 0.07 nmol GSSG/mg protein for 10 µM. Calculations of the respective GSSG/GSH ratios showed that incubation with 5 µM AURO led to a significant increase of the ratio after 3 h (from 0.84 ± 0.07 at solvent control to 0.98 ± 0.11) and after 24 h (from 0.79 ± 0.1 to 1.3 ± 0.34) in HT29 cells (Fig. 10c). Incubation with 10 µM AURO led to even higher GSSG/GSH ratios, reaching 1.14 ± 0.08 after 3 h and 1.6 ± 0.35 after 24 h of incubation.

3.9. Inhibition of human topoisomerase II α activity

A reduced amount of decatenated kDNA was observed after 1 h for a concentration of 1 µM AURO (39 ± 37% compared to the solvent control; Fig. 11a). Moreover, the decatenase activity of topo II α was further decreased to 30 ± 27% and 11 ± 12%, respectively for higher concentrations (5 and 10 µM). The activity of human topo II α was not affected after incubation with lower concentrations (0.01 and 0.1 µM).

3.10. Formation of topoisomerase II-DNA cleavage complexes

The formation of DNA-topo II complexes was measured in HT29 cells, using the ICE assay after 1 h of incubation. The immunofluorescent membranes, onto which the free and DNA-bound topo II fractions were blotted, showed incoherent results. The amount of detectable topo II-complexes varied strongly between the biological replicates, resulting in high standard deviations (Fig. 11b). Incubation with 0.1 and 1 µM AURO led to topo II-DNA complex formations of 163 ± 89% and 137 ± 79% of solvent control, respectively. Concentrations of 5 and 10 µM AURO induced cleavage complex stabilization of 193 ± 279% and 205 ± 276%, respectively. The high variances observed between the intracellular topo II-complex formation experiments may be caused by to the instability of AURO (Fig. 2).

3.11. DNA-intercalation

The ability of AURO to intercalate into double stranded calf thymus DNA was assessed by fluorescence measurements of the replacement of intercalating ethidium bromide by AURO. A significant decrease of fluorescence, indicating an increase of DNA-bound AURO, was observed after incubation of ethidium bromide-DNA with 1 µM AURO, to 96 ± 2% of solvent control (1% DMSO), followed by 88 ± 5% at 5 µM AURO and 83 ± 2% at 10 µM AURO (Fig. 12).

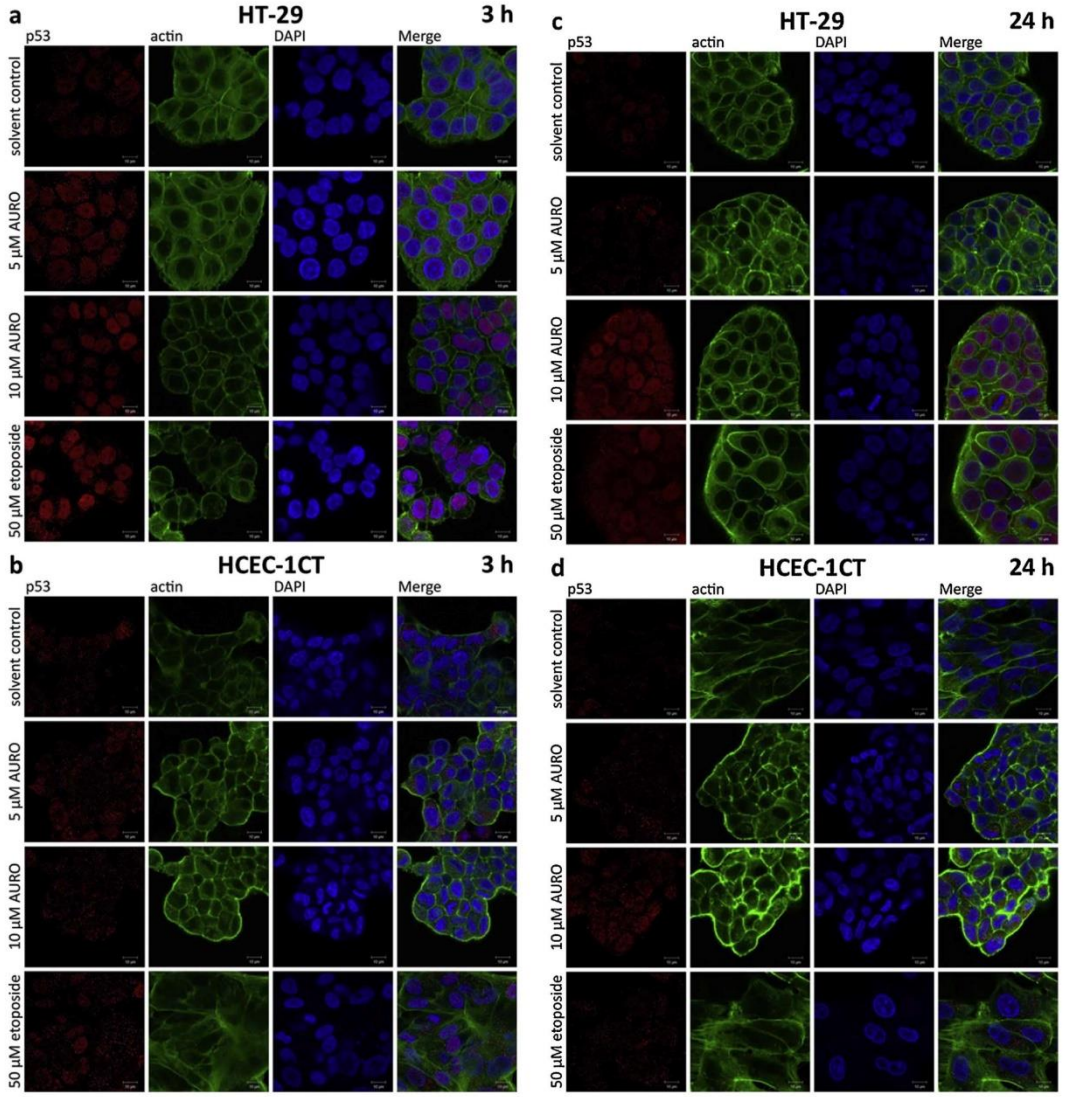

Fig. 6. Immunocytochemical evaluation of cellular p53-levels and cell morphology after incubation with AURO in HT29 and HCEC-1CT cells by confocal microscopy. Representative images of immunolocalization of p53 (*red*) using an anti-p53 antibody, f-actin cytoskeleton (*green*) stained by a fluorescently labeled phalloidin and cellular DNA content counterstained with DAPI (*blue*) in HT29 (a) and HCEC-1CT (b) cells after 3 h (Fig. 6a and b) and 24 h (Fig. 6 c and d) incubation with 5 and 10 µM AURO. 1% DMSO was used as solvent control, 50 µM etoposide as positive control. Scale bars (*white*) are equivalent to 10 µm. (For interpretation of the references to colour in this figure legend, the reader is referred to the web version of this article.)

3.12. Gene transcription levels of Nrf2, NQO1, γGCL and CYP1A1

The influence of AURO on the relative gene transcription of Nrf2, NQO1, γGCL and CYP1A1 in HT29 cells was assessed after 3 h and 24 h of incubation by qPCR. After 3 h a significant decrease of γGCL (0.48 ± 0.04-fold compared to the solvent control) was observed at a concentration of 10 µM. The mRNA levels of CYP1A1 were elevated after 3 h of 1 µM exposure 1.9 ± 0.42-fold, although not statistically significant. However, 5 µM AURO induced a significant 8.1 ± 0.93-fold increase (Fig. 13a). Incubation with 10 µM after 3 h resulted in gene transcription levels with a high variation of the biological replicates, leading to 2.5 ± 3-fold change of CYP1A1 transcription. Likewise, incubation of 24 h with 5 µM AURO led also to a high standard deviation of the relative gene transcription of CYP1A1 of 4.1 ± 3.9-fold (Fig. 13b). 24 h of incubation with 10 µM AURO led to a significant 6.5 ± 3.8-fold increase of CYP1A1 as well as a 1.1 ± 0.2-

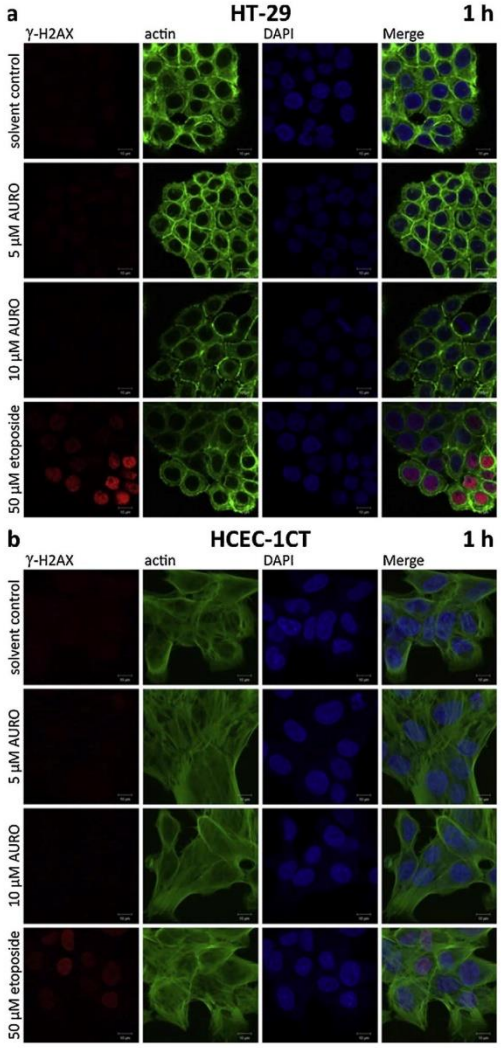

Fig. 7. Immunocytochemical evaluation of AURO-dependent H2AX phosphorylation and cell morphology after 1 h of incubation in HT29 and HCEC-1CT cells using confocal microscopy. Representative images of immunolocalization of γ-H2AX (*red*) using an anti-H2A.X (phospho S139) antibody, f-actin cytoskeleton (*green*) stained by a fluorescently conjugated phalloidin and cellular DNA content counterstained with DAPI (*blue*) in HT29 (a) and HCEC-1CT (b) cells after 1 h incubation with 5 and 10 µM AURO. 1% DMSO was used as solvent control, 50 µM etoposide as positive control. Scale bars (*white*) are equivalent to 10 µm. (For interpretation of the references to colour in this figure legend, the reader is referred to the web version of this article.)

fold increase of Nrf2 gene transcripts.

3.13. Activity of CYP1A1

After 24 h of incubation at 5 µM AURO a slight, but not significant increase of CYP1A1 activity was detected (117 ± 21% compared to solvent control (1% DMSO); Fig. 14) while 10 µM of AURO led to a

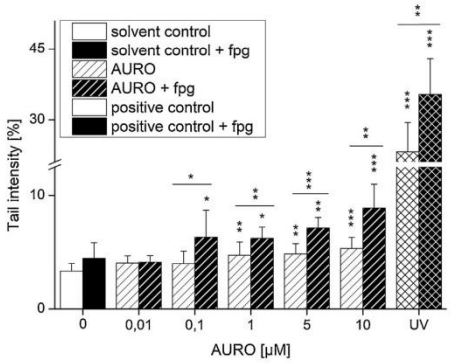

Fig. 8. Genotoxicity of AURO in the comet assay after 1 h of incubation in HT29 cells. The DNA-damaging potential of AURO was evaluated without (white bars, striped) and with addition of fpg (black bars, striped). 1% DMSO was used as solvent control (−fpg: white bar; +fpg: black bar) and UV-B radiation as positive control (−fpg white bar, patterned; +fpg: black bar, patterned). Results are depicted as mean ± SD relative to solvent control of 4 independent experiments, significances refer to comparison with solvent control ($^{*}p < 0.05$, $^{**}p < 0.01$, $^{***}p < 0.001$).

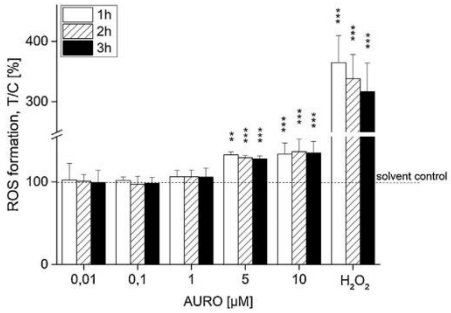

Fig. 9. Intracellular formation of ROS after incubation with AURO in HT29 cells in the DCF assay. Fluorescence values of dichlorofluorescein were measured after 1 h (white bars), 2 h (white bars, striped) and 3 h (black bars). 1% DMSO was used as solvent control (dotted line), H_2O_2 (50 µM) as positive control. Results are depicted as mean ± SD of three independent experiments, significances refer to comparison to solvent control ($^{**}p < 0.01$, $^{***}p < 0.001$).

significant increase of 139 ± 21% of the CYP1A1 activity.

4. Discussion

AURO is a secondary *Fusarium* metabolite, and contamination is prevalent in different types of cereal based food and feed commodities. Although detectable in many food samples at considerable concentrations, toxicological studies of AURO are scarce. In order to broaden the knowledge of the toxicity of this *Fusarium* metabolite, we investigated its impact on several endpoints of toxicological importance in the colon adenocarcinoma cell line HT29 and the primary extended colon cell line HCEC-1CT. A preceding analytical investigation applying LC–MS/MS technology revealed that the stability of the compound was not dependent on the used solvent, since both DMSO, which is routinely used in cell culture, and ACN, a solvent frequently used in analytical questions, did not affect the AURO concentration differently (Fig. 2a). Factors that did influence the stability of AURO were temperature and light, since storage conditions involving light-exposure and above room temperature led to a time-dependent decrease of AURO (Fig. 2b).

According to the results of the LC–MS/MS stability assessment,

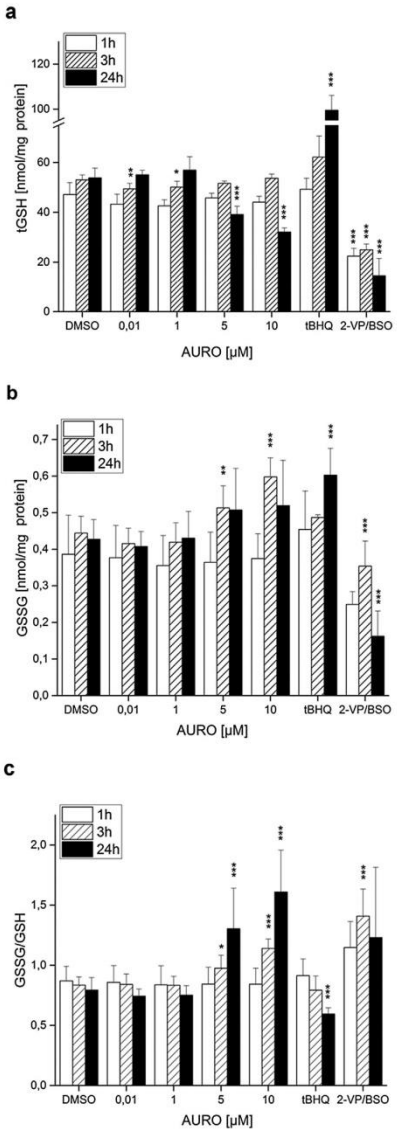

Fig. 10. Levels of a) tGSH, b) GSSG and the c) ratio of GSSG/GSH in HT29 cells after AURO incubation. Cells were incubated for 1 h (white bars), 3 h (white bars, striped) and 24 h (black bars) of incubation. 1% DMSO served as solvent control, tBHQ (200 µM) as positive control for all three incubation times, 2-VP (0.01%) for short term incubations (1 h and 3 h) and BSO (1 mM) for the long term incubation (24 h). Results are depicted as mean ± SD relative to solvent control of 5 independent experiments ($^{*}p < 0.05$, $^{**}p < 0.01$, $^{***}p < 0.001$).

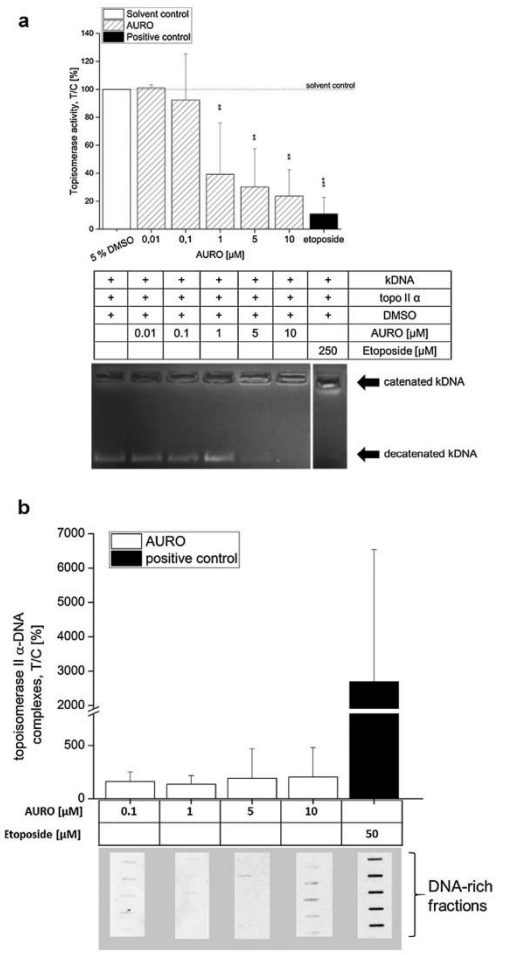

Fig. 11. Interference of AURO with the human topoisomerase II. a) The activity of the enzyme was measured in the cell-free decatenation assay after incubation with AURO for 1 h. Depicted is a representative gel; the etoposide control was located on the same gel, but in a different row, and added for reference next to the gel containing solvent control and AURO. The quantification of the decatenated kDNA fluorescence of 5–7 independent experiments. b) The ability to form covalent intermediate topo II-DNA (cleavage) complexes in HT29 cells after 1 h of incubation with AURO was investigated using the ICE assay. Depicted are representative membranes and the respective quantification of topo II-DNA complex formation of three independent experiments. DMSO (1%) was used as solvent control, etoposide (50 and 250 µM) as positive control. Significances refer to a comparison with 0.01 µM AURO ($^{**}p < 0.01$, $^{***}p < 0.001$).

AURO proved to be light-sensitive, hence the cell culture experiments were conducted under appropriate conditions (light exclusion as far as possible) in order to obtain reproducible results. 1,4-naphthoquinone derivatives have been described as cytotoxic in mammalian cells previously, a property which made this substance class promising tumor growth inhibitors in anticancer therapy (Freitas et al., 2012; Keizer et al., 1990; Pelageev et al., 2014; Pinto et al., 2014; Redaelli et al., 2015; Xu et al., 2012; Zakharova et al., 2011). The cytotoxic potential of AURO was evaluated with the WST-1 and the SRB assay in the extended primary colon cell line HCEC-1CT- and in the colon adenocarcinoma cells HT29. The data suggested that AURO induced pronounced cytotoxicity in both HCEC-1CT and HT29 cells after 24 h, 48 h and 72 h of incubation (Fig. 3). The cytotoxic effect of AURO was comparable in both cell lines, except for a slightly higher susceptibility of the non-tumorigenic HCEC-1CT cells towards lower concentrations.

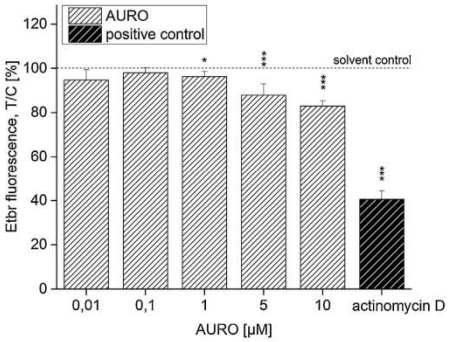

Fig. 12. Intercalation efficiency of AURO in calf thymus DNA. The relative change of fluorescence intensity of the DNA intercalating dye ethidium bromide (Etbr) served as indicator of the intercalation potential of AURO (white bars, black striped). 1% DMSO served as solvent control (dotted line), actinomycin D (3 µM) as positive control (black bar, white striped). Depicted are the respective ethidium bromide fluorescence values as mean ± SD relative to solvent control of 3 independent experiments. Significances refer to comparison with solvent control ($^{*}p < 0.05$, $^{***}p < 0.001$).

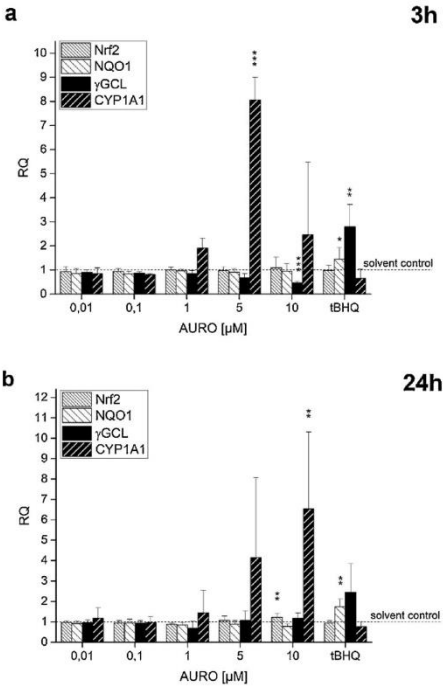

Fig. 13. Impact of AURO on the transcript level of Nrf2, NQO1, γGCL and CYP1A1 in HT29 cells after a) 3 h and b) 24 h incubation measured by qRT-PCR. 1% DMSO was used as solvent control (dotted line) and 200 µM tBHQ as positive control. Shown are the relative mRNA quantities (RQ) normalized to the mean value of mRNA levels of β-actin and GAPDH. The data presented are the mean ± SD of 4–6 independent experiments. Significances indicated display the significance level calculated on the basis of the underlying $\Delta\Delta C_T$ values as compared to 0.01 µM AURO ($^{*}p < 0.05$, $^{**}p < 0.01$, $^{***}p < 0.001$).

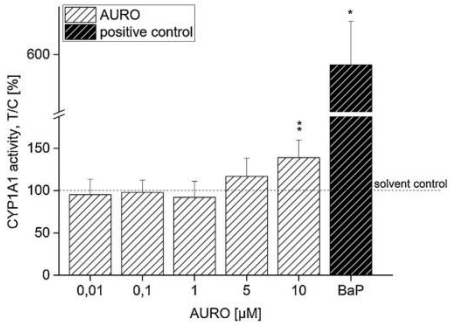

Fig. 14. Activity of CYP1A1 after incubation with AURO for 24 h in HT29 cells. The CYP1A1-dependent transformation of resorufin from 7-ethoxyresorufin by 7-ethoxyeethylase was measured using the EROD assay, following 24 h of incubation with AURO. The resorufin levels were divided by the amount of cellular protein and normalized to solvent control (1% DMSO; dotted line). Benzo-a-pyrene (BaP; 5 µM) was used as positive control. Depicted are mean ± SD relative to solvent control of 4–5 independent experiments ($^{*}p < 0.05$, $^{**}p < 0.01$).

This cell line had a significantly reduced proliferation after 72 h with 0.1 µM AURO, while in HT29 only an incubation for 72 h with 1 µM AURO led to a significant reduction of proliferation (Fig. 3b).

In order to evaluate the mechanism of action behind the cytotoxic effects of AURO, the impact of the secondary metabolite on cell cycle distribution of HT29 and HCEC-1CT cells was assessed using flow cytometry. Incubation with 10 µM AURO led to a significant decrease of HT29 cells in the S-phase (Figs. 4 and 5a). The slight rise of HT29 cells in the G_2/M-phase may indicate that the reduction of cellular proliferation observed in the SRB assay may be due to cytostatic, rather than cytotoxic effects of AURO.

Since the prevention of progression from $G_1$to S-phase has been associated with DNA-damage previously, the activation of p53, which serves as an indication of cell cycle arrest resulting from DNA damage, was evaluated by confocal microscopy (Baker et al., 1990; Diller et al., 1990). After 3 h of incubation with AURO, a slight increase of p53 was observed in HT29 cells (Fig. 6a) and HCEC-1CT cells (Fig. 6b). The activation of p53 was still detectable after 24 h of incubation with 10 µM AURO in both cell lines (Fig. 6c and d). The activation of p53 appeared higher in HT29 cells after 24 h, which matched the data of the cell cycle distribution, where a decrease of cells in the S-phase indicated DNA-damage after 24 h of incubation (Fig. 5a). The effects of AURO on the morphology of both cell lines showed an AURO-induced condensation of filamentous actin and a more rounded cellular shape of HT29 and HCEC-1CT after 3 h and 24 h of incubation (Figs. 6 and 7). The condensed chromatin observed in HCEC-1CT cells after 24 h of incubation with 10 µM AURO (Fig. 6d) may be indicative of the onset of apoptosis.

Further evaluation of potential DNA-damage showed no impact on the phosphorylation-levels of H2AX in either cell line (Fig. 7a and b), which suggested that AURO did not induce double strand breaks. These data are in accordance with the results in the ICE assay, which indicates that AURO does not act as a topoisomerase poison.

Based on the pronounced effects of AURO in HT29 cells, further experiments were focused on this cell line. Assessment of the DNA strandbreaking potential of AURO in the comet assay supported the results of enhanced p53 levels, underlining the DNA damaging potential of the compound (Fig. 8). It was previously reported that the cytotoxic effects of 1,4-naphthoquinone derivatives were partly attributed to redox cycling and the resulting formation of free radicals (Bachur et al., 1977; Handa and Sato 1975; Miller et al., 1986; Ross et al., 1986). In accordance with this concept, enhanced levels of fpg-sensitive sites were found after AURO treatment (Fig. 8). Fpg is an enzyme that

recognizes, amongst other damaged purines, 8-oxoguanine and thus serves as a marker of oxidative base damage (Chung et al., 1991). These pro-oxidative effects at the DNA level were supported by the observation that AURO induced the formation of intracellular ROS in the DCF assay in HT29 cells (Fig. 9). With this method, a significant induction of oxidative stress was noticed after 3 h of incubation. These results were in line with those of the assessment of the GSH/GSSG levels of HT29 cells. The data suggested that AURO had induced a shift of GSH/GSSG in the HT29 cells, since the ratio was significantly elevated (Fig. 10c). This effect was described e.g. for the 1,4-naphthoquinone menadione as well, which led to an increase of the amount of oxidized GSSG at the expense of GSH in rat hepatocytes (Di Monte et al., 1984). Feeding experiments with AURO in quail eggs had shown that the metabolite affected the antioxidant system in eggs and embryos (Dvorska et al., 2001, 2002).

The pro-oxidative effects of AURO might play a major role in the observed genotoxicity of the compound. However, significant DNA-damage occurred already at 0.1 μM, while ROS-induction was seen at concentrations > 5 μM, indicating the potential involvement of other mechanisms in the genotoxic impact of AURO.

Anthracyclines, 1,4-naphthoquinones used in cancer treatment, have been described as stabilizers of the ternary drug-DNA-topo II complex (cleavage complex), which is the major mechanism of action of these substances (Tewey et al., 1984a,b). Although AURO impaired the activity of human topo II in the cell-free decatenation assay (Fig. 11a), the interpretation of a potential stabilization of the cleavage complex in HT29 with the ICE assay were difficult due to comparable small effects and high variations between the biological repetitions (Fig. 11b). Since the cell-free decatenation assay is a method which is rapidly processed (less than 4 h), while assessment of cleavage complex formation with the ICE assay takes approximately 3 days from cell incubation to membrane evaluation, the experimental conditions of the latter might have been detrimental to the temperature- and light-dependent instability of AURO and could explain the inhomogeneous results. Overall, the results of the ICE assay suggest that stabilization of the topo II-DNA complex is not observable in HT29 cells after incubation with AURO. This finding is also supported by the microscopy results, which showed clearly that AURO did not enhance the phosphorylation of H2AX and thus did not induce double strand breaks in HT29 cells (Fig. 7a). However, the AURO-induced reduction of topo II activity in the gel-based decatenation assay was observable already at 1 μM, indicating that the metabolite may act as a catalytic inhibitor of topo II α (Fig. 11a). Impairment of this enzyme has been described previously for the *Alternaria* mycotoxins alternariol (AOH) and altertoxin II (ATX II) as well. The former was identified as stabilizer of the topo II complex, while ATX II as a catalytic inhibitor (Fehr et al., 2009; Tiessen et al., 2013).

For many naphthoquinone derivatives the formation of intercalative DNA-complexes has been described as a further mechanism contributing to genotoxicity (Esteves-Souza et al., 2007; Koch et al., 1993; Quigley et al., 1980). Comparably, in our study AURO induced a replacement of the intercalator ethidium bromide from calf thymus DNA, indicating mild intercalative properties of AURO, starting at a concentration of 1 μM (Fig. 12). The DNA-damage elicited by AURO in the comet assay was also observed at 1 μM, hence intercalative properties might contribute, although to a limited extent, to the overall genotoxic effect of the secondary metabolite (Ross et al., 1979).

In the next step we investigated the impact of AURO on the gene expression level of several targets associated with cellular defense against xenobiotic stressors in HT29 cells. While a clear induction of CYP1A1 mRNA was seen after 3 h of incubation, the data for gene expression of CYP1A1 after 3 h with 10 μM AURO and after 24 h with 5 and 10 μM varied between biological replicates, leading to high standard deviations (Fig. 13). Since cytotoxic effects were observed after 24 h incubation, the high standard deviations of the mRNA levels of CYP1A1 may be due to the onset of cytotoxic effects. In order to clarify the impact of AURO on CYP1A1, the activity of the enzyme after AURO incubation in HT29 cells was measured by the EROD assay, showing an induction of CYP1A1 activity (Fig. 13). CYP1A1 is regulated by the arylhydrocarbon receptor (AhR), an increase of CYP1A1 following incubation with AURO may thus be indicative for the activation of the AhR-pathway by the secondary metabolite (Delescluse et al., 2000). CYP1A1 was identified previously as metabolizing enzyme of 1,8-dihydroxyanthraquinones and its induction was discussed as possible biotransformation pathway, resulting either in the formation of a more potent genotoxic metabolite or serving as a detoxification step (Mueller et al., 1998). The role of CYP1A1 in the potency of AURO-mediated toxicity remains yet to be clarified.

In summary, the secondary *Fusarium* metabolite AURO was found to be cytotoxic in both, tumorigenic and non-tumorigenic colon cells. In both cell types enhanced levels of p53 protein, indicative for DNA damage, were observed. In accordance, AURO mediated DNA strand-breaks in the alkaline comet assay associated with an increase in fpg sensitive sites. As potentially contributing genotoxic mechanisms, induction of oxidative stress together with a decrease of intracellular tGSH, interference with topoisomerase activity and intercalative properties were identified. Moreover, AURO was found to enhance CYP1A1 expression, arguing for a function as Ah-receptor ligand. Considering the fact that AURO, although found in many mycotoxin contaminated food samples, is not legally regulated yet, these data may contribute to the discussion about classifying AURO not only as a secondary fungal metabolite but as a mycotoxin.

Conflicts of interest

None.

Acknowledgements

The authors would like to express their gratitude towards Dr. Giorgia Del Favero for skillful support during preliminary experiments.

LC–MS/MS measurements were performed at the Mass Spectrometry Center of the Faculty of Chemistry, University of Vienna.

References

Ashley, J.N., Hobbs, B.C., Raistrick, H., 1937. Studies in the biochemistry of micro-organisms. Biochem. J. 31, 385–397.
Bachur, N.R., Gordon, S.L., Gee, M.V., 1977. Anthracycline antibiotic augmentation of microsomal electron transport and free radical formation. Mol. Pharmacol. 13, 901–910.
Baker, P.M., Roberts, J.C., 1966. Studies in mycological chemistry. 21. Structure of aurofusarin a metabolite of some Fusarium species. J. Chem. Soc. C 2234.
Baker, S.J., Markowitz, S., Fearon, E.R., Willson, J.K., Vogelstein, B., 1990. Suppression of human colorectal carcinoma cell growth by wild-type p53. Science 249, 912–915.
Blandino, M., Scarpino, V., Vanara, F., Sulyok, M., Krska, R., Reyneri, A., 2015. Role of the european corn borer (Ostrinia nubilalis) on contamination of maize with 13 fusarium mycotoxins. Food Addit. Contamin. Part A Chem. Anal. Control Exposure Risk Assess. 32, 533–543.
Bottalico, A., Perrone, G., 2002. Toxigenic Fusarium species and mycotoxins associated with head blight in small-grain cereals in Europe. Eur. J. Plant Pathol. 108, 611–624.
Burma, S., Chen, B.P., Murphy, M., Kurimasa, A., Chen, D.J., 2001. ATM phosphorylates histone H2AX in response to DNA double-strand breaks. J. Biol. Chem. 276, 42462–42467.
Bradford, M.M., 1976. A rapid and sensitive method for the quantitation of microgram quantities of protein utilizing the principle of protein-dye binding. Anal. Biochem. 72, 248–254.
Chung, M.H., Kasai, H., Jones, D.S., Inoue, H., Ishikawa, H., Ohtsuka, E., Nishimura, S., 1991. An endonuclease activity of Escherichia coli that specifically removes 8-hydroxyguanine residues from DNA. Mutat. Res. DNA Repair 254, 1–12.
Chetsanga, C.J., Lozon, M., Makaroff, C., Savage, L., 1981. Purification and characterization of E. coli formamidopyrimidine-DNA glycosylase that excise damaged 7-methylguanine from DNA. Biochemistry 20, 5201–5207.
Collins, A.R., 2004. The comet assay for DNA damage and repair: principles, applications, and limitations. Mol. Biotechnol. 26, 249–261.
Commission, E., 2006. In: Commission, E. (Ed.), Commission Regulation (EC) No 1881/2006. Official Journal of the European Union.
Delescluse, C., Lemaire, G., De Souse, G., Rahmani, R., 2000. Is CYP1A1 related to AhR signaling pathway? Toxicology 153, 73–82.

Attachment: Publication 3

Demma, J., Hallberg, K., Hellman, B., 2009. Genotoxicity of plumbagin and its effects on catechol and NQNO-induced DNA damage in mouse lymphoma cells. Toxicol. In Vitro 23, 266–271.
Di Monte, D., Bellomo, G., Thor, H., Nicotera, P., Orrenius, S., 1984. Menadione-induced cytotoxicity is associated with protein thiol oxidation and alteration in intracellular Ca2+ homeostasis. Arch. Biochem. Biophys. 235, 343–350.
Diller, L., Kassel, J., Nelson, C.E., Gryka, M.A., Litwak, G., Gebhardt, M., Bressac, B., Ozturk, M., Baker, S.J., Vogelstein, B., 1990. p53 functions as a cell cycle control protein in osteosarcomas. Mol. Cell. Biol. 10, 5772–5781.
Donato, M.T., Gómez-Lechón, M.J., Castell, J.V., 1993. A microassay for measuring cytochrome P450IA1 and P450IIB1 activities in intact human and rat hepatocytes cultured on 96-well plates. Anal. Biochem. 213, 29–33.
Dvorska, J.E., Surai, P.F., Speake, B.K., Sparks, N.H.C., 2001. Effect of the mycotoxin aurofusarin on the antioxidant composition and fatty acid profile of quail eggs. Br. Poult. Sci. 42, 643–649.
Dvorska, J.E., Surai, P.F., Speake, B.K., Sparks, N.H.C., 2002. Antioxidant systems of the developing quail embryo are compromised by mycotoxin aurofusarin. Comp. Biochem. Physiol. Part C Toxicol. Pharmacol. 131, 197–205.
Esteves-Souza, A., Figueiredo, D.V., Esteves, A., Câmara, C.A., Vargas, M.D., Pinto, A.C., Echevarria, A., 2007. Cytotoxic and DNA-topoisomerase effects of lapachol amine derivatives and interactions with DNA. Braz. J. Med. Biol. Res. 40, 1399–1402.
Ezekiel, C.N., Bandyopadhyay, R., Sulyok, M., Warth, B., Krska, R., 2012a. Fungal and bacterial metabolites in commercial poultry feed from Nigeria. Food Addit. Contam. Part A Chem. Anal. Control Exposure Risk Assess. 29, 1288–1299.
Ezekiel, C.N., Sulyok, M., Warth, B., Krska, R., 2012b. Multi-microbial metabolites in fonio millet (acha) and sesame seeds in Plateau State, Nigeria. Eur. Food Res. Technol. 235, 285–293.
Fehr, M., Pahlke, G., Fritz, J., Christensen, M.O., Boege, F., Altemöller, M., Podlech, J., Marko, D., 2009. Alternariol acts as a topoisomerase poison, preferentially affecting the IIα isoform. Mol. Nutr. Food Res. 53, 441–451.
Freitas, H.P.S., Maia, A.I.V., Silveira, E.R., Marinho Filho, J.D.B., Moraes, M.O., Pessoa, C., Lotufo, L.V.C., Pessoa, O.D.L., 2012. Cytotoxic cordiaquinones from the roots of Cordia polycephala. J. Braz. Chem. Soc. 23, 1558–1562.
Frydman, B., Marton, L.J., Sun, J.S., Neder, K., Witiak, D.T., Liu, A.A., Wang, H.M., Mao, Y., Wu, H.Y., Sanders, M.M., Liu, L.F., 1997. Induction of DNA topoisomerase II-mediated DNA cleavage by β-lapacphone and related naphthoquinones. Cancer Res. 57, 620–627.
Grandela, C., Pera, M.F., Wolvetang, E.J., 2008. p53 is required for etoposide-induced apoptosis of human embryonic stem cells. Stem Cell Res. 1, 116–128.
Handa, K., Sato, S., 1975. Generation of free radicals of quinone group-containing anticancer chemicals in NADPH-microsome system as evidenced by initiation of sulfite oxidation. Gann Jpn. J. Cancer Res. 66, 43–47.
JECFA, 2011. Evaluation of Certain Food Additives and Contaminants. Seventy-fourth Report of the JECFA. Joint FAO/WHO Expert Committee on Food Additives, pp. 70–94.
Karawajew, L., Rhein, P., Czerwony, G., Ludwig, W.D., 2017. Stress-induced activation of the p53 tumor suppressor in leukemia cells and normal lymphocytes requires mitochondrial activity and reactive oxygen species. Blood 105, 4767–4775.
Kastan, M.B., Onyekwere, O., Sidransky, D., Vogelstein, B., Craig, R.W., 1991. Participation of p53 protein in the cellular response to DNA damage. Cancer Res. 51, 6304–6311.
Keizer, H.G., Pinedo, H.M., Schuurhuis, G.J., Joenje, H., 1990. Doxorubicin (adriamycin): a critical review of free radical-dependent mechanisms of cytotoxicity. Pharmacol. Ther. 47, 219–231.
Koch, T., Ropp, J.D., Sligar, S.G., Schuster, G.B., 1993. Photocleavage of DNA: irradiation of quinone-containing reagents converts supercoiled to linear DNA. Photochem. Photobiol. 58, 554–558.
Kuo, L.J., Yang, L.X., 2008. Gamma-H2AX − a novel biomarker for DNA double-strand breaks. In Vivo 22, 305–309.
Matumba, L., Sulyok, M., Monjerezi, M., Biswick, T., Krska, R., 2015. Fungal metabolites diversity in maize and associated human dietary exposures relate to micro-climatic patterns in Malawi. World Mycotoxin J. 8, 269–282.
Mikušová, P., Šrobárová, A., Sulyok, M., Santini, A., 2013. Fusarium fungi and associated metabolites presence on grapes from Slovakia. Mycotoxin Res. 29, 97–102.
Miller, M.G., Rodgers, A., Cohen, G.M., 1986. Mechanisms of toxicity of naphthoquinones to isolated hepatocytes. Biochem. Pharmacol. 35, 1177–1184.
Morgan, A.R., Evans, D.H., Lee, J.S., Pulleyblank, D.E., 1979. Review: ethidium fluorescence assay. Part II. Enzymatic studies and DNA-protein interactions. Nucleic Acids Res. 7, 571–594.
Mueller, S.O., Stopper, H., Dekant, W., 1998. Biotransformation of the anthraquinones emodin and chrysophanol by cytochrom P450 enzymes: Bioactivation o genotoxic metabolites. Drug Metab. Dispos. 26, 540–546.
Pelageev, D.N., Dyshlovoy, S.A., Pokhilo, N.D., Denisenko, V.A., Borisova, K.L., Keller-von Amsberg, G., Bokemeyer, C., Fedorov, S.N., Honecker, F., Anufriev, V.P., 2014. Quinone–carbohydrate nonglucoside conjugates as a new type of cytotoxic agents: synthesis and determination of in vitro activity. Eur. J. Med. Chem. 77, 139–144.
Pinto, E.G., Santos, I.O., Schmidt, T.J., Borborema, S.E.T., Ferreira, V.F., Rocha, D.R., Tempone, A.G., 2014. Potential of 2-hydroxy-3-phenylsulfanylmethyl-[1, 4]-naphthoquinones against Leishmania (L.) infantum: biological activity and structure-activity relationships. PLoS One 9, e105127.
Quigley, G.J., Wang, A.H.J., Ughetto, G., van der Marel, G., van Boom, J.H., Rich, A., 1980. Molecular structure of an anticancer drug-DNA complex: daunomycin plus d (CpGpTpApCpG). Proc. Natl. Acad. Sci. U. S. A. 77, 7204–7208.
Redaelli, M., Mucignat-Caretta, C., Isse, A.A., Gennaro, A., Pezzani, R., Pasquale, R., Pavan, V., Crisma, M., Ribaudo, G., Zagotto, G., 2015. New naphthoquinone derivatives against glioma cells. Eur. J. Med. Chem. 96, 458–466.
Ross, D., Thor, H., Threadgill, M.D., Sandy, M.S., Smith, M.T., Moldéus, P., Orrenius, S., 1986. The role of oxidative processes in the cytotoxicity of substituted 1,4-naphthoquinones in isolated hepatocytes. Arch. Biochem. Biophys. 248, 460–466.
Ross, W.E., Glaubiger, D., Kohn, K.W., 1979. Qualitative and quantitative aspects of intercalator-induced DNA strand breaks. Biochim. Biophys. Acta 562, 41–50.
Schwarz, C., Kreutzer, M., Marko, D., 2012a. Minor contribution of alternariol, alternariol monomethyl ether and tenuazonic acid to the genotoxic properties of extracts from Alternaria alternata infested rice. Toxicol. Lett. 214, 46–52.
Schwarz, C., Tiessen, C., Kreutzer, M., Stark, T., Hofmann, T., Marko, D., 2012b. Characterization of a genotoxic impact compound in Alternaria alternata infested rice as Altertoxin II. Arch. Toxicol. 86, 1911–1925.
Shibata, S., Morishita, E., Takeda, T., Sakata, K., 1966. The structure of aurofusarin. Tetrahedron Lett. 7, 4855–4860.
Skehan, P., Storeng, R., Scudiero, D., Monks, A., Mcmahon, J., Vistica, D., Warren, J.T., Bokesch, H., Kenney, S., Boyd, M.R., 1990. New colorimetric cytotoxicity assay for anticancer-drug screening. J. Natl. Cancer Inst. 82, 1107–1112.
Smith, P.K., Krohn, R.I., Hermanson, G.T., Mallia, A.K., Gartner, F.H., Provenzano, M.D., Fujimoto, E.K., Goeke, N.M., Olson, B.J., Klenk, D.C., 1985. Measurement of protein using bicinchoninic acid. Anal. Biochem. 150, 76–85.
Srinivas, P., Gopinath, G., Banerji, A., Dinakar, A., Srinivas, G., 2004. Plumbagin induces reactive oxygen species, which mediate apoptosis in human cervical cancer cells. Mol. Carcinog. 40, 201–211.
Tewey, K.M., Chen, G.L., Nelson, E.M., Liu, L.F., 1984a. Intercalative antitumor drugs interfere with the breakage-reunion reaction of mammalian DNA topoisomerase II. J. Biol. Chem. 259, 9182–9187.
Tewey, K.M., Rowe, T.C., Yang, L., Halligan, B.D., Liu, L.F., 1984b. Adriamycin-induced DNA damage mediated by mammalian DNA topoisomerase II. Science 226, 466–468.
Thor, H., Smith, M.T., Hartzell, P., Bellomo, G., Jewell, S.A., Orrenius, S., 1982. The metabolism of menadione (2-methyl-1,4-naphthoquinone) by isolated hepatocytes: a study of the implications of oxidative stress in intact cells. J. Biol. Chem. 257, 12419–12425.
Tiessen, C., Gehrke, H., Kropat, C., Schwarz, C., Bächler, S., Fehr, M., Pahlke, G., Marko, D., 2013. Role of topoisomerase inhibition and DNA repair mechanisms in the genotoxicity of alternariol and altertoxin-II. World Mycotoxin J. 6, 233–244.
Tietze, F., 1969. Enzymatic method for quantitative determination of nanogram amounts of total and oxidised glutathione: applications to mammalian blood and other tissues. Anal. Biochem. 27, 502–522.
Tola, S., Bureau, D.P., Hooft, J.M., Beamish, F.W.H., Sulyok, M., Krska, R., Encarnação, P., Petkam, R., 2015. Effects of wheat naturally contaminated with Fusarium mycotoxins on growth performance and selected health indices of red tilapia (Oreochromis niloticus × O. mossambicus). Toxins 7, 1929–1944.
Uhlig, S., Jestoi, M., Kristin Knutsen, A., Heier, B.T., 2006. Multiple regression analysis as a tool for the identification of relations between semi-quantitative LC-MS data and cytotoxicity of extracts of the fungus Fusarium avenaceum (syn. F. arthrosporioides). Toxicon 48, 567–579.
Uhlig, S., Eriksen, G.S., Hofgaard, I.S., Krska, R., Beltrán, E., Sulyok, M., 2013. Faces of a changing climate: semi-quantitative multi-mycotoxin analysis of grain grown in exceptional climatic conditions in Norway. Toxins 5, 1682–1697.
Vejdovszky, K., Warth, B., Sulyok, M., Marko, D., 2016. Non-synergistic cytotoxic effects of Fusarium and Alternaria toxin combinations in Caco-2 cells. Toxicol. Lett. 241, 1–8.
Wang, H., Joseph, J.A., 1999. Quantifying cellular oxidative stress by dichlorofluorescein assay using microplate reader11Mention of a trade name, proprietary product, or specific equipment does not constitute a guarantee by the United States Department of Agriculture and does not imply its approval to the exclusion of other products that may be suitable. Free Radic. Biol. Med. 27, 612–616.
Xu, H.L., Yu, X.F., Qu, S.C., Qu, X.R., Jiang, Y.F., Sui, D.Y., 2012. Juglone, from Juglans mandshurica Maxim, inhibits growth and induces apoptosis in human leukemia cell HL-60 through a reactive oxygen species-dependent mechanism. Food Chem. Toxicol. 50, 590–596.
Zakharova, O.D., Ovchinnikova, L.P., Goryunov, L.I., Troshkova, N.M., Shteingarts, V.D., Nevinsky, G.A., 2011. Cytotoxicity of new polyfluorinated 1,4-naphtoquinones with diverse substituents in the quinone moiety. Bioorg. Med. Chem. 19, 256–260.

Attachment: Abstract

Food-infesting moulds that produce mycotoxins pose a health risk to humans and animals. Hence, regulatory limits have been established for some secondary metabolites, for which sufficient data about toxicity and exposure exist, e.g. some mycotoxins from *Fusarium spp*. However, there are secondary metabolites for which no regulatory limits are in place yet, due to the limited amount of data. One example thereof are secondary metabolites produced by molds of the genus *Alternaria,* also referred to as "emerging mycotoxins". In this PhD thesis, eleven secondary metabolites from *Alternaria* and five from *Fusarium* moulds were investigated for their toxicological mechanisms.

One important *Alternaria* metabolite is the perylene quinone altertoxin II (ATX II), which has been identified as a major genotoxic impact component in *Alternaria alternata*-infested rice (Schwarz et al. 2012). However, the detoxification pathways of the altertoxin in the cell have not been elucidated yet. In this regard, ATX II constitutes an interesting candidate for induction of the Nrf2/ARE-pathway due to its epoxide group. Thus, the impact of the mycotoxin on this important cellular defense pathway was investigated in the first publication of this PhD thesis (Jarolim et al., 2016a). Altertoxin I (ATX I) was included in the experiments for comparison, since it resembles ATX II structurally, except for the missing epoxide. In publication 1, the impact of ATX I and II on the Nrf2/ARE-pathway activation and translocation of Nrf2 was investigated with the reporter gene assay in stably transfected Chinese hamster ovary (CHO) cells and with confocal microscopy in the colon adenocarcinoma cell line HT29. Furthermore, the induction of the Nrf2-dependent gene expression of γ-glumate cystein ligase (γ-GCL) was investigated with q-PCR and the amount of the enzymatic product of γ-GCL, glutathione (GSH), in the cells was measured with the GSH assay. The results indicate that ATX II acts as inducer of the Nrf2/ARE-pathway, while ATX I does not show any impact on the pathway (Jarolim et al., 2016a).

As mentioned above, the *Alternaria* mycotoxin ATX II was described as mutagenic and genotoxic. These effects could partially be associated with the targeting of a vital enzyme involved in the maintenance of the topology of DNA by ATX II, human topoisomerase II (topo II) (Schwarz et al. 2012; Stack and Prival 1986; Tiessen et al. 2013). Interestingly, inhibition of topo II was seen for the secondary *Alternaria* metabolites, alternariol (AOH) and

alternariol monomethyl ether (AME) as well (Fehr et al. 2009; Tiessen et al. 2016). This observation gave rise to the question if further secondary metabolites from *Alternaria spp*. were also active against topo II, which was examined in publication 2 of the PhD thesis (Jarolim et al., 2016b). For this purpose, eleven secondary *Alternaria* metabolites were investigated for their impact on the enzymatic activity of human topo IIα in the cell-free decatenation assay. The tested substances were chosen to reflect the chemical diversity of secondary metabolites produced by *Alternaria* fungi. Besides ATX I and II, the two perylene quinones alterperylenol (ALP) and stemphyltoxin III (STTX III), the dibenzo-α-pyrones AOH and AME as well as the *Alternaria* metabolites pyrenophorol (PYR), tentoxin (TEN), altersetin (ALN) and altenusine (ALS) were examined. For comparison, five *Fusarium* metabolites were also tested for their impact on human topo IIα, deoxynivalenol (DON), fumonisin B1 (FB1), fusarin C (FC), moniliformin (MON) and aurofusarin (AURO). The results of the decatenation assay experiments show that all tested *Alternaria* metabolites, except for TEN, reduce the activity of human topo IIα, while the only active substance from *Fusarium spp.* is the naphthoquinone AURO (Jarolim et al., 2016b). To investigate whether the targeting of human topo IIα by the fungal metabolites is based on the homology between human and bacterial topo II, the compounds were tested for their impact on gyrase from *E.coli* in the cell-free gyrase supercoiling assay. The results suggest that all four tested perylene quinones and the two dibenzo-α-pyrones from *Alternaria spp*. have a dual activity towards both human and bacterial topo II, while the remaining *Alternaria* metabolites are only active against the human enzyme. Of the five metabolites from *Fusarium spp*, that were examined, the naphthoquinone AURO is the only active compound against human, but not bacterial topo II. Interestingly, AURO is the most potent inhibitor of human topo IIα of all eleven tested secondary metabolites.

The observed potency of AURO in the decatenation assay made the dimeric naphthoquinone an interesting candidate for further investigations, since few studies about its toxicity were available. Hence, the toxicological profile of AURO was investigated in publication 3, in the adenocarcinoma cell line HT29 and in the non-transformed colon epithelial cells HCEC-1CT (Jarolim et al. 2018). The experiments showed that AURO is cytotoxic to both the cancer and the non-transformed cell line in the WST-1 and SRB assay. As a potential underlying mechanism, DNA-damaging properties of AURO were identified in the comet assay in HT29

cells, which is in accordance with an observed AURO-mediated cell cycle arrest in the G_2/M phase and an increase of p53 in both cell lines. The genotoxicity of the compound is presumably partly caused by the pro-oxidative effects that were seen in the comet assay, where AURO induced fpg-sensitive sites. This was also observed in the 2,7-dichlorofluorescein (DCF) assay, where an elevated level of reactive oygen species in HT29 cells was detected after incubation with AURO. Incubation of HT29 cells with the secondary *Fusarium* metabolite also led to an increase of the cellular GSSG/GSH ratio, which indicates oxidative process.

As mentioned above, AURO was shown to potently inhibit the activity of human topo IIα in the cell-free decatenation assay. To investigate whether the metabolite also leads to a stabilization of the DNA-topo II complex, the formation of these so called cleavage complexes was investigated in HT29 cells, using the *in vivo* complex of enzyme (ICE) assay. In this assay we could observe that an incubation with AURO caused to a mild, but not significant increase of topo II-DNA complexes. Many topo II-targeting substances are described to act as DNA intercalators (Chen and Liu 1994) and accordingly, AURO intercalates into calf thymus DNA in the cell-free intercalation assay. Interestingly, AURO increases the gene expression of cytochrome P450 1A1 (CYP1A1) in HT29 cells in q-PCR experiments. This was confirmed with the colorimetric 7-ethoxy-resorufin-O-deethylation (EROD) assay, where the activity of CYP1A1 is increased significantly after incubation with AURO. These two results indicate that AURO presumably acts as activator of the AhR pathway.

The results of publication 3 strongly suggest that AURO is cytotoxic and genotoxic *in vitro*. The findings of the cell culture experiments are even more intriguing, considering that the compound is rather unstable under the respective conditions, as measured by LC-MS/MS. The analytical experiments indicate that AURO is degraded in a light- and temperature-dependent manner.

Overall, the PhD thesis investigated sixteen secondary metabolites from *Alternaria* and *Fusarium* fungi for potential detoxification pathways and toxicologically relevant methods of action. The results of the three publications demonstrate that the Nrf2/ARE-pathway plays a role in cellular detoxification of ATX II (Jarolim et al. 2016a). The experiments could also identify human topo II as target of several tested *Alternaria* mycotoxins with diverse chemical

structures and of one *Fusarium* metabolite, which is presumably caused by the homology between human and bacterial topo II (Jarolim et al. 2016b). Furthermore, a novel secondary metabolite from *Fusarium* was identified as potently toxic in cell culture experiments, the dimeric naphthoquinone AURO (Jarolim et al. 2018).

Attachment: Zusammenfassung

Schimmelpilze, die Mykotoxine produzieren und so Lebensmittel kontaminieren, stellen ein Risiko für Mensch und Tier dar. Daher wurden für einige Mykotoxine Grenzwerte in Lebensmitteln aufgestellt, sofern ausreichend Daten über Toxizität und Verbreitung vorliegen, wie beispielsweise für Mykotoxine von Schimmelpilzen der Gattung *Fusarium spp*. Es existieren jedoch Sekundärmetabolite, für die zum jetzigen Zeitpunkt keine Grenzwerte benannt werden können, da die Datenlage nicht ausreichend ist. Dazu zählen die Schimmelpilze der Gattung *Alternaria*, welche auch als „emerging mycotoxins“ bezeichnet werden. Diese Dissertation hat die Untersuchung der Detoxifizierung, sowie von toxikologischen Mechanismen von elf ausgewählten *Alternaria* und fünf *Fusarium* Sekundärmetaboliten zum Ziel.

Ein wichtiger *Alternaria* Metabolit ist das Perylenchinon Altertoxin II (ATX II), welches als genotoxische Hauptkomponente in *Alternaria alternata*-befallenem Reis identifiziert wurde (Schwarz et al., 2012). Obwohl die Toxizität von ATX II untersucht wurde, ist dessen Detoxifizierung in der Zelle bis dato nicht bekannt. ATX II stellt aufgrund seiner Epoxidgruppe in diesem Zusammenhang einen interessanten Kandidaten für die Induktion des Nrf2/ARE-Signalwegs war, da das Molekül über ein Epoxid verfügt. Der Einfluss des Mykotoxins auf diesen wichtigen zellulären Signalweg wurde daher in der ersten Publikation der Dissertation untersucht (Jarolim et al. 2016a). Altertoxin I (ATX I) wurde aus Vergleichsgründen in die Experimente eingeschlossen, aufgrund der strukturellen Ähnlichkeit zu ATX II, bis auf die fehlende Epoxidgruppe. In Publikation 1 wurde der Einfluss von ATX I und II auf den Nrf2/ARE-Signalweg und die Translokation von Nrf2 mittels Reportergen Assay in stabil transfizierten chinesischen Hamsterzellen (CHO), sowie mit Konfokalmikroskopie in der Adenokarzinom Zellinie HT29, untersucht. Die Induktion der Nrf2-abhängigen Gentranskription der γ-Glutamyl Cystein Ligase (γ-GCL) wurde mit qPCR gemessen und die Menge des enzymatischen Synthese-Produkts der γ-GCL, Glutathion (GSH), wurde mit dem GSH Assay ermittelt. Zusammengenommen zeigen diese Ergebnisse, dass ATX II den Nrf2/ARE-Signalweg induziert, während ATX I keinen Einfluss auf dessen Aktivität hat (Jarolim et al., 2016a).

Wie oben erwähnt, wurde das *Alternaria* Mykotoxin ATX II als mutagen und genotoxisch beschrieben. Als möglicher zu Gründe liegender Mechanismus, wurde die Reduzierung der

Aktivität eines essentiellen Enzyms durch ATX II diskutiert, welches in die Aufrechterhaltung der DNA Topologie involviert ist, humane Topoisomerase II (Topo II) (Schwarz et al. 2012; Stack and Prival 1986; Tiessen et al. 2013). Interessanterweise wurde diese Inhibition ebenfalls für andere *Alterneria* Metabolite beobachtet, für Alternariol (AOH) und Alternariolmonomethylether (AME) (Fehr et al. 2009; Tiessen et al. 2016). Diese Beobachtung brachte die Frage auf, ob weitere Sekundärmetabolite von *Alternaria* Schimmelpilzen gegen Topo II gerichtet sind, was in Publikation 2 der Dissertation untersucht wurde (Jarolim et al. 2016b). Zu diesem Zweck wurden elf *Alternaria* Sekundärmetabolite auf ihren Einfluss auf die enzymatische Aktivität der humanen Topo IIα im zellfreien Dekatenierungs Assay untersucht. Die getesteten Substanzen wurden gewählt, um die breitgefächerte strukturelle Heterogenität der sekundären *Alternaria* Metabolite zu reflektieren. Daher wurden neben ATX I und II die beiden Perylenchinone Alterperylenol (ALP) und Stemphyltoxin III (STTX III), die Dibenzo-α-pyrone AOH und AME, sowie vier weitere *Alternaria* Metabolite Pyrenophorol (PYR), Tentoxin (TEN), Altersetin (ALN) und Altenusin (ALS) untersucht. Aus Vergleichsgründen wurden auch fünf Sekundärmetabolite von *Fusarium* Pilzen inkludiert, Deoxynivalenol (DON), Fumonisin B1 (FB1), Fusarin C (FC), Moniliformin (MON) und Aurofusarin (AURO).

Die Ergebnisse der Publikation 2 lassen darauf schließen, dass alle getesteten *Alternaria* Metabolite, außer TEN, sowie der *Fusarium* Metabolit AURO, die Aktivität der humanen Topo IIα reduzieren (Jarolim et al, 2016b). Um zu untersuchen, ob die Substanzen gegen die humane Topo IIα gerichtet sind, da diese strukturell der bakteriellen Topo II ähnelt, wurden die Sekundärmetabolite ebenfalls auf eine potentielle Wirkung auf Gyrase aus *E. coli* getestet, auch im zellfreien System. Die Ergebnisse des Gyrase Supercoling Assay zeigen, dass alle vier getesteten Perylenchinone und die zwei Dibenzo-α-Pyrone eine duale Inhibition der humanen und der bakteriellen Topo II verursachen, während die übrigen *Alternaria* Metabolite, außer TEN, nur gegen die humane Form aktiv waren. Dies unterstützte die These der dualen Inhibition der humanen und bakteriellen Topo II durch die Schimmelpilz Metabolite aufgrund der strukturellen Verwandtschaft der Enzyme. Von den fünf *Fusarium* Sekundärmetaboliten führte nur AURO zu einer Reduktion der Aktivität der humanen Topo IIα, aber nicht der Gyrase. Interessanterweise erwies sich AURO als der potenteste Inhibitor aller getesteten Sekundärmetabolite gegen humane Topo IIα.

Die beobachtete Topo II-Hemmung von AURO im Dekatenierungs Assay machte das dimere

Naphthochinon zu einem interessanten Kandidaten für weitere Untersuchungen, da wenige Studien zu dessen Toxizität existierten. Daher wurden toxikologische Mechanismen von AURO in Publikation 3 in der Krebszelllinie HT29 sowie in der nicht-transformierten Kolon Epithelzelllinie HCEC-1CT untersucht (Jarolim et al., 2018). Diese Experimente zeigten, dass AURO in beiden Zelllinien zytotoxisch im WST-1 und im SRB Assay ist. Ein potentiell zugrundeliegender Mechanismus könnte die DNA-schädigende Wirkung von AURO sein, die im Comet Assay in HT29 Zellen identifiziert wurde. Diese Beobachtung stimmt überein mit einem Zellzyklus Arrest in der G_2/M-Phase durch das Naphthochinon, sowie einem Anstieg von p53 in beiden Zelllinien. Vermutlich ist die Genotoxizität von AURO bedingt durch dessen pro-oxidative Effekte, die ebenfalls im Comet Assay ersichtlich sind, da die Testsubstanz fpg-sensitive Stellen induziert. Das pro-oxidative Potential von AURO konnte auch im 2,7-Dichlorofluorescein (DCF) Assay nachgewiesen werden, wo eine erhöhte Menge an reaktiven Sauerstoffspezies (ROS) in HT29 gemessen wurden. Zusätzlich führt die Inkubation mit AURO zu einer Zunahme des GSSG/GSH Verhältnisses in HT29 Zellen.

Wie oben erwähnt, wurde AURO als potentieller Inhibitor der humanen Topo IIα im zell-freien Dekatenierungsassay identifiziert. Um zu untersuchen, ob die Substanz in der Zelle zu einer Stabilisierung des DNA-Topo II-Komplexes führte, wurde die Stabilisierung dieses sogenannten Cleavage Komplexes in HT29 Zellen mit dem „in vivo Complex of Enzyme“ (ICE) Assay untersucht. Die Inkubation mit AURO führt in den Experimenten zu einer leichten, wenn auch nicht signifikanten Zunahme der DNA-Topo II-Komplexe. Viele Substanzen, die Topo II hemmen, wurden als DNA-Interkalatoren identifiziert (Chen und Liu 1994). Der zellfreie Interkalationsassay konnte dementsprechend auch für AURO eine Interkalation in Kalbsthymus DNA demonstrieren. Unerwarteterweise induziert AURO die Genexpression von CYP1A1 in HT29 Zellen in der q-PCR, was auch mittels Ethoxyresorufin (EROD) Assay bestätigt wurde, der zeigt, dass die Aktivität des Enzyms CYP1A1 nach Inkubation mit AURO erhöht ist. Diese beiden Ergebnisse sind ein Hinweis darauf, dass AURO als Aktivator des Arylhydrokarbonrezeptor (AhR) Signalwegs wirken könnte.

Die Resultate der LC-MS/MS Experimente zeigten, dass der Metabolit Licht- und Temperatur-empfindlich ist, weshalb die Zellkulturbedingungen vermutlich zu dessen Degradierung beigetragen haben. Trotz der Instabilität der Testsubstanz unter den experimentellen Bedingungen können die Ergebnisse aus Publikation 3 zeigen, dass AURO eine Reihe toxischer Effekte in Zellkultur verursacht. Die Messungen können daher als

Hinweis darauf betrachtet werden, dass der *Fusarium* Sekundärmetabolit AURO als vollwertiges Mykotoxin klassifiziert werden könnte, wenn weitere unterstützende Messungen durchgeführt werden.

Zusammengefasst wurden im Rahmen dieser Dissertation in Summe sechzehn Sekundärmetabolite, die von Pilzen der Gattungen *Alternaria* und *Fusarium* produziert werden, auf deren potentielle Detoxifizierung und toxikologische Wirkungen. Die Ergebnisse aus den drei Publikationen zeigen, dass der Detoxifizierungsweg Nrf2/ARE ein Ziel des *Alternaria* Mykotoxins ATX II darstellt. Die Experimente demonstrieren auch, dass humane Topoisomerase II ebenfalls ein Ziel für einige der getesteten *Alternaria* und *Fusarium* Mykotoxine darstellt, was vermutlich durch die Homologie zur bakteriellen Topo II bedingt ist. Weiters wurde ein neuer sekundärer *Fusarium* Metabolit identifiziert, der sich aufgrund seiner Toxizität in Zellkulturtests als interessant für weitere zukünftige Erforschung heraus kristallisiert hat.